

**Relationships between kinematic characteristics and  
ratio of forces during initial sprint acceleration**

**Daniel Thomas King**

**Submitted to Swansea University in fulfilment of the requirements for  
the Degree of MSc by Research in Sports Science**

**Swansea University**

**2021**

## Abstract

In track sprinting, the athlete generates around 70% of their maximum velocity during the initial acceleration phase (Nagahara et al., 2019a). Effective acceleration performance is largely determined by the technical ability of effectively orientating force applied to the track, quantified by the ratio of forces (RF; Morin et al., 2011). This thesis aimed to investigate the relationships between kinematic characteristics and RF during the initial acceleration phase of sprinting, as these important considerations remain unknown. Fourteen male sprinters completed two maximal 60 m sprint efforts from a block start. Whole-body kinematic data and external kinetic data were measured for the first four steps on the track. An initial analysis using semi-partial correlations (sr) determined that step-to-step variation in RF over the four steps was not related (sr = -0.280) to initial acceleration performance (normalised average horizontal external power; NAHEP), but that mean RF ( $RF_{MEAN}$ ) over these steps was strongly related to initial acceleration performance (sr = 0.683). To address the aim of this thesis, correlations with kinematic characteristics, using  $RF_{MEAN}$  as the dependent variable, revealed that placing the stance foot further behind the whole-body centre of mass at touchdown was strongly related to high RF ( $r = -0.672$ ). Specific stance leg configurations contributed to this favourable touchdown distance - a more anterior orientation (i.e., of the proximal end) of the foot and shank segments were both very strongly associated with RF ( $r = -0.724$  and  $r = -0.764$ , respectively). Following touchdown, ankle dorsiflexion range of motion was also very strongly related to RF ( $r = 0.728$ ). Touchdown distance was the only measure strongly related to both RF and performance ( $r = -0.710$  with NAHEP). These findings suggest coaches should focus on strategies which manipulate lower-leg configurations at touchdown and actions during early stance if they wish to improve RF ability.

## Declarations and Statements

This work has not previously been accepted in substance for any degree and is not being concurrently submitted in candidature for any degree.

Signed .. 

Date .....12/11/21.....

This thesis is the result of my own investigations, except where otherwise stated. Other sources are acknowledged by footnotes giving explicit references. A bibliography is appended.

Signed . 

Date .....12/11/21.....

I hereby give consent for my thesis, if accepted, to be available for photocopying and for inter-library loan, and for the title and summary to be made available to outside organisations.

Signed .... 

Date .....12/11/21.....

The University's ethical procedures have been followed and, where appropriate, that ethical approval has been granted.

Signed .. 

Date .....12/11/21.....

## Statements on Candidate Contributions

Due to restrictions associated with COVID-19, the raw data used in this thesis were collected as part of an earlier project at which the candidate was not involved. The candidate designed and conducted all analysis of the data presented in this thesis.

Signed .

A black rectangular redaction box covers the signature. There are some handwritten marks above and below the box, possibly initials or a flourish.

Date .....12/11/21.....

## Table of Contents

<b>CHAPTER 1: INTRODUCTION</b> .....	<b>1</b>
<b>1.1 Context</b> .....	<b>1</b>
<b>1.2 Research aim and questions</b> .....	<b>4</b>
<b>CHAPTER 2: LITERATURE REVIEW</b> .....	<b>6</b>
<b>2.1 Biomechanics of sprinting</b> .....	<b>6</b>
2.1.1 Sprint phases .....	7
2.1.2 Step phases .....	10
<b>2.2 Biomechanics of the initial acceleration phase</b> .....	<b>12</b>
2.2.1 Acceleration characteristics .....	12
2.2.2 Acceleration kinematics .....	13
2.2.3 Acceleration kinetics .....	15
2.2.4 Ratio of forces .....	17
<b>2.3 Relationships between kinematic characteristics and ratio of forces</b> .....	<b>24</b>
2.3.1 Investigations linking kinematics and RF .....	24
2.3.2 Kinematics and horizontal force .....	26
<b>2.4 Chapter summary</b> .....	<b>28</b>
<b>CHAPTER 3: METHODS</b> .....	<b>30</b>
<b>3.1 Participants</b> .....	<b>30</b>
<b>3.2 Experimental protocol</b> .....	<b>30</b>
<b>3.3 Data collection</b> .....	<b>30</b>
<b>3.4 Data processing</b> .....	<b>32</b>
3.4.1 Kinematic data .....	32
3.4.2 Kinetic data .....	34
<b>3.5 Data Analysis</b> .....	<b>36</b>
3.5.1 Spatiotemporal variables .....	36
3.5.2 Kinematic variables.....	37
3.5.3 Kinetic variables.....	40
<b>3.6 Statistical Analysis</b> .....	<b>41</b>
<b>CHAPTER 4: RESULTS</b> .....	<b>43</b>
<b>4.1 Overview</b> .....	<b>43</b>
<b>4.2 Ratio of forces and initial sprint acceleration performance</b> .....	<b>43</b>
<b>4.3 Kinematics and ratio of forces</b> .....	<b>46</b>
4.3.1 Descriptive linear kinematics .....	46
4.3.2 Descriptive angular kinematics .....	47
4.3.3 Relationships between linear kinematics and RF.....	55
4.3.4 Relationships between angular kinematics and RF.....	55
4.3.5 Relationships between kinematics favourable for RF and initial acceleration phase performance .....	57
<b>CHAPTER 5: DISCUSSION</b> .....	<b>59</b>

<b>5.1 Overview .....</b>	<b>59</b>
<b>5.2 How strongly do RF-associated measures derived from the RF-<math>v_H</math> profile, including the linearity of the fit, relate to initial acceleration phase performance? .....</b>	<b>60</b>
<b>5.3 What are the relationships between a sprinter's kinematics and RF during the initial acceleration phase? .....</b>	<b>63</b>
5.3.1 Touchdown kinematics .....	63
5.3.2 Kinematics during stance .....	66
5.3.3 Kinematic interactions across stance .....	68
5.3.4 Spatiotemporal variables .....	70
<b>5.4 How strongly do the kinematic characteristics, which are strongly related to RF, relate to initial acceleration phase performance?.....</b>	<b>71</b>
<b>5.5 Limitations and considerations for future research .....</b>	<b>74</b>
<b>5.6 Practical implications.....</b>	<b>76</b>
<b>5.7 Thesis conclusion .....</b>	<b>77</b>
<b><i>REFERENCE LIST</i>.....</b>	<b>79</b>
<b><i>APPENDICES</i>.....</b>	<b>87</b>
<b>Appendix A: Residual analysis to select the cut-off frequency of the Butterworth low-pass filter used to smooth the kinematic data .....</b>	<b>87</b>
<b>Appendix B: Pairwise comparisons for significant effects between steps.....</b>	<b>88</b>
<b>Appendix C: Relationships between performance measures and all measured variables .....</b>	<b>90</b>
<b>Appendix D: Multiple linear regression results .....</b>	<b>95</b>

## **Acknowledgements**

Firstly, I must give huge thanks to Dr Neil Bezodis and Dr Louise Burnie. Your endless support and supervision throughout the last year has developed my academic knowledge and skills and enabled me to accomplish things of which I didn't think I was capable.

Thanks to Dr Ryu Nagahara, for your insights and feedback throughout my project and for your time and resources spent collecting the data, with additional thanks to the sprinters at the National Institute of Fitness and Sports in Kanoya for participating in the data collection.

Thank you to my family and friends for your continued support, in all of its forms, along the way.

Finally, thank you to Ciera, for being my partner, and always giving me the boost of confidence that I very often need.

## Conference Papers

King, D., Burnie, L., Nagahara, R. and Bezodis, N. (2021) 'Linearity of the ratio of forces-velocity relationship is not related to initial acceleration performance in sprinting', *ISBS Proceedings Archive*: 39(1), Article 75.



## List of Tables

**Table 3.1.** Proximal and distal segment endpoint locations used for definition of the 15-segment body model. Page 34.

**Table 4.1.** Step-to-step GRF-derived and performance measures (Mean  $\pm$  SD) over each of the steps of the initial acceleration phase, with main effect of step number ( $p$ ). Page 44.

**Table 4.2.** GRF-derived measures (Mean  $\pm$  SD) averaged over the initial acceleration phase (i.e., 4 steps) and semi-partial correlations ( $sr$ ) with NAHEP over the initial acceleration phase. Page 46.

**Table 4.3.** Linear kinematics from steps one to four (Mean  $\pm$  SD), with main effect of step number. Page 47.

**Table 4.4.** Ankle angular kinematics from steps one to four (Mean  $\pm$  SD), with main effect of step number. Page 48.

**Table 4.5.** Knee angular kinematics from steps one to four (Mean  $\pm$  SD), with main effect of step number. Page 49.

**Table 4.6.** Hip angular kinematics from steps one to four (Mean  $\pm$  SD), with main effect of step number. Page 50.

**Table 4.7.** Foot angular kinematics from steps one to four (Mean  $\pm$  SD), with main effect of step number. Page 51.

**Table 4.8.** Shank angular kinematics from steps one to four (Mean  $\pm$  SD), with main effect of step number. Page 52.

**Table 4.9.** Thigh angular kinematics from steps one to four (Mean  $\pm$  SD), with main effect of step number. Page 53.

**Table 4.10.** Trunk angular kinematics from steps one to four (Mean  $\pm$  SD), with main effect of step number. Page 54.

**Table 4.11.** Mean ( $\pm$  SD) linear kinematics over four steps and correlation with  $RF_{MEAN}$ . Page 55.

**Table 4.12.** Mean ( $\pm$  SD) joint angular kinematics over four steps and correlation with  $RF_{MEAN}$ . Page 56.

**Table 4.13.** Mean ( $\pm$  SD) segment angular kinematics over four steps and correlation with  $RF_{MEAN}$ . Page 57.

**Table 4.14.** Relationships between kinematic characteristics favourable for  $RF_{MEAN}$  and their relationship ( $r$ ) with initial acceleration phase performance (NAHEP). Page 58.

## List of Figures

**Figure 1.1.** Ratio of forces-horizontal velocity (RF- $v_H$ ) profile from a single sprinter for each step over the entire sprint acceleration (orange markers) and its fitted linear trendline (orange), with steps over the initial acceleration phase overlaid (grey markers) and the corresponding fitted linear trendline (grey) (from Bezodis et al., 2020). Page 2.

**Figure 1.2.** Ratio of forces-horizontal velocity (RF- $v_H$ ) profile from a different sprinter for each step over the entire sprint acceleration (green markers) and its fitted linear trendline (green), with steps over the initial acceleration phase overlaid (grey markers) and the corresponding fitted linear trendline (grey) (Bezodis et al., 2020). Page 2.

**Figure 2.1.** Visual depiction of body positions between the four major sprint phases, from left to right. Beginning with the block phase (A; figure from Haugen et al., 2017), followed by the initial acceleration phase (B), transition phase (C) and maximum velocity phase (D); where grey to black positions depict the direction of changes in postural position (figure from Nagahara et al., 2014b). Page 7.

**Figure 2.2.** Comparison between parameters for major sprint phases between findings of Nagahara et al. (2014b) and Crick (2014) (von Lieres und Wilkau et al., 2018).  $\theta_{shank}$  and  $\theta_{trunk}$  denote shank and trunk angles at touchdown. CM-h denotes whole-body centre of mass height at touchdown. Page 8.

**Figure 2.3.** Visual depiction of the phases of the running step cycle, from left to right, where the stance and flight phases are delimited by touchdown and toe-off events (Dyson, 1973). Page 11.

**Figure 2.4.** Schematic representation of the ratio of forces (RF) and mathematical expression as a function of the total ( $F_{Tot}$ ) and horizontal ( $F_H$ ) step averaged GRF. The forward orientation of the total GRF vector is represented by the angle  $\alpha$  (Morin et al., 2011). Page 18.

**Figure 2.5.** Representation of the ratio of forces-horizontal velocity (RF- $v_H$ ) relationship over the initial acceleration phase (black o denote measured values during steps 1 to 4), featuring annotated RF-derived measures including  $D_{RF}$  (the gradient of the linear trendline),  $RF_0$  (red o; y-intercept at  $v_H = 0$ ) and mean step-averaged RF ( $RF_{MEAN}$ ) over the initial acceleration phase (steps 1 to 4). Page 19.

**Figure 2.6.** Representation of measured horizontal velocity-time ( $v_H$ -time, measured using a portable resistance device) (grey) compared to a mono-exponential fit to the  $v_H$ -time profile (black) typically observed over a maximal sprint (Cross et al., 2018). Page 20.

**Figure 2.7.** Comparison between force plate-derived measures of vertical GRF ( $F_V$ ), horizontal GRF ( $F_H$ ) and horizontal power ( $P_H$ ) and those derived from the Samozino et al. (2016) simple macroscopic model (Morin et al., 2019). Page 21.

**Figure 2.8.** Stick figure showing the positions of the trunk and stance leg, together with the actions of the muscles at different time samples. Time is expressed relative to the instant of toe-off (Jacobs and van Ingen Schenau, 1992). Page 26.

**Figure 2.9.** Schematic representation from Jacobs and van Ingen Schenau (1992; p. 954), depicting two positions during an early stance phase, based on a simple model of a sprinter illustrated by a heavy mass (box) and a simplified leg (l), which can rotate and extend. The angle ( $\theta$ ) in the bottom-left corner is 90 degrees and increases during stance.  $\dot{X}_{bcg}$  and  $\dot{Y}_{bcg}$  denote the horizontal and vertical velocity of the CM (here termed body centre of gravity (bcg)), respectively, where extension and rotation of the system combine to influence the change in these velocities (Jacobs & van Ingen Schenau, 1992). Page 26.

**Figure 3.1.** Locations of 47 retro-reflective markers affixed to each participants body (from Suzuki et al., 2014, p.146). Page 31.

**Figure 3.2.** Kinetic data capture experimental set-up with force plates mounted under the starting blocks (left) and in series for approximately 50 m along the indoor track (right). Page 32.

**Figure 3.3.** Marker positions (grey spheres) creating the 15-segment model (yellow lines) with whole-body centre of mass location (large turquoise sphere) based on data while stationary in the blocks, generated in Visual3D. Page 33.

**Figure 3.4.** Centre of mass displacement as determined from integration of the antero-posterior GRF data after accounting for the effects of drag (blue) and anteroposterior centre of pressure data (black) with respect to time. Red crosses represent touchdown and green crosses represent toe-off (based on the 50 N threshold used for the raw vertical GRF data). These data are for a single trial of participant 4 and are used for illustrative purposes only. Note: The

centre of pressure data return to  $\sim 0$  during each flight phase and are thus only of interest during each stance phase. Following toe-off from a number stance phases, the figure appears to show black bars – these depict noise in the centre of pressure data during the flight phase. Page 36.

**Figure 3.5.** Joint angle conventions for three stance leg joints; ankle, knee, and hip. JC denotes joint centre. Extension/plantar flexion were defined as positive. Page 38.

**Figure 3.6.** Segment angle conventions for four segments; foot, shank, thigh, and trunk. JC denotes joint centre. Conventions for the positive direction are displayed on the stance leg, following the conventions of Nagahara et al. (2014b). Page 39.

**Figure 4.1.** RF- $v_H$  profiles for all 14 sprinters (A-N, labels above each sub-figure) across the initial acceleration phase with individual linear trendlines fitted through all four steps. Technical ability descriptors based on the slope ( $D_{RF}$ ) and y-intercept ( $RF_0$ ) of this trendline, and the goodness of fit ( $R^2$ ), for each individual are stated in the top right of each plot, while  $RF_{MEAN}$  over initial acceleration is stated in the bottom left. Plot backgrounds are colour coded according to initial acceleration performance (NAHEP) from lowest (red) to highest (green) – see colour scale in bottom right of figure. Page 45.

**Figure 4.2.** Joint angle-time and angular velocity-time history for the ankle joint of the stance leg during stance phase for steps one to four from each of the 14 sprinters. Page 48.

**Figure 4.3.** Joint angle-time and angular velocity-time history for the knee joint of the support leg during stance phase for steps one to four from each of the 14 sprinters. Page 49.

**Figure 4.4.** Joint angle-time and angular velocity-time history for the hip joint of the support leg during stance phase for steps one to four from each of the 14 sprinters. Page 50.

**Figure 4.5.** Segment angle-time and angular velocity-time history for the foot segment of the support leg during stance phase for steps one to four from each of the 14 sprinters. Page 51.

**Figure 4.6.** Segment angle-time and angular velocity-time history for the shank segment of the support leg during stance phase for steps one to four from each of the 14 sprinters. Page 52.

**Figure 4.7.** Segment angle-time and angular velocity-time history for the thigh segment of the support leg during stance phase for steps one to four from each of the 14 sprinters. Page 53.

**Figure 5.1.** RF- $v_H$  profiles for one sprinter from the current thesis, created from left: ‘early acceleration (includes block exit; method used by Bezodis et al., 2020) and right: initial acceleration (excludes block exit; method used in this thesis) with linear trendlines fitted. Technical performance descriptors based on the slope ( $D_{RF}$ ) and y-intercept ( $RF_0$ ) of this trendline, are stated in the bottom left of each plot. Page 62.

**Figure 5.2.** Representation of two examples of whole-body configurations with different angular kinematics to achieve the same touchdown distance. Left figure with a more posteriorly extended leg and more upright upper body, right figure with a more forward leaning upper body and less posteriorly extended leg. Red circle denotes the whole-body CM position, green circle denotes the base of support (toe marker), example normalised touchdown distance of -0.15 (arbitrary units). Page 65.

# CHAPTER 1: INTRODUCTION

## 1.1 Context

An athlete's ability to accelerate effectively can be a determining factor for success in track sprinting. During a maximal sprint, the first steps on the track are when the largest forward accelerations are observed, with the athlete often having reached ~70% of their maximum velocity by step four (Nagahara et al., 2019a; 2020). The initial acceleration phase of maximal sprinting can be defined as the first four steps following block exit (Nagahara et al., 2014b). This phase of the sprint has been the subject of considerable biomechanical research to understand the principles underpinning high acceleration performance.

Previous investigations in the sprint running literature have revealed that a key element of high acceleration performance is effective orientation of force output (Morin et al., 2011; Rabita et al., 2015; Samozino et al., 2016). This 'technical ability' is typically measured by the ratio of forces (RF), which describes the proportion of the step-averaged resultant force vector ( $F_R$ ) that is directed horizontally ( $F_H$ ), i.e.,  $RF = F_H/F_R$  (Morin et al., 2011). When quantifying technical performance during sprint acceleration, a linear trendline is often fitted to step-averaged RF with respect to step-averaged horizontal velocity ( $v_H$ ), denoted as the RF- $v_H$  profile (Rabita et al., 2015). This profile is typically created using data from each step of the entire acceleration phase. The gradient of the trendline fitted to the RF- $v_H$  profile quantifies the ability to maintain RF as  $v_H$  increases, termed rate of decline in RF ( $D_{RF}$ ; Morin et al., 2011). The y-intercept provides the theoretical maximal RF at null velocity, termed  $RF_0$  (Rabita et al., 2015), whilst other measures such as  $RF_{MAX}$  (RF value at 0.3 s; Samozino et al., 2016) are also sometimes extracted. Bezodis et al. (2020) found a very strong relationship between mean RF and performance (quantified by normalised average horizontal external power; NAHEP) over the block phase and first four steps ( $r = 0.88$ ). Their study also found  $D_{RF}$  and  $RF_0$  combined to explain 93-95% of the variance in performance over this phase. However, Bezodis et al. (2020) found that the RF- $v_H$  profile over the whole acceleration phase was not always closely related to the RF- $v_H$  profile during just the early part of acceleration, as considerable step-to-step

variation in RF can be observed, particularly during the initial acceleration phase (i.e., first four steps on the track; Figure 1.1); while, in other cases, there may be little variation from a linear decrease over these first four steps, but the trend is considerably different from the profile during the entire acceleration phase (Figure 1.2).

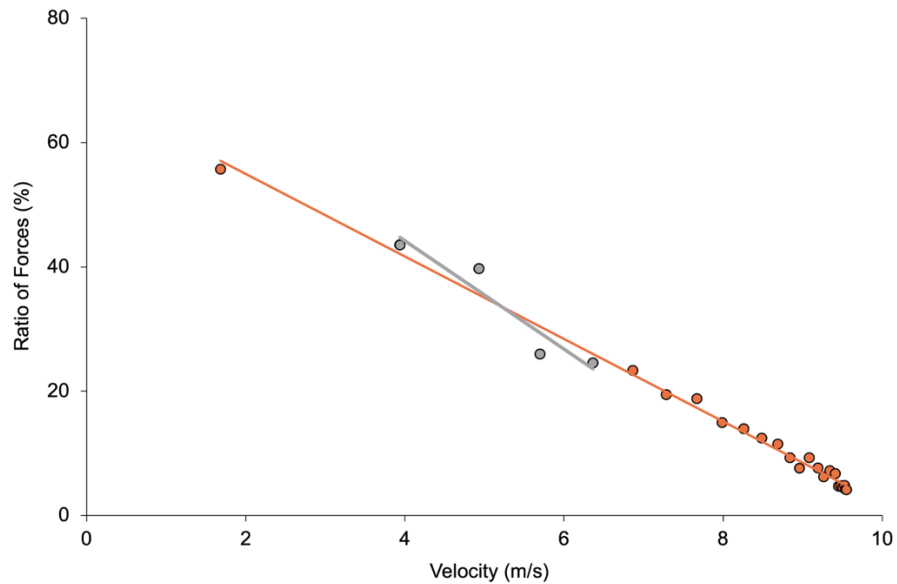


**Figure 1.1.** Ratio of forces-horizontal velocity (RF- $v_H$ ) profile from a single sprinter for each step over the entire sprint acceleration (orange markers) and its fitted linear trendline (orange), with steps over the initial acceleration phase overlaid (grey markers) and the corresponding fitted linear trendline (grey) (from Bezodis et al., 2020).

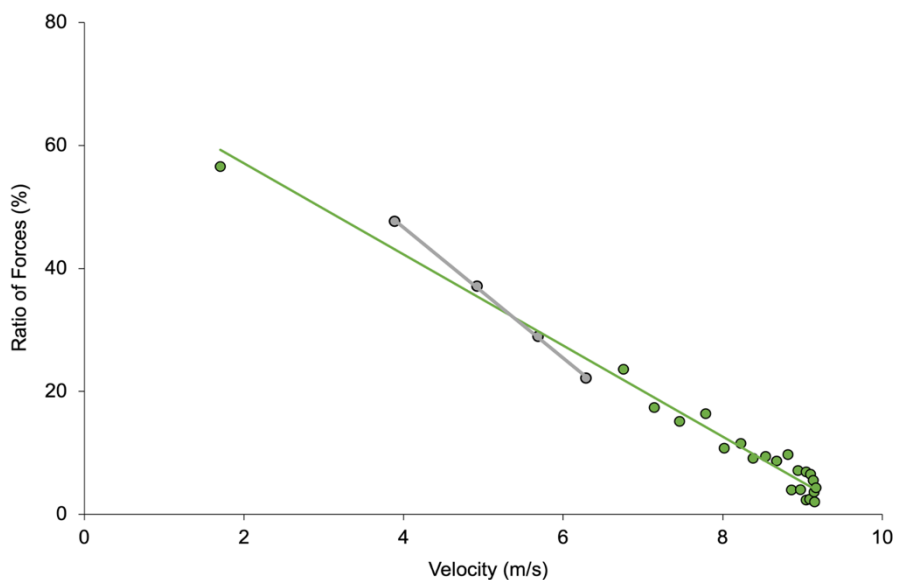


**Figure 1.2.** Ratio of forces-horizontal velocity (RF- $v_H$ ) profile from a different sprinter for each step over the entire sprint acceleration (green markers) and its fitted linear trendline (green), with steps over the initial acceleration phase overlaid (grey markers) and the corresponding fitted linear trendline (grey) (Bezodis et al., 2020).



This variation in RF during the initial acceleration phase of the sprint can be quantified from the coefficient of determination (adjusted  $R^2$ ) of the linear trendline fitted to the RF- $v_H$  profile. Hereafter termed the ‘linearity’ of the profile (fitted to data from the first four steps), this coefficient allows objective assessment of an athlete’s step-to-step variation in the decreasing RF values over the initial acceleration phase. It remains unknown whether step-to-step variation in RF is associated with acceleration performance and investigating the strength of the relationship between the linearity of the RF- $v_H$  profile and performance over the initial acceleration phase could therefore provide valuable insight. This would enable researchers to determine whether step-to-step variation in RF is important to consider for initial acceleration performance, as well as providing knowledge to inform the practice of sprinters and coaches during the initial acceleration phase.

Although it has been widely established that RF is a determining factor for sprint acceleration performance, as it is more strongly related to acceleration performance than resultant force magnitude (Morin et al., 2011; Rabita et al., 2015; Bezodis et al., 2020), it currently remains unknown what kinematic characteristics of the body and stance leg during acceleration are associated with the ability to produce high RF. As such, there is currently no empirical evidence which has directly associated kinematic characteristics with RF measures (i.e.,  $RF_{MEAN}$ ,  $RF_0$  and  $D_{RF}$ ) using an observational, cross-sectional design. However, many previous investigations have highlighted kinematic characteristics that are strongly related to performance, and postural positions that may be favourable for producing horizontal propulsive forces during acceleration (Jacobs & van Ingen Schenau, 1992; Kugler & Janshen, 2010; Bezodis et al., 2015b; 2017). For instance, Jacobs and van Ingen Schenau (1992) found that highly trained sprinters delayed extension of the whole-body centre of mass (CM) away from the base of support until the CM had been rotated further forwards, relative to the base of support. However, the study by Jacobs and van Ingen Schenau (1992) analysed only the second stance phase of the sprint effort and used a simple body model of only four segments (foot, lower leg, upper leg, and upper body). Hence, further investigation using more comprehensive modelling and data collection of the whole initial acceleration phase is warranted. Later studies by Kugler and Janshen (2010) and Bezodis et al. (2015b) provided additional evidence that the general movement strategy observed by Jacobs and van Ingen Schenau (1992) may be favourable for

performance; Kugler and Janshen (2010) found that greater forward lean of the body, facilitated by more posterior foot placement, led to greater production of propulsive forces. Additionally, Bezodis et al. (2015b) found, using computer simulation, that placing the foot further behind the CM at touchdown (termed negative touchdown distance) led to a near linear increase in RF during the stance phase. More recently, Bezodis et al. (2017) suggested that rotating the CM rapidly about the stance foot at touchdown, with a foot further behind the CM could improve RF capability even further. However, it is important to consider that the stance leg is multi-segmented, so achieving a postural position in which the whole-body CM is ahead of the stance foot at touchdown is largely a function of the angles at the ankle, knee, and hip. The aforementioned studies who provided these findings either did not report stance leg joint kinematics and investigated a non-sprint trained population (Kugler & Janshen, 2010), or theoretically manipulated specific joint kinematics to achieve changes in touchdown distance and investigated a simulated model (Bezodis et al., 2015b). Therefore, further investigation is warranted encompassing both linear and angular kinematic characteristics during initial acceleration, using a sprint trained population, to assess the strength of the relationships between such kinematics and RF measures, and ultimately, how these features contribute to initial sprint acceleration performance.

## **1.2 Research aim and questions**

The aim of this thesis is to *investigate the relationships between kinematic characteristics and RF during the initial acceleration phase of sprinting*. Before this aim can be achieved, a preliminary investigation will be required to explore the relationships surrounding RF-associated measures of technical performance and initial acceleration performance, to address the first research question. This will inform the study design for the second research question to address the aim of this thesis. Research question three will finally be addressed as a supplementary investigation to explore the relationships between any RF-associated kinematics and acceleration performance. The culmination of these three research questions will ensure kinematic characteristics that may be associated with RF, and their potential relationship with initial sprint acceleration performance are systematically explored in detail:

1. *How strongly do RF-associated measures derived from the RF- $v_H$  profile, including the linearity of the fit, relate to initial acceleration phase performance?*
2. *What are the relationships between a sprinter's kinematics and RF during the initial acceleration phase?*
3. *How strongly do the kinematic characteristics which are strongly related to RF relate to initial acceleration phase performance?*

## **CHAPTER 2: LITERATURE REVIEW**

### **2.1 Biomechanics of sprinting**

Often referred to as the blue-ribbon event of track and field, the 100 m sprint holds its place as a key event within the Olympic Games, bringing millions to watch when a new ‘fastest athlete on earth’ emerges victor. This complex movement pattern is often analysed in scientific literature to understand the features and mechanisms that underpin performance and hence identify avenues to potentially improve sprint running performance. Biomechanical analysis of sprint performance is often focussed on one of, or an interaction between, two branches of analysis: kinematics and kinetics. Kinematics is the study of motion without regard to causes (Robertson et al., 2013). Literature in this area explores how segments of the body move and interact to facilitate motion. For the context of sport biomechanics, it often investigates the movement pattern of athletes during specific sporting movements in order to elucidate key features that contribute to more successful performance. Kinetics is the study of the relationships between the force system acting on a body and the changes it produces in body motion (Hall, 2019). This branch of sport biomechanics explains how movement patterns are initiated by forces generated by the body and the interaction of these forces with the external environment. Section 2.1 will describe the composition of the 100 m sprint event, which consists of four major sprint phases which are, in turn, each comprised of multiple steps containing stance and flight phases. Biomechanical characteristics of the sprint phases and the sub-phases within each step will be explored to build a foundation for understanding of the determinants of acceleration performance discussed later in this review. As the majority of biomechanical sprint research has been conducted using male populations, throughout this literature review it is assumed that ‘sprinter’ and ‘athlete’ refers to males unless otherwise stated.

### 2.1.1 Sprint phases

The track sprint begins with a block phase, with the athlete having set the starting blocks to their personal preference of angle and spacing. These settings allow the athlete to assume their preferred position during the sprint start, in order to propel the body's centre of mass (CM) at a lower angle than could be achieved from a standing start (Sandstrom, 1983). This low CM trajectory upon leaving the blocks, sometimes termed block exit angle, is advantageous to facilitate acceleration (di Prampero et al., 2005). In a review by Harland and Steele (1997), the common kinematic features adopted by sprinters in the block phase were highlighted. These were medium block spacing (30 to 50 cm inter-block distance), with front and rear knee angles at 90° and 130°, respectively, resulting in the hips held moderately high (Figure 2.1, A), followed by a block exit angle of 40-45°. The common kinetic characteristics of the block phase are large peak ankle plantar flexor moment and power (Mero et al., 2006), and hip extension moment (Brazil et al., 2017) which contribute to a high horizontal ground reaction force impulse (Baumann, 1976; Mero et al., 1983) to produce high block exit velocity.

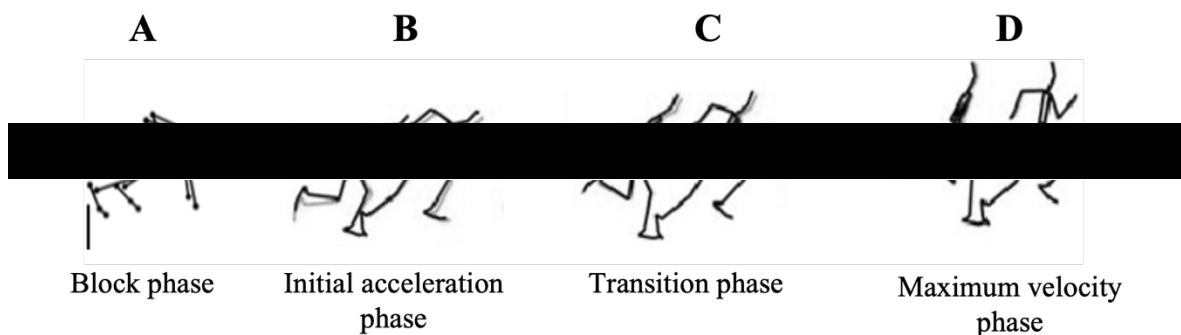


**Figure 2.1.** Visual depiction of body positions between the four major sprint phases, from left to right. Beginning with the block phase (A; figure from Haugen et al., 2017), followed by the initial acceleration phase (B), transition phase (C) and maximum velocity phase (D); where grey to black positions depict the direction of changes in postural position (figure from Nagahara et al., 2014b).

The next phase of a sprint, constituting the first contact phases with the track following block exit, was termed the initial acceleration phase by Delecluse et al. (1995). The defined parameters for the length of the initial acceleration phase have been subject to some discrepancy between the scientific and coaching literature. Although Maćkała et al. (2015) defined the initial acceleration phase, by distance on the track,

as the first 12 m of the sprint, many biomechanical analyses investigate kinematic and kinetic characteristics on a step-to-step basis. Therefore, other researchers have attempted to identify breakpoint steps, through differences in kinematic and kinetic features, that signal the change between the major sprint phases (Figure 2.2).

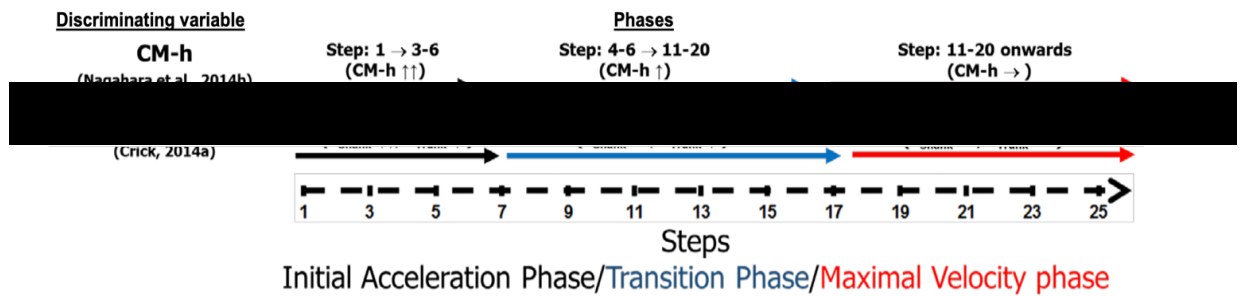


**Figure 2.2.** Comparison between parameters for major sprint phases between findings of Nagahara et al. (2014b) and Crick (2014) (figure from von Lieres und Wilkau et al., 2018).  $\theta_{\text{shank}}$  and  $\theta_{\text{trunk}}$  denote shank and trunk angles at touchdown. CM-h denotes whole-body centre of mass height at touchdown.

The distinction between the initial acceleration phase and following sprint phases can be achieved by observing the changes in an athlete's kinematics. For example, Nagahara et al., (2014b) measured CM height (CM-h) over the entire acceleration phase and found the largest increase through steps 1-4, compared to the subsequent transition phase. Hence, Nagahara et al. (2014b) used this difference in CM-h to identify the breakpoint step between phases (Figure 2.2). However, it was suggested by Crick (2014), in the coaching literature, that the initial acceleration phase ends at steps 5-7 when step-to-step changes in shank angles end as the shank becomes perpendicular to the ground at touchdown (Figure 2.2). This suggestion is more questionable than the findings of Nagahara et al. (2014b) due to its basis on coaching supposition rather than objective evidence. Also, the suggestion by Crick (2014) was based exclusively on evaluation of lower limb angular characteristics, which cannot give a holistic representation of whole-body postural position. Due to the discrepancy between phase definitions, von Lieres und Wilkau et al. (2018) investigated the distinction between sprint phases using both methods from Crick (2014) and Nagahara et al. (2014b). Their findings concluded that CM-h (suggested by Nagahara et al. (2014b)) provides a more robust and holistic measure that is more representative of overall postural changes during initial acceleration. Therefore, in the current thesis the

initial acceleration phase will be defined as the first four steps on the track following block exit, as suggested by Nagahara et al. (2014b) and used in several recent studies (e.g., Bayne et al., 2020; Donaldson et al., 2020).

When considering kinetic characteristics, it is clear that the initial phase of sprint acceleration is a period where substantial magnitudes of force are produced by the athlete (Maćkała, 2007; Nagahara et al., 2014a; Rabita et al., 2015). Kinematic and spatiotemporal characteristics associated with the generation of these ground reaction forces (GRF) are longer ground contact times, compared to later sprint phases, and the whole-body CM positioned in front of the contact foot for some or all of the initial acceleration phase (Figure 2.1). The interaction between kinematic and kinetic features during this phase can be used to develop a more complete understanding of the determinants of performance. The aforementioned CM position, with respect to the contact foot, is typically measured at the stance events of touchdown and toe-off (discussed in section 2.3.2) and termed the touchdown distance or toe-off distance, respectively. In this instance, a negative distance represents a stance foot in a position posterior to the whole-body CM. Such a negative position at touchdown allows for the greatest potential for the production of antero-posterior (A-P) forces (Bezodis et al., 2015a). This A-P component of force is accompanied by a sufficient vertical component to overcome the effect of gravity, providing sufficient flight time for repositioning of the lower limbs before the next stance phase (Weyand et al., 2000; Hunter et al., 2005; Nagahara et al., 2019a) and to allow the gradual rise of the CM into upright running (Nagahara et al., 2014a). Research pertaining to this phase of acceleration has applicability to sport of many disciplines where good acceleration ability can be advantageous (Moir et al., 2007; Lockie et al., 2013; Newans et al., 2019). However, given the aims of this thesis, the current review will only focus on studies which have used trained sprinters from block starts because other types of sprint starts and athletic populations are not comparable (Wild et al., 2018).

The ‘transition phase’ follows the initial acceleration phase. During the transition phase, the body must adapt from the typical forward leaning position in the acceleration phase (Figure 2.1, B), to a more upright position as velocity increases (Figure 2.1, C). Kinematic and kinetic characteristics displayed by the athlete change to reflect these adaptations to postural position. Schache et al. (2019) found that there

was a progressive decrease in the magnitude of horizontal acceleration during the transition phase, and the trunk gradually became more upright during stance, the hip and knee became less flexed at touchdown, and the ankle became more plantar flexed at touchdown. Schache et al. (2019) accredited this decrease in acceleration magnitude to both a notable decrease in propulsive horizontal impulse and an increase in braking impulse, while vertical impulse remained nearly unchanged. However, the relationships between the joint and segment angular kinematics with horizontal acceleration magnitude were not explored.

In the maximum velocity phase, the body position assumes a more upright posture, compared to that of the initial acceleration phase, with the whole-body CM in a more posterior position relative to the stance foot (Nagahara et al., 2014b) (Figure 2.1, D). Similar to that observed in the transition phase, there is an increased braking period during the stance phase, compared to the initial acceleration phase. These large braking forces have been attributed to the shift in CM position (von Lieres und Wilkau et al., 2017). These forces are generated throughout the entire sprint as a result of the impact as an athlete's foot strikes the floor. However, as touchdown distance becomes continually more positive as a sprint progresses beyond the initial acceleration phase (von Lieres und Wilkau et al., 2017), the impact forces generated by the foot contact, and in particular the horizontal component of these, increase (Hay, 1994; Hunter et al., 2005), which produces a deceleration effect that is detrimental to sprint performance. Matsuo et al. (2019) found a very strong correlation ( $r = 0.89$ ) between the positive (propulsive) work done in the horizontal direction and 50 m sprint time, while negative (braking) work done revealed a moderate negative correlation ( $r = -0.49$ ). Reduction in work done during the braking phase can potentially be facilitated by reducing touchdown distance and foot touchdown velocity (von Lieres und Wilkau et al., 2017).

### **2.1.2 Step phases**

The three major sprint phases after the block phase (i.e., as block phase precedes any steps on the track); initial acceleration phase, transition phase and maximum velocity phase, are each fundamentally underpinned by the sub-phases that form each step of sprinting. These step phases are the 'stance phase' and 'flight phase', which combine to form each step cycle. The stance phase represents the period in which the athlete's



foot is in contact with the ground (Figure 2.3). The action of the sprinter during this phase is responsible for the outcome of the following flight phase. During the flight phase, after the athlete's foot leaves the floor (Figure 2.3), the body acts as a projectile and no external work can be done during this phase to affect the trajectory of the CM (Hojka et al. 2016). During the flight, the only external effects present are that of air resistance and gravity. For this reason, the biomechanical sprint literature investigating external kinetics is almost solely interested in researching the stance phase. However, when analysing the flight phase from a kinematic perspective, movements made by the athlete during flight can directly influence the effectiveness of the subsequent stance phase. The flight phase serves as an opportunity to reposition the body, and in particular the lower limbs, into a favourable configuration for the following touchdown (e.g., where the leading foot is in relation to the CM, therefore influencing the subsequent touchdown distance), thereby directly affecting the kinetics of the subsequent touchdown event.



**Figure 2.3.** Visual depiction of the phases of the running step cycle, from left to right, where the stance and flight phases are delimited by touchdown and toe-off events (Dyson, 1973).

The ratio to which each of the two step phases constitutes the complete step cycle changes with each of the major sprint phases (Plamondon & Roy, 1984; Nagahara et al., 2014a). During the initial acceleration phase, long ground contact times are observed ( $\sim 0.18$  s; Nagahara et al., 2014a), where the sprinter generates large propulsive impulses to achieve maximal acceleration (Golden et al., 2009). This phase therefore features short flight phases which, as mentioned previously, serve only long enough to reposition the legs before the next stance phase. Stance phases begin to

decrease in duration through the transition phase, as there is less horizontal propulsive force produced, with increasing vertical force resulting in longer flight phases (Colyer et al., 2018). During the maximum velocity phase, vertical forces take precedence and cause long flight phases and minimal ground contact times ( $\sim 0.10$  s; Nagahara et al., 2014a). When the horizontal velocity of the CM has reached its peak, the only purpose of stance phase is to propel the body back into flight phase and maintain this velocity (van Ingen Schenau et al., 1994).

## **2.2 Biomechanics of the initial acceleration phase**

This section will build on the introduction of the initial acceleration phase in section 2.1.1, firstly outlining the typical spatiotemporal, kinematic, and kinetic variables that are characteristic of the initial acceleration phase of maximal sprinting, before exploring previous literature that has detailed the performance determinants among the aforementioned biomechanical characteristics that will be of interest for this thesis.

### **2.2.1 Acceleration characteristics**

As previously detailed, the duration of each stance phase during initial acceleration is considerably longer than the subsequent sprint phases (Nagahara et al., 2014a). This extended ground contact time is key to maximising the acceleration of the athlete's CM and is therefore fundamental to sprint performance. During these contact phases, the athlete creates the foundation for performance during the later sprint phases by producing large net horizontal impulses to increase their velocity (Lockie et al., 2012). Although the resultant magnitude of the ground reaction forces which underpin these impulses hold importance throughout the sprint effort, many previous studies have found that, during acceleration, the orientation of these forces are more strongly related to sprint performance than the magnitude of the resultant force (Morin et al., 2011; Rabita et al., 2015; Samozino et al., 2016; Bezodis et al. 2020). Hence, during the initial acceleration phase, performance is largely dictated by highly effective application of force during longer ground-contact times to maximise the horizontal

component of the resultant GRF impulse (Morin et al., 2011; 2012). This will be explored in greater detail in section 2.2.4.

It has been suggested that producing a larger horizontal component of the resultant ground reaction force during initial acceleration is associated with a forward leaning position (Debaere et al., 2013), and proximal-distal joint extension patterns of the lower limbs (Charalambous et al., 2012; Jacobs & van Ingen Schenau, 1992). A forward leaning posture of the athlete allows the athlete to minimise braking forces during the stance phase by positioning the stance foot behind the whole-body CM at touchdown (Mero et al., 1983). The proximal-distal joint extension patterns present during the initial acceleration phase act to transfer torque generated by the powerful lower-limb extensor muscles to the ground to generate large horizontal propulsive forces (Hunter et al., 2005).

### **2.2.2 Acceleration kinematics**

Kinematics can be separated further into their linear and angular components. While linear kinematics in sprint acceleration typically cover spatiotemporal characteristics such as displacements and absolute segment positions in space (and their derivatives), angular kinematics are associated with the relative angles at joints, and angles of segments relative to global axes (and their derivatives). The linear kinematic characteristics associated with the initial acceleration phase will firstly be discussed, followed by the angular kinematics, and throughout the performance implications of these features will be considered.

The spatiotemporal variables of step length (SL) and step frequency (SF) are examples of linear kinematics that receive great attention in the sprint running literature, as sprint velocity is mechanically the product of these variables, i.e.,  $\text{velocity} = \text{SL} \times \text{SF}$ . Very simply, if athletes can increase SL or SF, without a proportional decrease in the other, they will increase their velocity. However, these variables are subject to a level of mutual dependency, such that it is difficult to increase both variables equally, where increasing SL can cause a decrease in SF (or vice versa) (Hunter et al., 2004). Debaere et al. (2013) found that, in a cohort of high-level male and female athletes, neither SL

nor SF (on average from 0-10 m) were strongly related to sprint performance from the start to the 10 m mark. Nagahara et al. (2014a) suggested this is because SL and SF continually change on a step-to-step basis during the entire acceleration phase. Nagahara et al. (2014a) investigated the association between rates of changes in step length and step frequency and acceleration performance. Their study found positive correlations between acceleration and rates of changes in step frequency up to the second step, and positive correlations between acceleration and rates of changes in step length from the 5<sup>th</sup> to the 19<sup>th</sup> step. The findings by Nagahara et al. (2014a) suggest that, when looking at the broader entire acceleration phase (i.e., encompassing the initial acceleration and transition phases), exploring the rate of changes in step length and step frequency may be most appropriate due to their continual step-to-step changes. However, conclusions have been left unclear as to what relationships exist between such spatiotemporal variables and acceleration performance on a smaller scale, such as from steps one to four constituting the initial acceleration phase.

di Prampero et al. (2005) suggested that the ‘whole-body orientation’ of the sprinter is related to their acceleration. Kugler and Janshen (2010) found that greater forward lean of the body (i.e., CM angle, defined as the angle of the whole-body CM to the vertical axis in the sagittal plane), typically facilitated by more posterior foot placement, led to greater production of propulsive forces during the acceleration phase, reinforcing the suggestion by di Prampero et al. (2005). These findings were expanded by von Lieres und Wilkau et al. (2018), who found that, as sprinters assume a more forward-inclined posture during the initial acceleration phase, their horizontal CM acceleration was larger compared with the later phases of a sprint when the sprinters adopted a less forward-inclined posture. However, this postural position (i.e., CM angle) depends on both the CM height and horizontal distance between the contact foot and the CM, which in turn are dependent on the orientation of the segments of the stance leg and trunk. These stance leg and trunk segment configurations have been explored in recent literature (e.g., Bezodis et al., 2017; Walker et al., 2021), with studies aiming to quantify the contributions of each stance leg joint to sprint performance through measurement of joint angular characteristics at key events of the stance phase, such as touchdown and toe-off. Walker et al. (2021) analysed the relationships between kinematic variables and performance, quantified by normalised average horizontal external power (NAHEP), during the first step of the initial acceleration phase. They

found that only thigh separation and trunk angles at toe-off demonstrated strong relationships with first stance performance. Bezodis et al., (2017) found, from data collected at the step nearest 5 m from the start, that better performing sprinters had a more dorsiflexed ankle, more flexed knee, and extended their hip more rapidly at touchdown. The findings by Bezodis et al., (2017) and Walker et al., (2021) provide valuable insights into the relationships between sprint acceleration performance and stance leg configurations on individual steps during the initial acceleration phase. However, the sprint running literature has yet to explore such relationships for each step during the initial acceleration phase or present the step-to-step changes that may be present in stance leg kinematics over the initial acceleration phase.

### **2.2.3 Acceleration kinetics**

With respect to kinetic research, the initial acceleration phase is associated with the effective application of force to achieve high acceleration of the athlete's CM. The primary objective is to maximise horizontal displacement of the CM in as short a time as possible, therefore performance measures highlighted in the literature, that will be discussed in this section, reflect the athlete's ability to facilitate this horizontal acceleration. This is evident from early studies of Baumann (1976) and Mero et al. (1983), where sprinters who produced larger horizontal impulses possessed faster 100 m personal-best times. These findings were supported more recently by Colyer et al. (2019) and Morin et al. (2011; 2012), who found that greater acceleration performance was associated with the production of more horizontally orientated forces. Colyer et al. (2019) suggested that the production of high forces with a more horizontal orientation should be encouraged from the onset of the sprint.

Impulse is a function of the force applied and the time over which it acts. Hence, if an athlete produces a high magnitude of force and applies it over a long contact time, the impulse produced will be considerably higher than producing the same magnitude of force during a shorter ground contact, or a lower magnitude of force over a long contact time. With regards to sprint performance, caution must be applied when attempting to enforce this principle, as accumulating many ground contacts that are long in duration may negatively impact the time taken to reach the finish line and the goal of the

maximal sprint is to reach the finish line in the lowest possible time. The horizontal velocity of a sprinter's CM is determined by the net antero-posterior impulses generated. During the steps constituting the initial acceleration phase, the production of greater propulsive forces during mid-late stance has been found to be particularly important (Colyer et al., 2018) and is a widely recognised desirable feature for individual sprinters (Nagahara et al., 2018a). These propulsive impulse forces constitute the majority of net anteroposterior impulse produced by the athlete, where Bezodis et al. (2014) found peak propulsive forces of around  $1.3\times$  bodyweight are generated during the first stance phase. The magnitude of the peak propulsive forces have been shown to be related to mean 40 m velocity (Morin et al., 2015). Murata (2018) suggested that changes in spatiotemporal variables like step length and frequency are the product of greater propulsive impulse produced during the initial acceleration phase, as well as greater net anteroposterior impulse during the entire acceleration phase. Braking impulse is also generated during the ground contact phase and during early acceleration is primarily the result of the impact GRF generated as an athlete's foot strikes the floor (Kawamori et al., 2013). The impulse generated upon impact acts posteriorly and produces a deceleration effect, which can be a detriment to overall sprint performance. For this reason, it is advised that suppressing the work done during this braking phase is essential to achieve high sprint performance (Matsuo et al., 2019). Previous research has found that a potential strategy to achieve this is minimising horizontal foot velocities prior to touchdown (von Lieres und Wilkau et al., 2017).

Block phase performance is commonly quantified by the horizontal CM velocity at block exit, and acceleration performance is often quantified as the velocity at a given step, distance, or time. Velocity-based measures are dictated by the net propulsive impulse generated but do not account for the time taken to achieve this velocity, leading to a potentially biased interpretation of performance (Bezodis et al., 2010). As stated previously, performance with regards to propulsive impulse generation can be compromised by pushing for a longer duration, which produces high impulse but takes longer to achieve. Therefore, with regards to sprint success being dictated by the minimal time taken to reach the finish line, it is important that a sufficient change in horizontal velocity is achieved if an athlete spends more time in contact with the blocks and ground. To account for these determining factors for sprint start performance, a

measure was proposed by Bezodis et al. (2010), in the form of average external power ( $\bar{P}$ ), which is calculated based on horizontal motion (equation 2.1) given the horizontal demand of sprint running, and normalised to participant characteristics (equation 2.2)

$$\bar{P} = \frac{m(v_f^2 - v_i^2)}{2 \cdot \Delta t} \quad (2.1)$$

$$P_N = \frac{\bar{P}}{m \cdot g^{3/2} \cdot l^{1/2}} \quad (2.2)$$

where  $v_i$  and  $v_f$  are the horizontal velocities at the start and end of the period of interest, respectively,  $\Delta t$  is the duration of this period,  $m$  is the mass of the sprinter,  $g$  is the acceleration due to gravity, and  $l$  is the leg length of the sprinter. This normalised average horizontal external power (NAHEP;  $P_N$ ) provides a single measure that accounts for the change in velocity and the time taken to achieve this change (Bezodis et al., 2019). NAHEP is normalised using both mass and leg length because smaller sprinters require less power to translate their CM to the same extent as a larger sprinter, so these anthropometric factors must be accounted for to enable a fair comparison between sprinters of different stature (Bezodis et al., 2010). This measure can be quantified across any phase of interest, for example just the block phase or a specific step, the initial acceleration phase, or the entire acceleration during a sprint, while exclusively accounting for the effects of the horizontal components of the impulse generated.

#### 2.2.4 Ratio of forces

Technical sprint ability concerns the effective application of force during sprinting, which can be quantified as an athlete's ability to apply a resultant force to the ground with a more horizontal orientation. This is measured throughout the literature as the ratio of forces (RF) (Morin et al., 2011; Figure 2.4). Ratio of forces was first transferred from the cycling literature by Morin et al. (2011), drawing from the concept of force effectiveness used in pedalling mechanics (Zameziati et al., 2006; Dorel et al., 2010). Morin et al. (2011) found that force application technique, quantified using step-averaged RF (RF calculated using forces on average over a step) during acceleration,

was a determinant of 100 m sprint performance, but the magnitude of the resultant GRF ( $F_R$ ) was not. This finding has been replicated by many recent investigations into sprint technical ability (Rabita et al., 2015; Willwacher et al., 2016; Colyer et al., 2019).

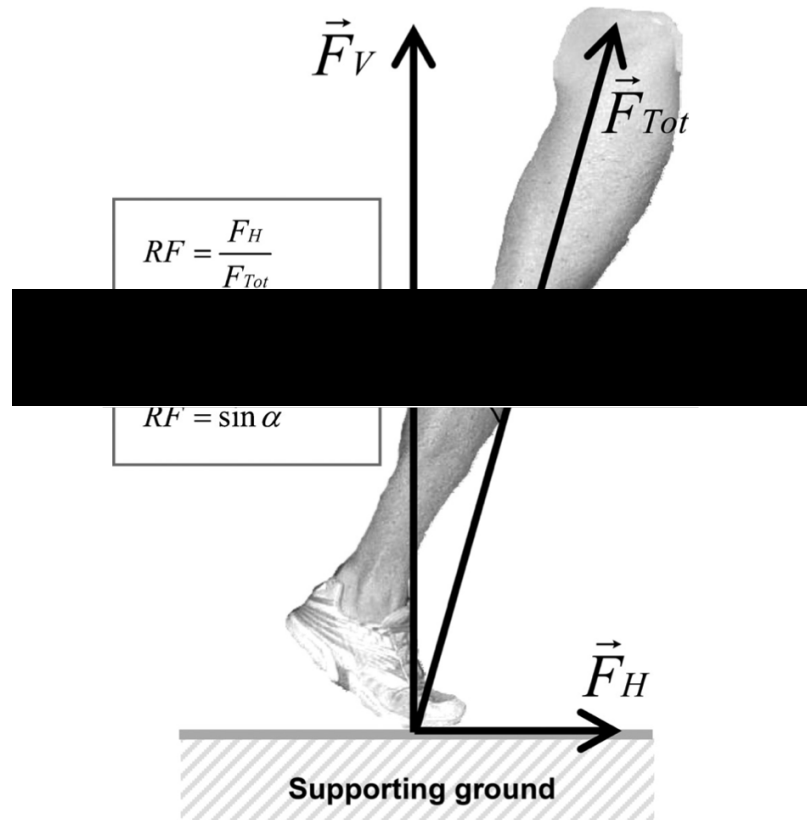


**Figure 2.4.** Schematic representation of the ratio of forces (RF) and mathematical expression as a function of the total ( $F_{Tot}$ ) and horizontal ( $F_H$ ) step averaged GRF. The forward orientation of the total GRF vector is represented by the angle  $\alpha$  (Morin et al., 2011).

An athlete's production of higher RF is reflective of a higher horizontally orientated proportion of the resultant force vector (where 100% represents entirely horizontal force and 0% entirely vertical). Using the orthogonal components of the resultant GRF ( $F_R$ , also sometimes termed  $F_{Tot}$ ), that is mean vertical ( $F_V$ ) and horizontal ( $F_H$ ) force over the total stance phase, ratio of forces can be calculated through  $F_H/F_R$  (Figure 2.4; Morin et al., 2011). Higher average ratio of forces has also been found to be a differentiating factor for sprint start and early acceleration performance (Willwacher et al., 2016; Bezodis et al., 2020). Therefore, provided sufficient  $F_R$  magnitude can be produced, sprinters should endeavour to orientate the force vector more horizontally



to improve acceleration performance (Otsuka et al., 2014; Rabita et al., 2015; Willwacher et al., 2016; Colyer et al., 2019).

Since the introduction of this measure, other RF-associated measures have been presented in the literature, including the maximum measured RF (Morin et al., 2011) or  $RF_{MEAN}$  over specific distances (Samozino, 2018) or time durations (Morin et al., 2011; Bayne, 2018). In their study that conceptualised RF, Morin et al. (2011) also aimed to quantify an athlete's capacity to maintain high RF despite increasing velocity. To quantify this, they proposed the measure 'rate of decline in RF' ( $D_{RF}$ ). This variable is obtained from a linear trendline which is fitted to step-averaged RF with respect to step-averaged horizontal velocity ( $v_H$ ), termed the RF- $v_H$  relationship. The gradient of the linear trendline is extracted as  $D_{RF}$ , where the higher the  $D_{RF}$  value (i.e., less negative; a shallower RF- $v_H$  relationship), the less RF reduces as velocity increases (Figure 2.5). The average RF over a particular period of interest or number of steps is defined as  $RF_{MEAN}$ . An additional key feature that can be obtained from the RF- $v_H$  relationship is the theoretical maximal RF at null velocity ( $RF_0$ ; Rabita et al., 2015). This measure is extracted as the y-intercept of the linear trendline (Figure 2.5). Although this theoretical value is not directly obtained from the force output, it gives another valuable representation of an athlete's RF capacity.

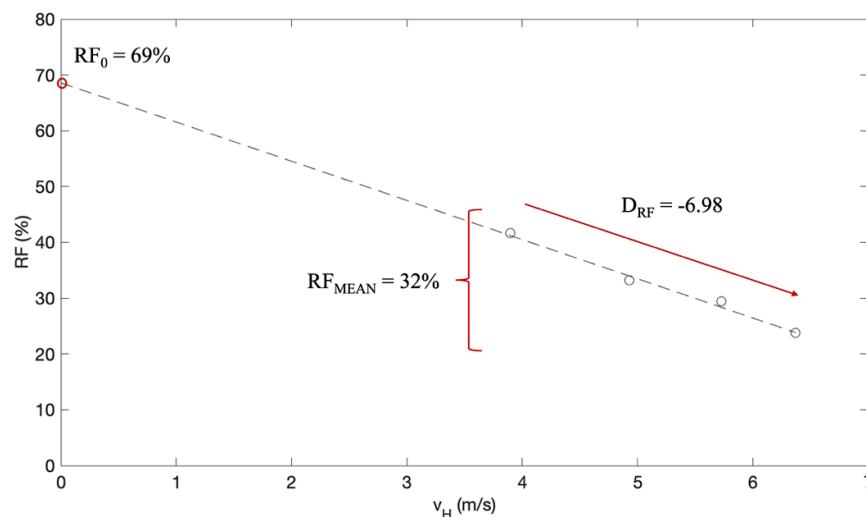


**Figure 2.5.** Representation of the ratio of forces-horizontal velocity (RF- $v_H$ ) relationship over the initial acceleration phase (black o denote measured values during steps 1 to 4), featuring annotated RF-derived measures including  $D_{RF}$  (the gradient of the linear trendline),  $RF_0$  (red o; y-intercept at  $v_H = 0$ ) and mean step-averaged RF ( $RF_{MEAN}$ ) over the initial acceleration phase (steps 1 to 4).

As both  $D_{RF}$  and  $RF_0$  are components of the linear trendline fitted to the  $RF-v_H$  relationship, they are both contributing factors to the  $RF_{MEAN}$  measure. Since  $RF_{MEAN}$  is influenced by its peak and rate of decrease, sprinters must achieve both a high  $RF_0$  and a low  $D_{RF}$  to obtain a higher  $RF_{MEAN}$  throughout a given period of acceleration (Bayne, 2018).

Many recent studies have obtained the aforementioned  $RF$ -associated measures based on a simple macroscopic model, introduced by Samozino et al. (2016). This model is based on a mono-exponential fit to the horizontal velocity-time ( $v_H-t$ ) profile over the entire acceleration phase which is well established throughout the literature (Figure 2.6).

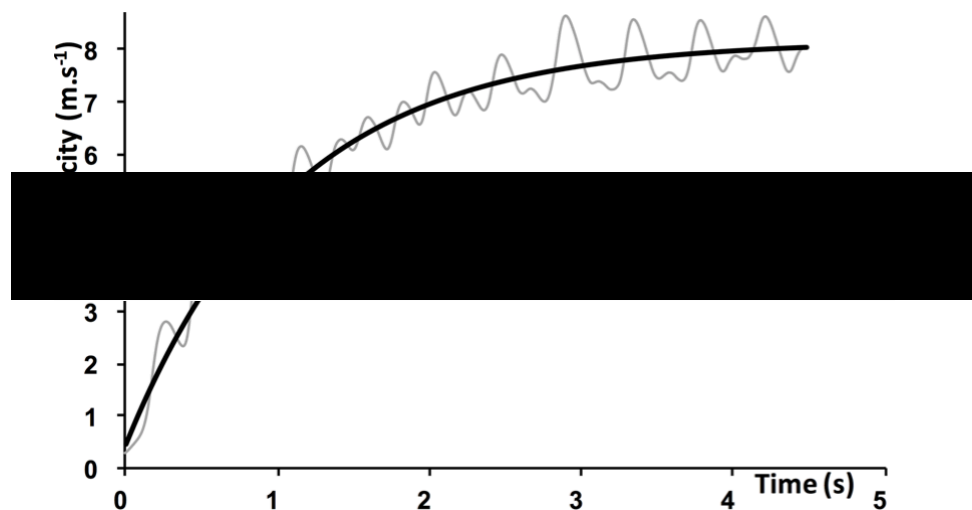


**Figure 2.6.** Representation of measured horizontal velocity-time ( $v_H$ -time, measured using a portable resistance device) (grey) compared to a mono-exponential fit to the  $v_H$ -time profile (black) typically observed over a maximal sprint (Cross et al., 2018).

This mono-exponential fit follows the function presented in equation 2.3:

$$v_H(t) = v_{H_{max}} \cdot (1 - e^{-t/\tau}) \quad (2.3)$$

where  $v_{H_{max}}$  is the maximal velocity reached at the end of the acceleration and  $\tau$  is the acceleration time constant. The horizontal acceleration of the CM ( $a_H$ ) can be expressed after derivation of  $v_H(t)$  over time (equation 2.4).

$$a_H(t) = \left(\frac{v_{max}}{\tau}\right) \cdot e^{-\frac{t}{\tau}} \quad (2.4)$$

From this acceleration profile, the net horizontal antero-posterior GRF ( $F_H$ ) applied to the body CM can be modelled over time, by applying the fundamental laws of dynamics in the horizontal direction (equation 2.5).

$$F_H(t) = m \cdot a_H(t) + F_{aero}(t) \quad (2.5)$$

where  $m$  is the runner's body mass (in kg) and  $F_{aero}(t)$  is the aerodynamic drag. Using modelled step-averaged  $F_H$  and step-averaged  $F_V$  (assumed as the bodyweight of the sprinter), modelled step-averaged  $F_R$  can be calculated using Pythagoras' theorem, and hence, modelled step-averaged RF can be determined. The model provides a useful and accurate approximation of many other performance measures (Figure 2.7) to researchers who lack the instruments required to measure ground reaction forces or those collecting data in a competition environment.

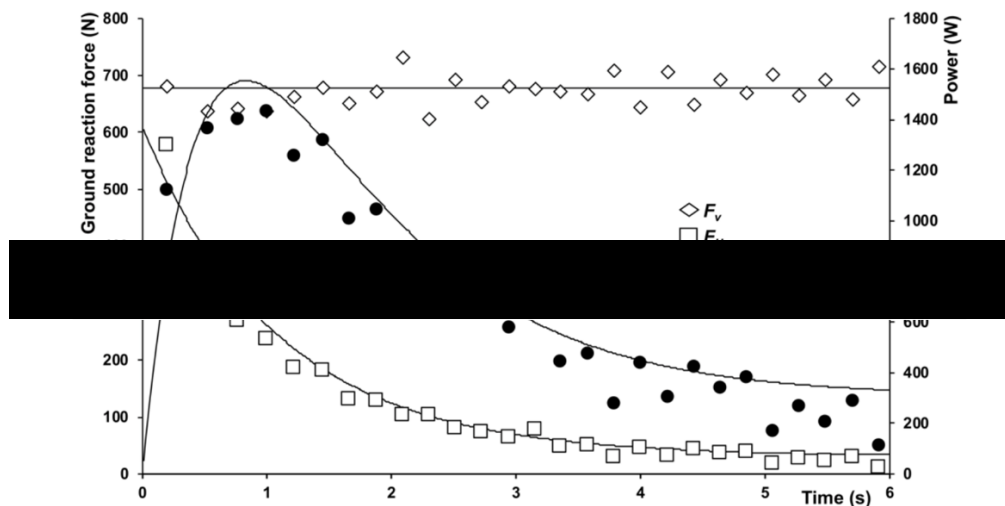


**Figure 2.7.** Comparison between force plate-derived measures of vertical GRF ( $F_V$ ), horizontal GRF ( $F_H$ ) and horizontal power ( $P_H$ ) and those derived from the Samozino et al. (2016) simple macroscopic model (Morin et al., 2019).

The simple model provides an additional RF-associated measure of sprint technical ability,  $RF_{MAX}$ . This represents the RF value at 0.3 s based on a linear fit to modelled  $RF-v_H$  from 0.3 s onwards. Although similar to the theoretical  $RF_0$  measure

(Figure 2.5),  $RF_{MAX}$  is a direct measure extracted from a model fitted to the  $v_H$ -time profile across an entire phase of the sprint effort, hence it could be considered a quasi-direct measure of an athlete's maximum RF capacity. Its more direct nature than  $RF_0$  could explain why  $RF_{MAX}$  was recently found to be nearly perfectly correlated ( $r = 0.94$ ) with early acceleration performance, quantified through NAHEP, while  $RF_0$  showed a large correlation ( $r = 0.59$ ) (Bezodis et al., 2020).

The simple macroscopic model has been criticised due to the simplicity of the underlying  $v_H$ -time model (Haugen et al., 2019), the estimation of  $RF_{MAX}$  at low speeds where deviations are observed in the supposedly linear RF- $v_H$  relationship, and the lack of consideration for within-step kinetics (Pavei et al., 2019). However, Bezodis et al. (2020) investigated the relationships between modelled RF and RF-associated measures (i.e.,  $RF_0$ ,  $D_{RF}$ ) with those from direct GRF measurement. They found that RF- $v_H$  parameters calculated from the simple model aligned well with values calculated directly from the GRF measured by the force plates. The findings by Bezodis et al. (2020) extended the findings by Morin et al. (2019) to include RF and its associated measures, alongside the previously explored measures of vertical and horizontal GRF, and horizontal power. However, Bezodis et al. (2020) importantly noted that the data from which the simple model was fitted was obtained using a 'gold standard' force platform system, hence less sophisticated and accurate measurement tools may not hold the same predictive capabilities. As the current thesis will investigate the first steps on the track constituting the initial acceleration phase, and there have been concerns about measures derived from the model at low speeds (Pavei et al., 2019), this thesis will present RF measures calculated from direct measurement of ground reaction forces on a 'gold standard' force plate system.

In their recent study, Bezodis et al. (2021) addressed discrepancies existing in the current body of literature surrounding the methods used for calculation of RF from measured external force data. Although many studies report step-averaged RF, some have achieved this value from calculating instantaneous RF (at each frame sampled) before calculating the average across a given stance phase (Rabita et al., 2015), while others have averaged antero-posterior and resultant forces across the step before calculating RF (Morin et al., 2011; 2012) or calculated the ratio between the step-averaged antero-posterior component and the resultant of the step-averaged antero-

posterior and vertical components (Samozino et al., 2016; Morin et al., 2019). Although each of the methods are similar in theory, the difference in computation of each approach yields a different value for  $RF_{MEAN}$  and their mechanical reality differs considerably. This can consequently lead to different interpretations of an athlete's 'technical ability' if one approach is not widely adopted, or the method is not explicitly detailed by each author. As detailed by Bezodis et al. (2021), there are evident computational differences between approaches. When taking an average of forces over an entire step including flight phase, before calculating RF, a more true representation of the RF- $v_H$  profile is obtained, as long as mean  $F_R$  for each step is determined directly from the instantaneous resultant forces and not the step-averaged horizontal and vertical components. In contrast, using instantaneous RF values to obtain step-averaged RF can bias the determined values because instantaneous RF can reach high values during late stance where forces are relatively low (Bezodis et al., 2021). Bezodis et al., (2021) observed that this effect on the RF- $v_H$  relationship became more pronounced as acceleration phase progressed. Given these considerations, it was suggested that future research should use force data averaged across the step before calculating RF to provide a more appropriate assessment of 'mechanical effectiveness'.

In the preprint to their 2021 study, Bezodis et al. (2020) created RF- $v_H$  profiles using data from the entire acceleration phase. Although it was not their primary focus, Bezodis et al. (2020) highlighted a concern about the step-to-step variation in the RF- $v_H$  relationship that could be observed during the first four steps (i.e., the initial acceleration phase), which was often apparently non-linear and also did not align with the linear trendline fitted to the entire acceleration phase. This suggests that there may not always be a strong linear fit to the RF- $v_H$  relationship during the initial acceleration phase. It is unknown whether differences in the 'linearity' of the profile, particularly during initial acceleration, is a differentiating factor between sprinters and/or is related to acceleration performance. Therefore, future research must consider this potential issue before using RF-derived measures to understand early acceleration technique and performance.

## **2.3 Relationships between kinematic characteristics and ratio of forces**

Sprint running literature suggests that greater acceleration is accompanied by a forward-leaning posture (Kugler & Janshen, 2010; Van Caekenberghe et al., 2013; Bezodis et al., 2015b; Nagahara et al., 2018b). Although acceleration performance also shows strong relationships with effective force application (i.e., RF), there is a lack of literature detailing the interaction of RF with specific kinematic characteristics. Presently, only two studies have tried to investigate the link between kinematic characteristics and RF, and their influence on sprint performance (Bezodis et al., 2017; Nagahara et al., 2019b). Both studies attempted to manipulate RF capability by modifying an athlete's kinematics. In both investigations, the researchers did not find that any intentional changes to kinematics resulted in improved RF or overall acceleration performance. However, it should be noted that the study by Nagahara et al. (2019b) did not collect motion capture data and, while Bezodis et al. (2017) did present this data, it was confined to the stance phase which contacted closest to the 5 m mark, limiting the conclusions that can be drawn for performance over the initial acceleration phase. Therefore, while the findings of both investigations are not directly relevant to the current aim and research questions, aspects of these studies can be used to inform the rationale and theory behind, and the methodology of, the current thesis.

This section will explore the aforementioned investigations by Bezodis et al. (2017) and Nagahara et al. (2019b), explaining their methodology and conclusions with respect to the interaction between kinematic characteristics and RF. Following this, kinematic characteristics identified throughout the literature that could contribute to achieving greater technical performance but have yet to be investigated in relation to this, will be described.

### **2.3.1 Investigations linking kinematics and RF**

The first known study to investigate the relationship between kinematics and RF was undertaken by Bezodis et al. (2017). Their study used a cohort of team sports athletes and attempted to enhance RF capability through internal and external forms of verbal

cueing, e.g., instructed to focus on ‘pulling the leg backwards’ or ‘clawing the ground backwards’ at touchdown for internal and external focus instructions, respectively. The use of these manipulative cues resulted in decreased RF in the step nearest 5 m and in overall acceleration performance (assessed through 10 m sprint time), when compared to a control condition. These findings suggest that acute technical changes can affect RF capability, but that they caused a detrimental effect to both RF and performance. Nagahara et al. (2019b) used a cohort of physically active adults who were instructed to lean the whole body forward, attempting to increase the production of propulsive force. Nagahara et al. (2019b) found no change in performance variables (i.e., running speed and net antero-posterior impulse) with this intent, only increased step frequency in the first two steps, which was attributed to decreases in contact time and flight time. Nagahara et al. (2019b) suggested these changes were due to a notable decrease in vertical and braking impulse, without an increase in propulsive horizontal impulse.

The findings by Nagahara et al. (2019b) support previous research by Kugler and Janshen (2010), who found smaller vertical force and higher horizontal propulsive forces were associated with a greater forward lean of the whole-body during acceleration. Kugler and Janshen (2010) also used a relatively untrained population; 28 male and 13 female physical education students. Although not observed in the population used by Nagahara et al. (2019b), the findings by Kugler and Janshen suggest that higher propulsive forces can be associated with forward lean. Within a more highly and/or sprint trained population (i.e., those more capable of producing higher propulsive force), there may be positive relationships between these kinematics associated with forward lean (e.g., whole body orientation, smaller contact and flight times, higher step frequency) and more propulsive and horizontally orientated force (i.e., RF). However, before attempting to design any interventions, future research needs to better understand the relationships between RF and kinematic characteristics during early acceleration, and for the purposes of specificity, this is particularly required from a population of trained sprinters.

### 2.3.2 Kinematics and horizontal force

Although the relationship between kinematics and RF has not been directly considered, there is a considerable body of literature detailing the relationships between linear and angular kinematic characteristics, GRF output and performance. With regards to linear kinematics, the interaction between the CM and the contact foot during the stance phase may help to elucidate its relationship with RF. For example, it was first determined by Jacobs and van Ingen Schenau (1992) that highly trained sprinters delay the extension of their CM away from the base of support (BoS) until the CM had been rotated further forwards (Figure 2.8; Figure 2.9).

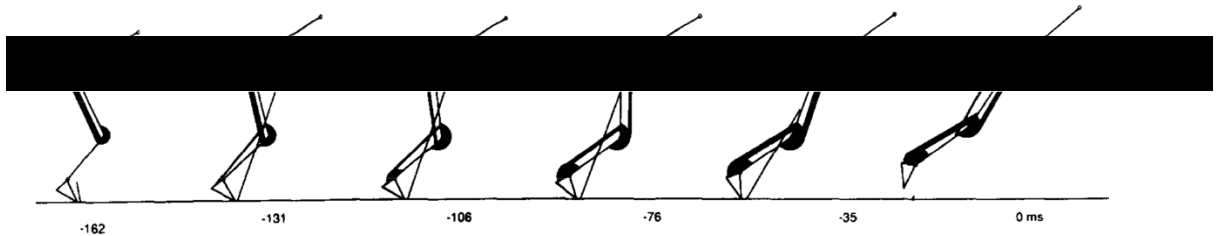


**Figure 2.8.** Stick figure showing the positions of the trunk and stance leg, together with the actions of the muscles at different time samples. Time is expressed relative to the instant of toe-off (Jacobs and van Ingen Schenau, 1992).

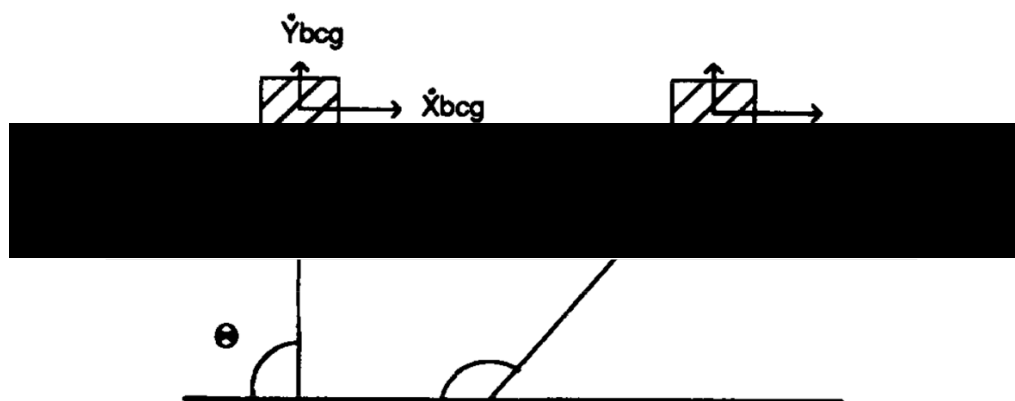


**Figure 2.9.** Schematic representation from Jacobs and van Ingen Schenau (1992; p. 954), depicting two positions during an early stance phase, based on a simple model of a sprinter illustrated by a heavy mass (box) and a simplified leg (l), which can rotate and extend. The angle ( $\theta$ ) in the bottom-left corner is 90 degrees and increases during stance.  $\dot{X}_{bcg}$  and  $\dot{Y}_{bcg}$  denote the horizontal and vertical velocity of the CM (here termed body centre of gravity (bcg)), respectively, where extension and rotation of the system combine to influence the change in these velocities (Jacobs & van Ingen Schenau, 1992).



This creates a more forward leaning posture, and the subsequent leg extension has a greater horizontal component. The movement strategy described by Jacobs and van Ingen Schenau (1992) therefore depicts the action of the sprinter which could facilitate a greater toe-off distance.

Kugler and Janshen (2010) also later found that performers who were able to achieve greater acceleration demonstrated more negative touchdown distance. The finding by Kugler and Janshen (2010) was investigated further using a computer simulation by Bezodis et al. (2015b), who found that placing the foot further back behind the CM at touchdown led to a near linear increase in RF during the stance phase, supporting the findings of Kugler and Janshen (2010). It has been suggested that attempting to utilise both previously mentioned movement strategies (i.e., Jacobs & van Ingen Schenau (1992) and Bezodis et al. (2015b)) by rotating the CM rapidly at touchdown (relative to the stance foot) with the stance foot further behind the CM, could exaggerate RF capability even further (Bezodis et al., 2017). However, adopting the strategy described by Kugler and Janshen (2010) with a larger negative touchdown distance (i.e., stance foot further behind the CM) may prove more beneficial for performance than that described by Jacobs and van Ingen Schenau (1992), as less time is needed to anteriorly translate the CM ahead of the stance foot before extension can occur. Theoretically, this strategy would be favourable for sprint performance where horizontal displacement in the shortest time possible is the ultimate goal. All of the above evidence suggests the placement of the stance foot in relation to the CM at touchdown, and the action during stance to translate the CM into a favourable toe-off position, are potentially important features relating to RF. However, it is important to note that previous research reporting touchdown distance have either not reported the stance leg joint kinematics and investigated a non-sprint trained population (Kugler & Janshen, 2010), or theoretically manipulated specific joint kinematics using computer simulation to achieve changes in touchdown distance (Bezodis et al., 2015b). As the stance leg is multi-segmented, changes in the position of the stance foot relative to the position of the CM at touchdown, will likely largely be due to the configuration and orientation of the joints and segments within the stance leg. The relationships between touchdown distance, stance leg joint and segment kinematics, and RF, are therefore fundamental for future research to understand, and the associations of these with initial acceleration performance should also ultimately be considered.

With regards to these stance leg joint configurations, Bezodis et al. (2017) found that sprinters who demonstrated higher RF had a more dorsiflexed ankle, a more flexed knee and higher hip extension velocity at touchdown. In their study, Bezodis et al, (2017) found that the largest between condition effects occurred at the ankle joint. This was in line with the findings of a systematic review by Napier et al. (2015), who found that ankle kinematics are altered to a greater extent than the more proximal joints in studies designed to achieve technical changes in foot strike. Bezodis et al. (2017) suggested that it is possible that greater ankle dorsiflexion and/or knee flexion at touchdown may help to acutely increase RF. Such kinematics could affect this change either due to geometric differences simply affecting the orientation of the resultant force or factors such as muscle-tendon unit lengths differing and thus affecting the force output of different muscle groups. They concluded that the specific joint configurations of the stance leg may be more important than the distance of the leg from the CM at touchdown, and that this could be assessed in a cross-sectional, experimental, or theoretical investigation, something which has yet to occur.

## **2.4 Chapter summary**

This literature review introduced biomechanical research of the maximal sprint, before exploring more deeply into the biomechanics of the initial acceleration phase to develop understanding of the principles that underpin effective sprint acceleration performance. The importance of achieving high RF has been clearly demonstrated by previous research (Morin et al., 2011; Rabita et al., 2015; Bezodis et al., 2020). However, many studies have analysed RF-associated measures (i.e.,  $RF_{MEAN}$ ,  $D_{RF}$ ,  $RF_0$ ) from RF- $v_H$  profiles created over the entire acceleration phase, without considering the potential performance implications of the large step-to-step variation in RF that can be observed during the initial acceleration phase. Previous investigations attempting to understand the kinematic characteristics that may be associated with RF capability have thus far done so by implementing acute technical changes in kinematics to attempt to enhance RF, ultimately finding either no improvement or a reduction in RF (Bezodis et al., 2017; Nagahara et al., 2019b). This

literature review explored a number of studies that have demonstrated the relationships between linear and angular kinematics (i.e., whole-body CM position, stance leg configurations) with the production of higher propulsive antero-posterior impulse forces or sprint performance (Jacobs & van Ingen Schenau, 1992; Kugler & Janshen, 2010; Bezodis et al., 2015b). However, previous research has yet to observe the relationships between such kinematics and an athlete's ability to generate high RF during sprint acceleration and using a sprint trained population.

## **CHAPTER 3: METHODS**

### **3.1 Participants**

Fourteen male sprinters (mean  $\pm$  SD; age:  $19 \pm 1$  years, height:  $1.74 \pm 0.66$  m, leg length:  $88.9 \pm 5.1$  cm, mass:  $68.3 \pm 4.9$  kg, 100 m personal best time:  $11.15 \pm 0.33$  s) were provided with full study details and gave written informed consent to participate. Prior to data collection, the study was approved by the research ethics committee of the National Institute of Fitness and Sports in Kanoya. At the time of data collection, all participants were healthy and injury-free.

### **3.2 Experimental protocol**

Participants completed their preferred self-led warm-up routine. After setting the starting blocks to their preference, two maximal sprint efforts were performed up to 60 m, wearing spiked shoes. Participants were provided with a rest period of at least 10 minutes between sprint efforts. The data was collected from five sessions over a total period of 10 days, with temperature and atmospheric pressure (mean  $\pm$  SD) of  $31.3 \pm 0.9^{\circ}\text{C}$  and  $1010 \pm 2$  kPa, respectively.

### **3.3 Data collection**

Three-dimensional kinematic data was captured through 16 cameras (Kestrel 4200, Motion Analysis Corporation, California, USA) recording at 250 Hz and positioned to capture data up to the end of the fourth step of a maximal sprint effort. A total of 47 retro-reflective markers were placed on each participant using the marker model of Suzuki et al. (2014; Figure 3.1).

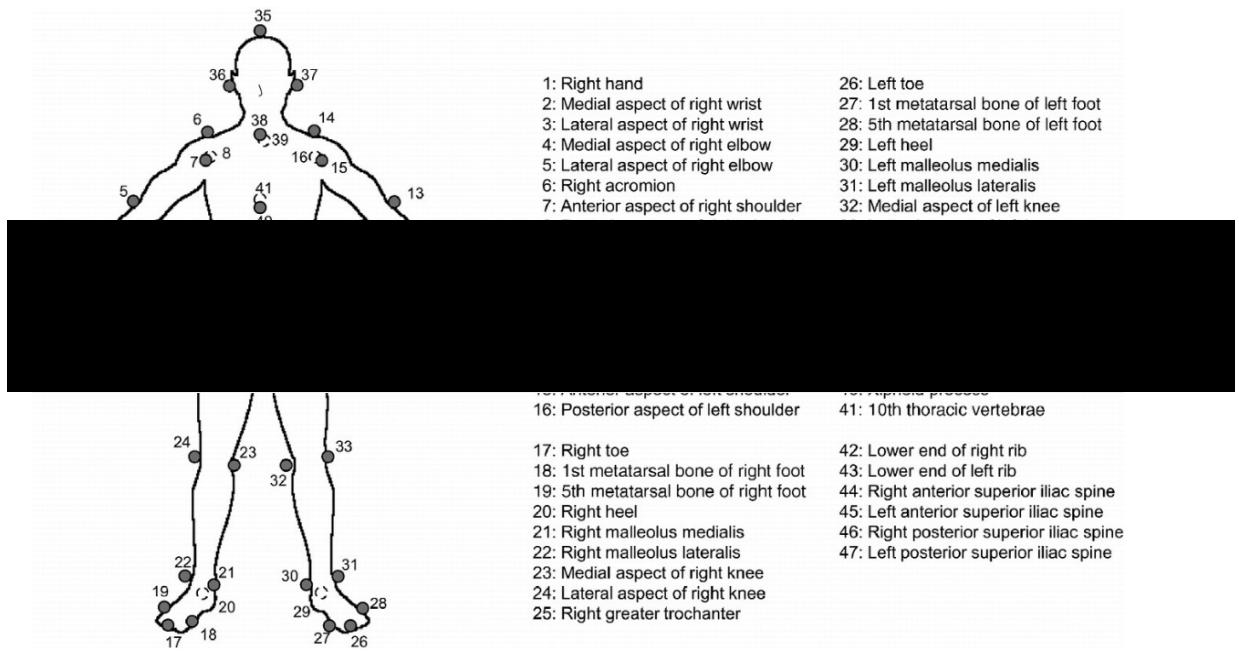


**Figure 3.1.** Locations of 47 retro-reflective markers affixed to each participants body (from Suzuki et al., 2014, p.146).

Ground reaction force (GRF) data was collected from force plates (TF-3055, TF-32120, TF-90100, Tec Gihan, Uji, Japan) mounted in series under the indoor athletics track (Figure 3.2). Force plates under the starting blocks and sequentially along the track formed a total capture volume of  $\sim 52 \text{ m} \times 1 \text{ m}$ . GRF data was collected at a sampling frequency of 1000 Hz.

An electric starting gun was used to synchronously initiate the GRF data collection, emit an auditory starting signal for the participants, and provide a spike in an analogue signal in the kinematic data stream. During data collection, the kinematic data capture was started prior to the starting signal. As the electronic starting gun was responsible for both the initiation of GRF data collection and the starting signal, the length of kinetic data captured was less than kinematic data, and the two datasets were synchronised during post-processing (see section 3.3). All data was recorded, and then later processed, in MATLAB (R2021a, Natick, USA) using custom written scripts.

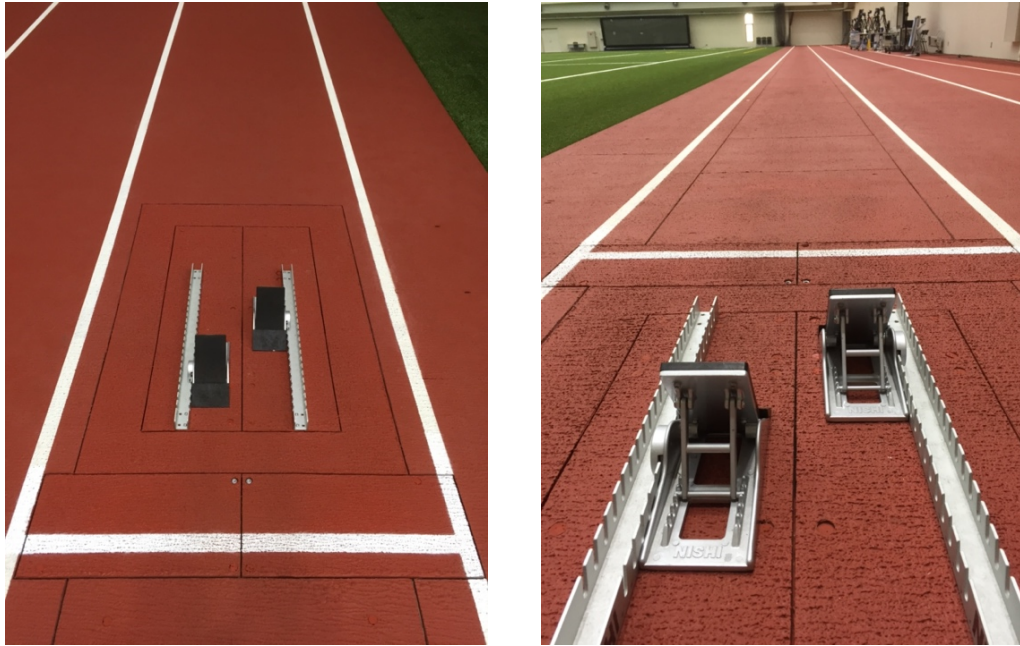


**Figure 3.2.** Kinetic data capture experimental set-up with force plates mounted under the starting blocks (left) and in series for approximately 50 m along the indoor track (right).

### 3.4 Data processing

#### 3.4.1 Kinematic data

Kinematic data was up sampled from 250 Hz to 1000 Hz using an interpolating cubic spline function to match the sampling frequency of kinetic data. This allowed the frames defining each stance phase (i.e., touchdown and toe-off) to be exactly matched between both data sets. The spike in the kinematic data stream caused by firing of the starting gun was used to synchronise the two datasets. Following synchronisation, kinematic data prior to the starting signal was discarded so both datasets were the same length.

Three-dimensional marker coordinates were exported to Visual3D (v6, C-Motion, Maryland, USA), where they were smoothed using a fourth order zero-lag low-pass Butterworth filter with a cut-off frequency of 14 Hz which was selected using residual analysis (Winter, 2009). A residual analysis was conducted on four markers (toe, lateral ankle, lateral knee & hip markers of the stance leg) for three randomly selected participants, with the average value then taken as the cut-off frequency for all markers (for full details of the residual analysis, refer to appendix A). A 15-segment body

model was created, consisting of hands, forearms, upper arms, feet, shanks, thighs, head, upper trunk, and lower trunk, in accordance with the data collection procedures of Nagahara et al. (2014b) and as used in other previous studies (Suzuki et al., 2014; Nagahara et al., 2017). The 15-segment model was applied to the mean marker positions during the first fifty frames of data, while each participant was stationary in the blocks (Figure 3.3) and then reconstructed from the marker trajectories during each sprinting trial using a six degrees of freedom approach for each segment.

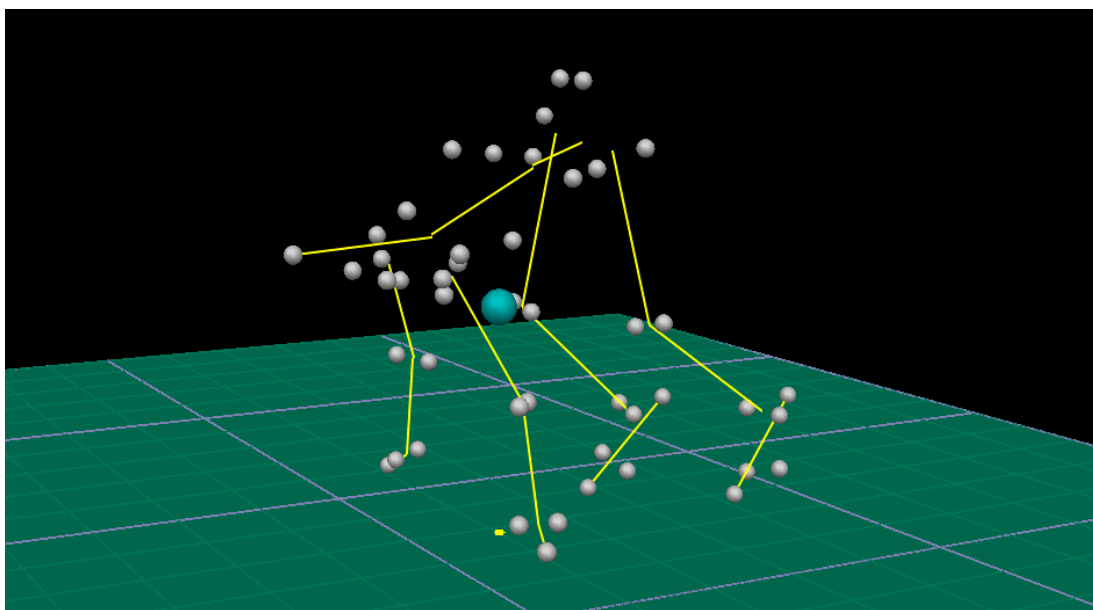


**Figure 3.3.** Marker positions (grey spheres) creating the 15-segment model (yellow lines) with whole-body CM location (large turquoise sphere) based on data while stationary in the blocks, generated in Visual3D.

The hip joint centre location was determined using the method recommended by the Japan Clinical Gait Analysis Forum as this was the most suitable for Japanese individuals. This method defined the hip joint centre for each leg as the point located 18% of the medial distance between the right and left great trochanters from the point located at one-third of the distance from each greater trochanter to the respective anterior superior iliac spine. The midpoint of the two hip joint centres was taken as the distal end point of the lower trunk and each hip joint centre gave the proximal endpoint of the thigh. The position of the whole-body CM was calculated according to the

15-segment body model, using the segmental inertia parameters of Japanese athletes (Ae et al., 1992), with the typical mass of a running shoe (200 g) added to each foot (Hunter et al., 2004).

**Table 3.1.** Proximal and distal segment endpoint locations used for definition of the 15-segment body model.

<b>Segment</b>	<b>Proximal endpoint</b>	<b>Distal endpoint</b>
Head	Suprasternal notch	Vertex <sup>^</sup>
Upper trunk	Lowest point of ribs	Suprasternal notch
Lower trunk	Lowest point of ribs	Hips
Upper arm	Shoulder	Humeral epicondyle
Lower arm	Humeral epicondyle	Ulna styloid process
Hand	Ulna styloid process	Third dorsal metacarpal head <sup>^</sup>
Thigh	Hip joint centre <sup>^</sup>	Femoral condyle
Shank	Femoral condyle	Malleolus
Foot	Posterior aspect of calcaneus <sup>^</sup>	Toes <sup>^</sup>

<sup>^</sup> denotes the use of a single endpoint marker. All other endpoints were calculated as the midpoint of lateral and medial markers at the location, except suprasternal notch which used the midpoint of the anterior and posterior markers.

### 3.4.2 Kinetic data

To define the instant of movement onset, the raw vertical GRF signal during the block phase was first visually checked to identify an initial period while each participant was clearly stationary in the blocks (i.e., no considerable fluctuation in the signal), and a mean value over this period was calculated. Movement onset was then defined as the instant at which the raw vertical GRF signal exceeded, and remained, two standard deviations above the mean signal from the clear stationary period, in accordance with previous research (Bezodis et al., 2020). A 50 N threshold in raw vertical GRF data was used to define contact with the track or blocks. This enabled the detection of block exit, followed by the touchdown and toe-off events of each stance phase. Following the definition of stance events using raw signals, each component of the raw GRF data was smoothed using a 4<sup>th</sup> order zero-lag low-pass Butterworth filter with a cut-off frequency of 50 Hz, in accordance with previous research (Nagahara et al., 2017; 2018).



To calculate horizontal velocity ( $v_H$ ) over each sprint effort, the filtered anteroposterior GRF was divided by body mass, integrated (using the trapezium rule), and adjusted for the influence of aerodynamic drag force (Colyer et al., 2018; Samozino et al., 2016). Following the procedures of Arsac and Locatelli (2002), aerodynamic drag force ( $F_{air}$ ) during each trial was estimated using the athlete's height and mass, along with the aerodynamic friction coefficient as follows:

$$F_{air} = k \cdot (v_H)^2 \quad (3.1)$$

where  $v_H$  represents horizontal velocity and  $k$  is the athlete's aerodynamic friction coefficient, which was estimated using values of air density ( $\rho$ , in  $\text{kg/m}^3$ ), frontal area of the athlete ( $Af$ , in  $\text{m}^2$ ) and drag coefficient ( $Cd = 0.9$ ; van Ingen Schenau et al., 1991):

$$k = 0.5 \cdot \rho \cdot Af \cdot Cd \quad (3.2)$$

with

$$\rho = \rho_0 \cdot \frac{Pb}{760} \cdot \frac{273}{273+T^\circ} \quad (3.3)$$

$$Af = (0.2025 \cdot h^{0.725} \cdot m^{0.425}) \cdot 0.266 \quad (3.4)$$

where  $\rho_0 = 1.293 \text{ kg/m}^3$  representing the  $\rho$  at 760 Torr and 273°K,  $Pb$  was the measured barometric pressure (in Torr),  $T^\circ$  was the measured air temperature (in °C),  $m$  was the athlete's body mass (in kg), and  $h$  was the athlete's height (in m). Wind speed was not included as the data was collected indoors.

Horizontal velocity was integrated (using the trapezium rule) with respect to time to calculate horizontal displacement of the CM. This CM displacement was visually inspected and compared to the anteroposterior centre of pressure (CoP) data measured by the force plates (e.g., Figure 3.4) to qualitatively assess the GRF data quality including the assumption of a stationary position in the blocks, and the adjustment made to account for aerodynamic drag effects. For valid trials, the CM and CoP displacement were deemed to be closely aligned, providing confidence in the above data processing used to determine  $v_H$ . However, two trials were deemed invalid as the

athlete was not stationary prior to movement onset, causing the CM displacement and CoP to not align correctly (see section 3.5.2).

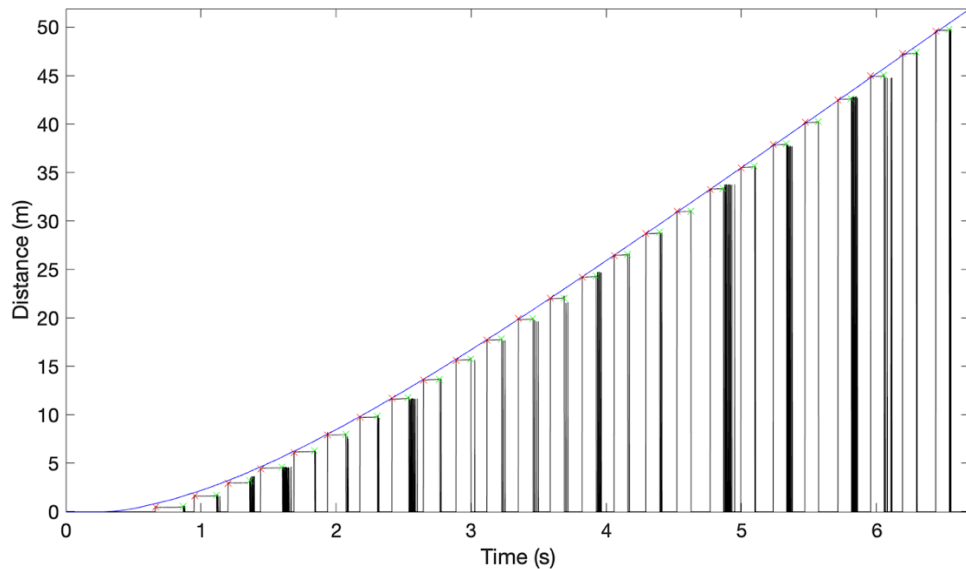


**Figure 3.4.** Centre of mass displacement as determined from integration of the antero-posterior GRF data after accounting for the effects of drag (blue) and anteroposterior centre of pressure data (black) with respect to time. Red crosses represent touchdown and green crosses represent toe-off (based on the 50 N threshold used for the raw vertical GRF data). These data are for a single trial of participant 4 and are used for illustrative purposes only. Note: The centre of pressure data return to  $\sim 0$  during each flight phase and are thus only of interest during each stance phase. Following toe-off from a number stance phases, the figure appears to show black bars – these depict noise in the centre of pressure data during the flight phase.

## 3.5 Data Analysis

### 3.5.1 Spatiotemporal variables

Contact time and flight time for each of the first four steps were calculated from touchdown and toe-off timings, defined using a 50 N threshold with the raw vertical GRF data as described above. As this analysis focussed on the initial acceleration phase, the first flight after block exit was not included (i.e., can be considered flight 0). Therefore, each flight phase followed the prior contact phase, e.g., flight 1 followed the first contact on the track. Step time was then calculated as the sum of contact time and flight time, and the inverse of total step time was calculated to determine step frequency ( $\text{steps}\cdot\text{s}^{-1}$ ). Step length was determined from the anteroposterior CoP data,

where values were extracted from the instant of mid-stance. The difference in anteroposterior CoP calculated between each stance phase provided step length (m).

Horizontal displacement and velocity of the whole-body CM were extracted at each touchdown and toe-off event alongside vertical displacement of the CM at each of these events. Horizontal displacement was defined relative to the participants' stationary block phase CM position and vertical displacement was defined relative to the track.

### **3.5.2 Kinematic variables**

Joint angles were calculated for the ankle, knee, and hip joints based on the respective adjacent segments. Flexion-extension angles (x-axis) were extracted, with extension/plantar flexion defined as positive (Figure 3.6). Ankle angle was measured as the angle between the shank segment and a rearfoot segment, which was defined from the ankle joint centre to the metatarsophalangeal (MTP) joint centre (i.e., defined as the midpoint between the first and fifth metatarsals). Angular velocities for each joint were defined as the vector describing the relative angular velocity of the distal segment relative to the proximal segment; using the proximal segment as the resolution coordinate system to define the direction of change in joint angle.

For one participant, kinematic data ended prior to the end of step four during their first trial, so the data could not be used from this trial to calculate the kinematic variables across all four steps. For this participant's second trial, the kinematic data ended at the frame of toe-off for step four. To allow the inclusion of this participant in the analysis, angular velocities of joints and segments at toe-off for step four were calculated by linear extrapolation from the three prior angular velocity values to the next (touchdown) frame. Two other trials from different sprinters also could not be used for analyses because the participant was not stationary prior to movement onset, as confirmed by the analysis described above (section 3.4.2; Figure 3.4), or markers were lost during the trial. These trials were therefore removed from any subsequent analysis and the other trial for each participant was used (only one trial was used for each of the 14 participants in the final analysis based on their highest NAHEP value – see end of section 3.5).

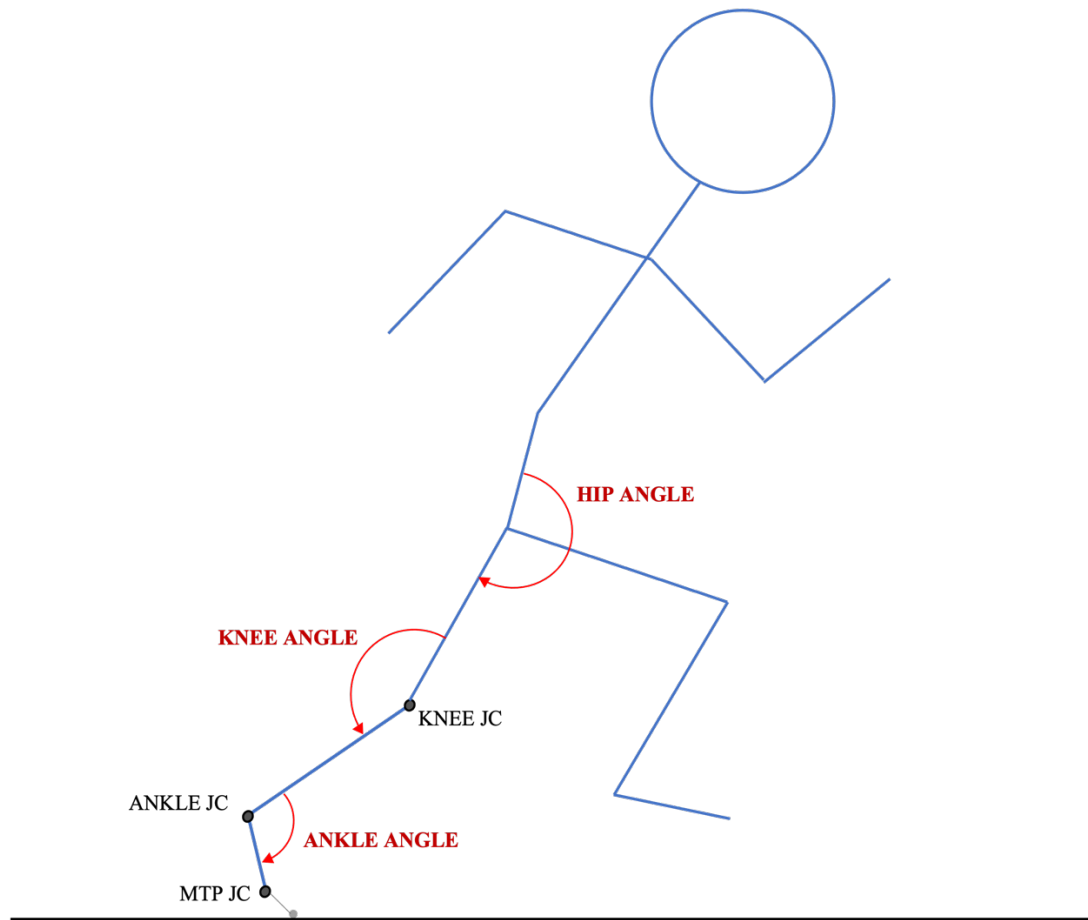


**Figure 3.5.** Joint angle conventions for three stance leg joints; ankle, knee, and hip. JC denotes joint centre. Extension/plantar flexion were defined as positive.

Absolute segment angles were also calculated for the foot, shank, thigh, and trunk. These were reconstructed in six degrees of freedom for each segment and were expressed relative to the global coordinate system – segment orientations about the global medio-lateral (X) axis were extracted, with  $0^\circ$  representing a horizontally oriented segment and positive rotation representing an anti-clockwise rotation of the proximal end about the distal end (Figure 3.7). For these absolute segment angles, the foot was modelled as a single rigid segment from the toe marker to the heel marker to give a closer representation of the whole foot orientation (as described previously, the rearfoot segment – i.e., ankle to MTP – was used when determining ankle angle to provide a more accurate representation of the true ankle joint angle). The trunk angle was defined using the upper trunk segment orientation, to give a closer representation of upper body orientation.

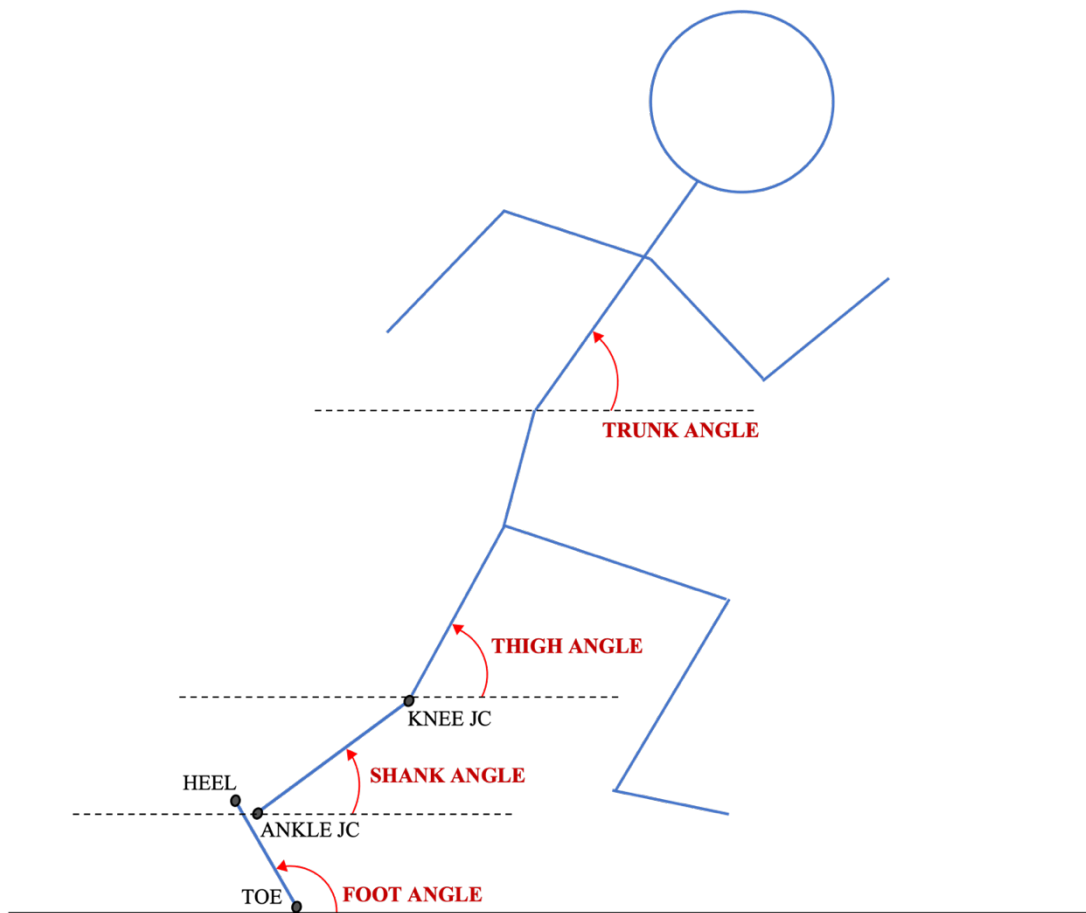


**Figure 3.6.** Segment angle conventions for four segments; foot, shank, thigh, and trunk. JC denotes joint centre. Conventions for the positive direction are displayed on the stance leg, following the conventions of Nagahara et al. (2014a).

Linear foot velocity was defined as the distal endpoint velocity of the foot segment with reference to the global coordinate system, and the anteroposterior component at the instant of touchdown for each step was defined as foot touchdown velocity. The anteroposterior displacement between each toe marker and the whole-body CM was calculated and was extracted at touchdown and toe-off to define touchdown distance and toe-off distance, respectively, for each step. Touchdown and toe-off distances, CM height and step length were normalised to account for differences in leg length between sprinters by dividing each by the individual's greater trochanter height.

Continuous joint and segment angular kinematics were plotted with respect to time from touchdown to toe-off for steps one to four from all fourteen sprinters to visually assess movement patterns across the cohort. Discrete angular kinematics (e.g., angles

at touchdown and toe-off, peak, minimum, range of motion) were then extracted from these continuous data.

### 3.5.3 Kinetic variables

Step-averaged data from each of the first four stance phases were determined from the resultant GRF ( $F_R$ ) and its vertical ( $F_V$ ) and antero-posterior ( $F_H$ ) components. Step-averaged ratio of forces ( $RF$ ) was then calculated from these step averaged forces as:

$$RF = \frac{F_H}{F_R} \cdot 100 \quad (3.5)$$

with

$$F_R = \sqrt{F_H^2 + F_V^2} \quad (3.6)$$

A linear trendline was fitted through the four step-averaged RF values with respect to the corresponding four step-averaged  $v_H$  values, forming the RF- $v_H$  profile (Figure 2.5; Rabita et al., 2015). The gradient of the linear trendline was determined as the rate of decline in RF ( $D_{RF}$ ) and its y-intercept was extracted as the theoretical maximal RF at null velocity ( $RF_0$ ) (Rabita et al., 2015). The coefficient of determination (adjusted  $R^2$ ) of this trendline was also calculated to quantify the linearity of the relationship between RF and  $v_H$  across the initial acceleration phase. RF over each of the first four steps was averaged and defined as  $RF_{MEAN}$  over the entire initial acceleration phase. Mean resultant GRF magnitude ( $F_{R\ MEAN}$ ) was also calculated over these four steps.

For use as an objective measure of initial acceleration performance, average horizontal external power (AHEP;  $\bar{P}$ ), based on the rate of change in mechanical energy in a horizontal direction (Bezodis et al., 2010), was calculated over each of the four steps as follows:

$$\bar{P} = \frac{m(v_f^2 - v_i^2)}{2 \cdot \Delta t} \quad (3.7)$$

where  $v_i$  and  $v_f$  are the horizontal velocities at touchdown and toe-off of each stance phase, respectively,  $\Delta t$  is the duration of the stance phase, and  $m$  is the mass of the sprinter. These external power data were normalised to dimensionless values to account for differences in stature (Bezodis et al., 2010; Hof, 1996):

$$P_N = \frac{\bar{P}}{m \cdot g^{3/2} \cdot l^{1/2}} \quad (3.8)$$

where  $m$  is the mass of the sprinter,  $g$  is the acceleration due to gravity, and  $l$  is the leg length (defined as the greater trochanter height) of the sprinter.

AHEP and NAHEP were calculated from touchdown to toe-off for each step over the initial acceleration phase during the preliminary investigation, to provide step-to-step descriptive progressions of GRF-derived measures. However, NAHEP calculated from the beginning of first contact to the end of fourth contact was used as a criterion measure of initial acceleration phase performance. For the eleven sprinters who had two valid trials, the trial in which each participant displayed the highest NAHEP was used for all subsequent analyses.

### 3.6 Statistical Analysis

Statistical analyses were conducted in SPSS (v28.0, IBM, Illinois, USA). Descriptive statistics are presented as mean values ( $\pm$  SD) of the group of fourteen sprinters. Statistical significance was accepted at  $p < 0.05$ . To assess whether variables changed between the four steps of the initial acceleration phase, between step analyses for steps one to four were conducted on all measures through a repeated measures ANOVA to identify if there was a main effect of step number. Mauchly's sphericity test was conducted, and if the assumption of sphericity was not met (i.e., where  $p < 0.05$ ), the Greenhouse-Geisser adjustment was applied. If a main effect was identified, pairwise comparisons with Bonferroni adjustment were calculated to identify any pairwise significant effects between each of the four steps (for full pairwise comparison details,

see appendix B). To quantify relationships between kinematic and kinetic measures of interest over the initial acceleration phase, the mean value over the four steps was calculated and used for all subsequent analyses. Semi-partial correlation coefficients ( $sr$ ) which accounted for the prior effects of the block phase using  $v_H$  at first touchdown were calculated between NAHEP and each of the associated performance measures (i.e.,  $F_{R\text{ MEAN}}$ ,  $RF_{\text{MEAN}}$ ,  $RF_0$ ,  $D_{RF}$ , linearity of the RF- $v_H$  fit).

Bivariate correlations between the four-step mean value of each of the kinematic variables and  $RF_{\text{MEAN}}$  were performed (for 95% confidence intervals, see appendix C). Following this, bivariate correlations between each of the variables which were strongly related to  $RF_{\text{MEAN}}$  were performed against NAHEP. Thresholds for the magnitudes of all correlations were defined according to Batterham and Hopkins (2006) as trivial (0.0), small (0.1), moderate (0.3), large (0.5), very large (0.7), nearly perfect (0.9) and perfect (1.0).



## CHAPTER 4: RESULTS

### 4.1 Overview

This chapter will systematically describe the two investigations that were conducted to address the three research questions in order to achieve the aim of this thesis. Firstly, the results of the preliminary investigation that addressed research question one will be described (section 4.2). This will present the GRF-derived kinetic measures for each of the four steps encompassing the initial acceleration phase to provide context and describe the performance of the sprinters over this period. This will be followed by the individual RF- $v_H$  profiles from the 14 sprinters. Lastly, an assessment of the relationships between the GRF and RF-derived measures and performance during the initial acceleration phase will be presented.

The second investigation addressed the second and third research questions. Section 4.3 will therefore firstly present the joint and segment angular kinematic time-histories across each of the four steps to provide the necessary context for understanding the discrete parameters which are subsequently used to address the two research questions. The relationships between these discrete kinematic characteristics, RF, and performance during the initial acceleration phase will then be presented.

### 4.2 Ratio of forces and initial sprint acceleration performance

There were significant main effects of step number for all GRF variables over the initial acceleration phase ( $p < 0.05$ ). Average  $F_R$  and  $F_V$  progressively increased across the four steps, while average and peak propulsive  $F_H$  progressively decreased (Table 4.1). Step-averaged ratio of forces (RF) decreased with each step across the initial acceleration phase whilst step-averaged horizontal velocity ( $v_H$ ) progressively increased (Table 4.1). The differences between each pair of adjacent steps were significant for both RF and  $v_H$  ( $p < 0.05$ ). The performance measures (AHEP and NAHEP) also progressively increased with each step (Table 4.1).

**Table 4.1.** Step-to-step GRF-derived and performance measures (Mean  $\pm$  SD) over each of the four steps of the initial acceleration phase, with main effect of step number (p).

Measure	Units	Step 1	Step 2	Step 3	Step 4	Main Effect (p)
<b>F<sub>R</sub></b>						
Average	(BW)	1.48 $\pm$ 0.13	1.51 $\pm$ 0.17	1.67 $\pm$ 0.16	1.74 $\pm$ 0.14	< 0.01
Peak	(BW)	2.27 $\pm$ 0.20	2.17 $\pm$ 0.28	2.40 $\pm$ 0.23	2.42 $\pm$ 0.26	< 0.01
<b>F<sub>H</sub> component</b>						
Average	(BW)	0.61 $\pm$ 0.06	0.54 $\pm$ 0.06	0.50 $\pm$ 0.06	0.45 $\pm$ 0.05	< 0.01
Peak propulsive	(BW)	1.11 $\pm$ 0.09	0.96 $\pm$ 0.07	0.93 $\pm$ 0.07	0.90 $\pm$ 0.06	< 0.01
Peak braking	(BW)	-0.39 $\pm$ 0.22	-0.32 $\pm$ 0.22	-0.45 $\pm$ 0.31	-0.45 $\pm$ 0.13	0.04
<b>F<sub>V</sub> component</b>						
Average	(BW)	1.31 $\pm$ 0.12	1.37 $\pm$ 0.16	1.54 $\pm$ 0.15	1.63 $\pm$ 0.14	< 0.01
Peak	(BW)	2.02 $\pm$ 0.20	2.01 $\pm$ 0.29	2.29 $\pm$ 0.24	2.36 $\pm$ 0.27	< 0.01
Step-averaged RF	(%)	41.67 $\pm$ 1.57	36.66 $\pm$ 2.78	30.42 $\pm$ 2.90	26.68 $\pm$ 2.27	< <b>0.01</b>
Step-averaged v <sub>H</sub>	(m.s <sup>-1</sup> )	3.73 $\pm$ 0.17	4.75 $\pm$ 0.19	5.52 $\pm$ 0.20	6.17 $\pm$ 0.20	< <b>0.01</b>
AHEP	(W)	1582 $\pm$ 208	1775 $\pm$ 214	1879 $\pm$ 263	1901 $\pm$ 192	< 0.01
NAHEP		0.80 $\pm$ 0.11	0.89 $\pm$ 0.12	0.95 $\pm$ 0.15	0.96 $\pm$ 0.12	< 0.01

Main effects highlighted in **bold** showed significant step-to-step differences across all steps through pairwise post-hoc comparisons (p < 0.05).

RF-v<sub>H</sub> profiles created from step-averaged RF and v<sub>H</sub> over the initial acceleration phase varied considerably between the fourteen sprinters (Figure 4.1). While some sprinters displayed a largely linear RF-v<sub>H</sub> relationship over the initial acceleration phase (sprinters A, E, H & N; all R<sup>2</sup>  $\geq$  0.98) (Figure 4.1), the majority of the group displayed more variation over the four steps. The sprinters with more variation typically displayed either of two patterns; either higher RF on step two (sprinters B, F, L & M; R<sup>2</sup> range = 0.63-0.92) or lower RF on step three before an increase on step 4 (sprinters G, I, J & K; R<sup>2</sup> range = 0.72-0.90). However, two sprinters had notably different RF-v<sub>H</sub> profiles; sprinter D displayed higher RF on step three (R<sup>2</sup> = 0.873) and sprinter C displayed lower RF on step four (R<sup>2</sup> = 0.72). The highest initial acceleration phase performance was achieved by sprinter C (NAHEP = 0.750, most green background), whilst the lowest performance was achieved by sprinter L (NAHEP = 0.563, most red background; Figure 4.1).

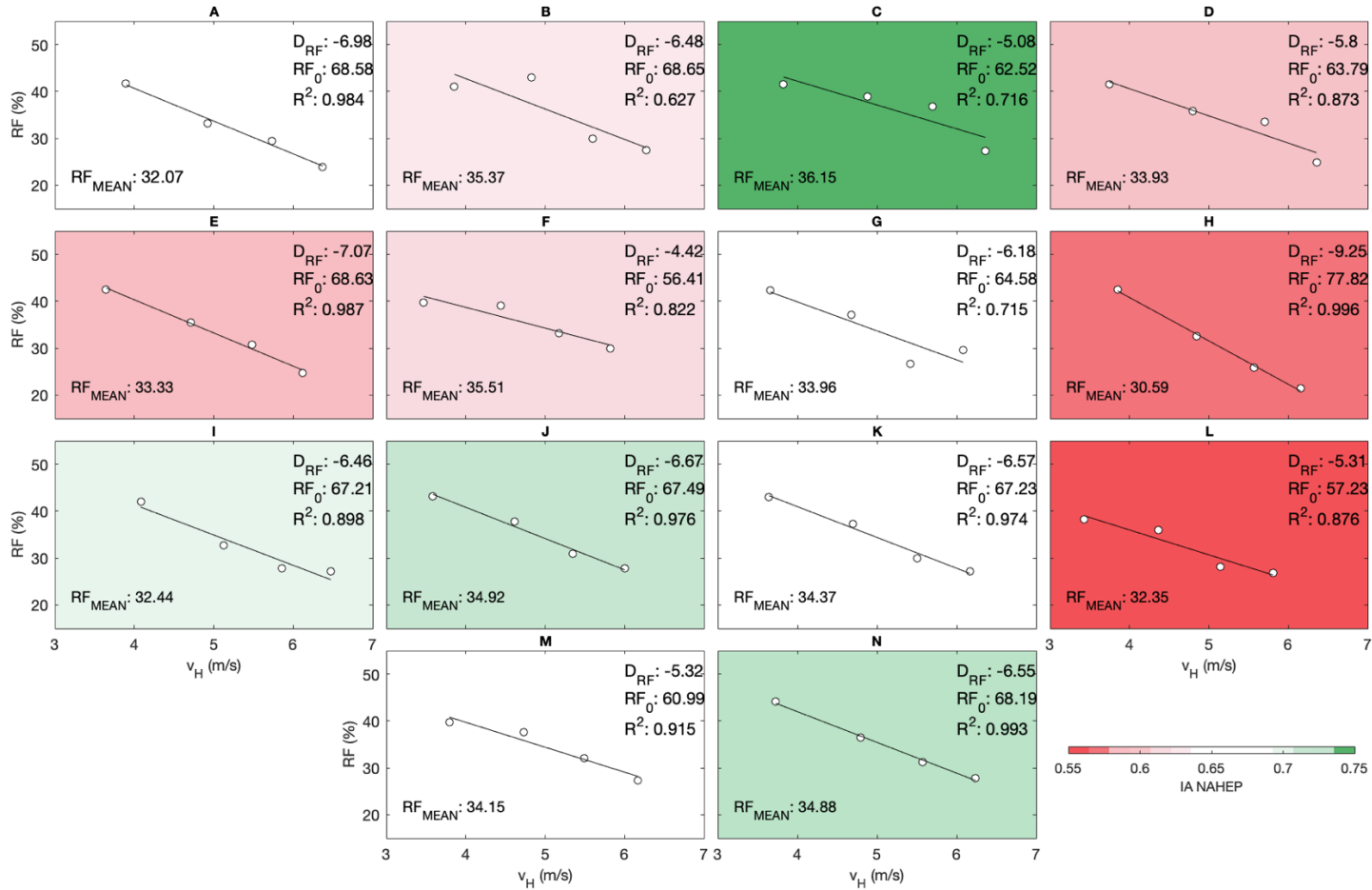


**Figure 4.1.** RF- $v_H$  profiles for all 14 sprinters (A-N, labels above each sub-figure) across the initial acceleration phase with individual linear trendlines fitted through all four steps. Technical ability descriptors based on the slope ( $D_{RF}$ ) and y-intercept ( $RF_0$ ) of this trendline, and the goodness of fit ( $R^2$ ), for each individual are stated in the top right of each plot, while  $RF_{MEAN}$  over initial acceleration is stated in the bottom left. Plot backgrounds are colour coded according to initial acceleration performance (NAHEP) from lowest (red) to highest (green) – see colour scale in bottom right of figure.

The initial acceleration phase performance, defined by NAHEP (from the beginning of first contact to the end of fourth contact) on average for the 14 sprinters, was  $0.65 \pm 0.04$ . A large, significant relationship ( $sr = 0.683$ ) was observed between  $RF_{MEAN}$  and initial acceleration phase performance (Table 4.2). No other large or significant relationships were observed between technical ability measures and performance over the initial acceleration phase (Table 4.2).

**Table 4.2.** GRF-derived measures (Mean  $\pm$  SD) averaged over the initial acceleration phase (i.e., 4 steps) and semi-partial correlations (sr) with NAHEP over the initial acceleration phase.

Measure	Units	4-step Mean	sr with NAHEP
$F_{R\ MEAN}$	(BW)	$1.60 \pm 0.15$	0.379
$RF_{MEAN}$	(%)	$33.86 \pm 1.55$	0.683**
$RF_0$	(%)	$66.01 \pm 5.44$	-0.090
$D_{RF}$	(%·s/m)	$-6.36 \pm 1.15$	0.333
Linearity of $RF-v_H$ fit ( $R^2$ )		$0.891 \pm 0.124$	-0.280

\*\* Correlation is significant at the 0.01 level (2-tailed). Semi-partial correlation coefficients (sr) were used to account for the potential prior effects of the block phase using  $v_H$  at first touchdown.

## 4.3 Kinematics and ratio of forces

### 4.3.1 Descriptive linear kinematics

All linear kinematics associated with the CM progressively increased from steps one to four (Table 4.3). All of the spatiotemporal measures increased from steps one to four, except contact time which decreased (Table 4.3). Significant main effects of step number were observed for all linear kinematic and spatiotemporal characteristics (Table 4.3).

**Table 4.3.** Linear kinematics from steps one to four (Mean  $\pm$  SD), with main effect of step number.

	Units	Step 1	Step 2	Step 3	Step 4	Main Effect (p)
<b>Centre of Mass</b>						
Displacement at TD <sup>^</sup>	(m)	0.81 $\pm$ 0.08	1.79 $\pm$ 0.18	2.95 $\pm$ 0.26	4.26 $\pm$ 0.36	-
Displacement at TO <sup>^</sup>	(m)	1.51 $\pm$ 0.10	2.56 $\pm$ 0.19	3.76 $\pm$ 0.28	5.09 $\pm$ 0.39	-
Velocity at TD	(m.s <sup>-1</sup> )	3.26 $\pm$ 0.16	4.39 $\pm$ 0.18	5.25 $\pm$ 0.19	5.96 $\pm$ 0.20	-
Velocity at TO	(m.s <sup>-1</sup> )	4.39 $\pm$ 0.18	5.25 $\pm$ 0.20	5.97 $\pm$ 0.20	6.56 $\pm$ 0.20	-
Normalised Height at TD		0.81 $\pm$ 0.04	0.86 $\pm$ 0.04	0.88 $\pm$ 0.03	0.91 $\pm$ 0.04	<b>&lt; 0.01</b>
Normalised Height at TO		0.90 $\pm$ 0.04	0.94 $\pm$ 0.04	0.97 $\pm$ 0.04	0.99 $\pm$ 0.04	<b>&lt; 0.01</b>
Normalised TDD <sup>§</sup>		-0.15 $\pm$ 0.05	-0.05 $\pm$ 0.07	0.02 $\pm$ 0.06	0.07 $\pm$ 0.06	< 0.01
Normalised TOD <sup>¶</sup>		-0.94 $\pm$ 0.06	-0.90 $\pm$ 0.03	-0.87 $\pm$ 0.05	-0.84 $\pm$ 0.05	<b>&lt; 0.01</b>
<b>Spatiotemporal</b>						
Contact time	(s)	0.189 $\pm$ 0.014	0.162 $\pm$ 0.016	0.147 $\pm$ 0.014	0.135 $\pm$ 0.014	<b>&lt; 0.01</b>
Flight time <sup>†</sup>	(s)	0.063 $\pm$ 0.021	0.075 $\pm$ 0.016	0.083 $\pm$ 0.017	0.091 $\pm$ 0.013	< 0.01
Normalised step length <sup>§</sup>		1.22 $\pm$ 0.13	1.37 $\pm$ 0.10	1.52 $\pm$ 0.13	1.64 $\pm$ 0.11	<b>&lt; 0.01</b>
Step frequency	(steps.s <sup>-1</sup> )	4.00 $\pm$ 0.33	4.25 $\pm$ 0.27	4.36 $\pm$ 0.31	4.43 $\pm$ 0.24	< 0.01
<b>Foot</b>						
Velocity at TD	(m.s <sup>-1</sup> )	0.37 $\pm$ 0.55	0.08 $\pm$ 0.50	0.37 $\pm$ 0.64	0.47 $\pm$ 0.36	0.02

<sup>^</sup>Relative to position at/time of movement onset. TD = touchdown, TO = Toe-off, TDD = Touchdown distance. TOD = Toe-off distance. <sup>†</sup>Following contact phase. <sup>§</sup>Touchdown to next touchdown. Both displacement and velocity of the CM at touchdown and toe-off are expected to increase with each step and as such, these were not assessed for a main effect over four steps. Main effects highlighted in **bold** showed significant step-to-step differences across all steps through pairwise post-hoc comparisons (p < 0.05).

### 4.3.2 Descriptive angular kinematics

For all fourteen sprinters, the ankle joint dorsiflexed on touchdown for approximately the first quarter of each stance phase, then remained relatively stationary for a period, before plantar flexion towards the end of stance phase (Figure 4.2). The peak dorsiflexion velocity during early stance was less than the subsequent peak plantar flexion velocity (Figure 4.2, Table 4.4). Significant main effects of step number were observed for ankle dorsiflexion range of motion, plantar flexion range of motion, and ankle angle at toe off. Significant main effects were also observed in each of the angular velocity characteristics (p < 0.05; Table 4.4) except for peak plantar flexion velocity.

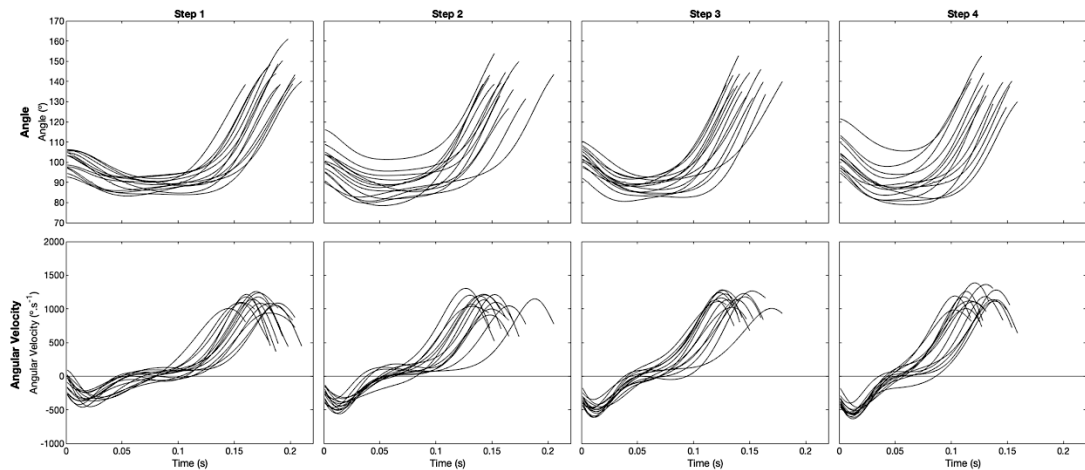


**Figure 4.2.** Joint angle-time and angular velocity-time history for the ankle joint of the stance leg during stance phase for steps one to four from each of the 14 sprinters.

**Table 4.4.** Ankle angular kinematics from steps one to four (Mean  $\pm$  SD), with main effect of step number.

	Units	Step 1	Step 2	Step 3	Step 4	Main Effect (p)
<b>Ankle</b>						
<u>Angle</u>						
Touchdown	(°)	101 $\pm$ 5	101 $\pm$ 7	103 $\pm$ 5	104 $\pm$ 8	0.24
Dorsiflexion RoM	(°)	13 $\pm$ 4	13 $\pm$ 3	15 $\pm$ 3	16 $\pm$ 3	0.01
Peak dorsiflexion	(°)	88 $\pm$ 3	87 $\pm$ 7	88 $\pm$ 4	88 $\pm$ 7	0.80
Plantar flexion RoM	(°)	56 $\pm$ 5	53 $\pm$ 5	52 $\pm$ 3	49 $\pm$ 4	< 0.01
Toe-off	(°)	144 $\pm$ 7	140 $\pm$ 7	140 $\pm$ 6	137 $\pm$ 7	0.01
<u>Angular velocity<sup>A</sup></u>						
Touchdown	(°·s <sup>-1</sup> )	-101 $\pm$ 126	-267 $\pm$ 91	-342 $\pm$ 72	-374 $\pm$ 76	< 0.01
Peak dorsiflexion	(°·s <sup>-1</sup> )	-342 $\pm$ 74	-438 $\pm$ 79	-504 $\pm$ 74	-545 $\pm$ 61	< 0.01
Peak plantar flexion	(°·s <sup>-1</sup> )	1117 $\pm$ 90	1127 $\pm$ 106	1171 $\pm$ 88	1174 $\pm$ 117	0.05
Toe-off	(°·s <sup>-1</sup> )	660 $\pm$ 217	788 $\pm$ 152	908 $\pm$ 139	904 $\pm$ 178	< 0.01

<sup>A</sup>Negative angular velocity values are representative of dorsiflexion, positive for plantar flexion. RoM = range of motion.

Through the majority of each stance phase, the knee extended, with both mean peak extension angle and angle at toe-off remaining almost constant across the four steps (Figure 4.3; Table 4.5). As steps progressed, the knee was more extended at touchdown, but extension velocity at touchdown decreased across the four steps (Figure 4.3; Table 4.5). Relatively low extension velocity was observed at the knee for approximately the first half of each stance phase, followed by an increased extension velocity during mid-to-late stance (Figure 4.3). For steps one and two, during late stance, the knee began to flex in most of the sprinters, but the magnitude of flexion and the number of sprinters flexing the knee during late stance decreased with each

step (Figure 4.3). Significant main effects of step number were observed in all of the knee angular characteristics except peak extension angle and toe-off angle ( $p < 0.05$ ), but significant step-to-step differences between all steps were only found for knee angle at touchdown and peak flexion angle (Table 4.5).

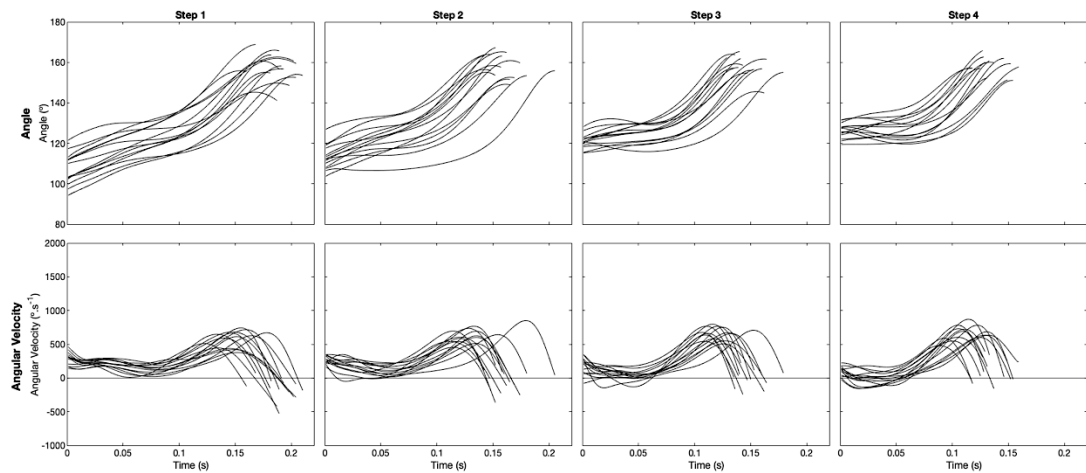


**Figure 4.3.** Joint angle-time and angular velocity-time history for the knee joint of the support leg during stance phase for steps one to four from each of the 14 sprinters.

**Table 4.5.** Knee angular kinematics from steps one to four (Mean  $\pm$  SD), with main effect of step number.

	Units	Step 1	Step 2	Step 3	Step 4	Main Effect (p)
<b>Knee</b>						
<u>Angle</u>						
Touchdown	(°)	107 $\pm$ 8	113 $\pm$ 6	121 $\pm$ 4	126 $\pm$ 4	<b>&lt; 0.01</b>
Early flexion RoM	(°)	0 $\pm$ 0	0 $\pm$ 0	0 $\pm$ 1	1 $\pm$ 2	0.04
Peak flexion	(°)	107 $\pm$ 8	113 $\pm$ 6	120 $\pm$ 4	126 $\pm$ 4	<b>&lt; 0.01</b>
Extension RoM	(°)	51 $\pm$ 8	45 $\pm$ 6	37 $\pm$ 4	32 $\pm$ 4	< 0.01
Peak extension	(°)	158 $\pm$ 6	158 $\pm$ 6	158 $\pm$ 5	158 $\pm$ 4	0.99
Late flexion RoM	(°)	1 $\pm$ 2	0 $\pm$ 1	0 $\pm$ 0	0 $\pm$ 0	0.01
Toe-off	(°)	157 $\pm$ 7	158 $\pm$ 6	158 $\pm$ 5	158 $\pm$ 4	0.71
<u>Angular velocity</u>						
Touchdown	(°·s <sup>-1</sup> )	294 $\pm$ 95	271 $\pm$ 60	190 $\pm$ 121	108 $\pm$ 72	< 0.01
Peak Extension	(°·s <sup>-1</sup> )	583 $\pm$ 118	632 $\pm$ 108	662 $\pm$ 91	668 $\pm$ 105	< 0.01
Peak Flexion	(°·s <sup>-1</sup> )	-182 $\pm$ 154	-78 $\pm$ 137	-66 $\pm$ 98	-63 $\pm$ 71	< 0.01
Toe-off	(°·s <sup>-1</sup> )	-178 $\pm$ 161	-53 $\pm$ 160	18 $\pm$ 174	106 $\pm$ 171	< 0.01

Main effects highlighted in **bold** showed significant step-to-step differences across all steps through pairwise post-hoc comparisons ( $p < 0.05$ ). Negative angular velocity values are representative of flexion, positive for extension. RoM = range of motion.

As steps progressed, the hip was more extended at both touchdown and toe-off, showing a significant main effect of step number ( $p < 0.01$ ; Table 4.6), although there was no significant main effect of step number on the range of motion at the hip during stance. Hip extension velocity at touchdown and peak extension velocity showed unclear trends across steps one to four, while a significant main effect of step number was observed for hip extension velocity at toe-off (Table 4.6). Hip extension velocity at touchdown was relatively constant over the four steps and the pattern of extension, including some fluctuation in extension velocity, throughout stance remained relatively unchanged with each step (Figure 4.4). While most of the sprinters extended their hip throughout late stance until toe-off across all steps, some sprinters began to flex the hip prior to toe-off on steps one and two (Figure 4.4).

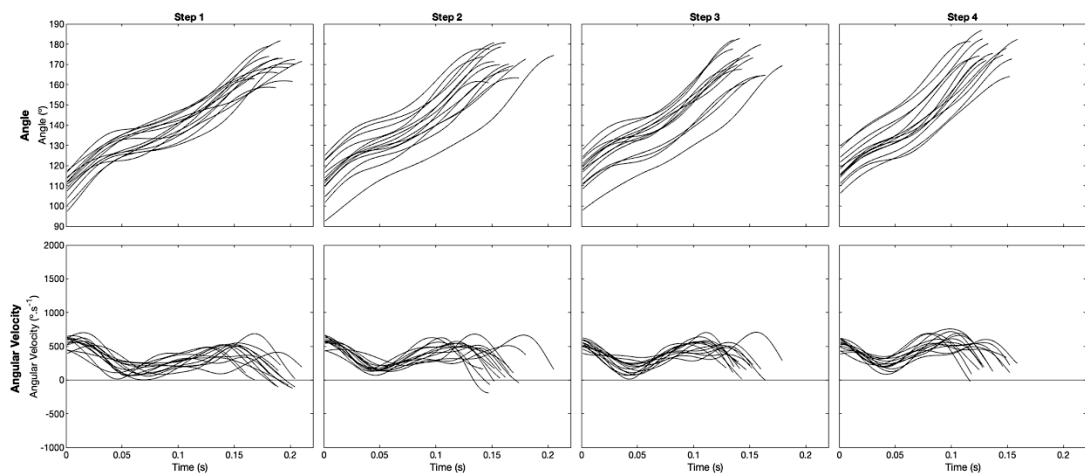


**Figure 4.4.** Joint angle-time and angular velocity-time history for the hip joint of the support leg during stance phase for steps one to four from each of the 14 sprinters.

**Table 4.6.** Hip angular kinematics from steps one to four (Mean  $\pm$  SD), with main effect of step number.

	Units	Step 1	Step 2	Step 3	Step 4	Main Effect (p)
<b>Hip</b>						
<u>Angle</u>						
Touchdown	(°)	110 $\pm$ 6	112 $\pm$ 9	116 $\pm$ 8	117 $\pm$ 7	< 0.01
Extension RoM	(°)	60 $\pm$ 7	60 $\pm$ 9	56 $\pm$ 6	59 $\pm$ 5	0.49
Toe-off	(°)	170 $\pm$ 7	172 $\pm$ 6	172 $\pm$ 7	176 $\pm$ 6	< 0.01
<u>Angular velocity</u>						
Touchdown	(°·s <sup>-1</sup> )	556 $\pm$ 82	576 $\pm$ 72	533 $\pm$ 63	529 $\pm$ 75	0.21
Peak Extension	(°·s <sup>-1</sup> )	591 $\pm$ 62	615 $\pm$ 45	581 $\pm$ 77	631 $\pm$ 73	0.19
Toe-off	(°·s <sup>-1</sup> )	29 $\pm$ 115	81 $\pm$ 138	158 $\pm$ 96	167 $\pm$ 101	< 0.01

Negative angular velocity values are representative of flexion, positive for extension. RoM = range of motion.



For most of the fourteen sprinters, the foot became slightly flatter (i.e., foot angle increased) during early stance, although for some the foot became gradually more vertical during early stance (i.e., foot angle decreased). As steps progressed, the early decrease in foot angle became more prominent (i.e., more sprinters with decreasing foot angle compared to increasing; Figure 4.5). As each stance phase progressed the anterior foot rotation gradually increased in velocity before slowing slightly just prior to toe-off (Figure 4.5). A significant main effect of step number was observed in all foot angular kinematics ( $p < 0.01$ ; Table 4.7).

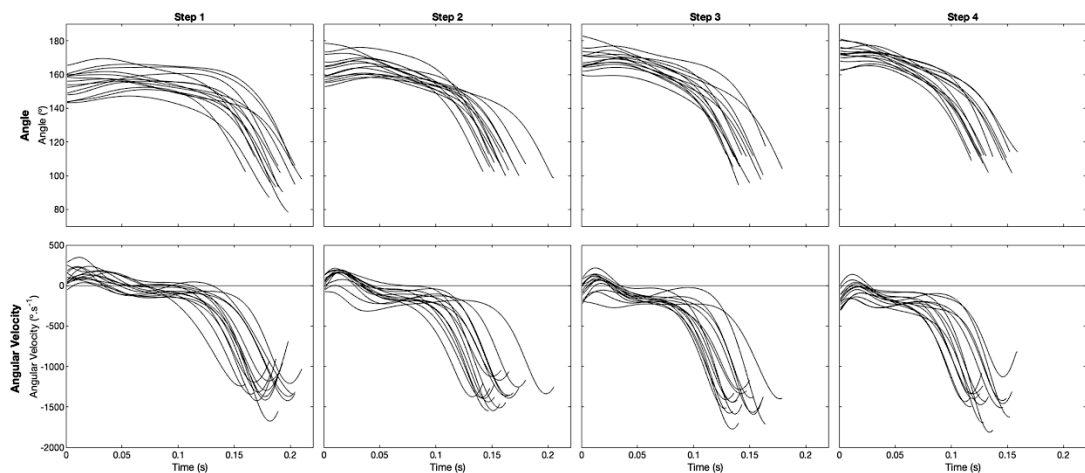


**Figure 4.5.** Segment angle-time and angular velocity-time history for the foot segment of the support leg during stance phase for steps one to four from each of the 14 sprinters.

**Table 4.7.** Foot angular kinematics from steps one to four (Mean  $\pm$  SD), with main effect of step number.

	Units	Step 1	Step 2	Step 3	Step 4	Main Effect (p)
<b>Foot</b>						
<u>Angle</u>						
Touchdown	(°)	154 $\pm$ 7	163 $\pm$ 8	169 $\pm$ 6	172 $\pm$ 5	< 0.01
Toe-off	(°)	97 $\pm$ 9	105 $\pm$ 5	106 $\pm$ 7	110 $\pm$ 4	< 0.01
<u>Angular velocity</u>						
Touchdown	(°·s <sup>-1</sup> )	99 $\pm$ 96	45 $\pm$ 68	-66 $\pm$ 105	-178 $\pm$ 92	< 0.01
Toe-off	(°·s <sup>-1</sup> )	-1133 $\pm$ 228	-1285 $\pm$ 145	-1435 $\pm$ 149	-1388 $\pm$ 252	< 0.01

During the majority of each stance phase, the shank became gradually more horizontal (i.e., anterior rotation; decrease in angle) (Figure 4.6). However, during mid-to-late stance, a more vertical rotation of the shank was observed for some sprinters. As steps progressed, the shank was more vertical at touchdown and toe-off (i.e., larger angle; Table 4.8), while its angular velocity at touchdown decreased with each step and increased at toe-off (Table 4.8). The shank rotated through a greater angle with each step (Table 4.8). Significant main effects of step number were observed for shank angle at touchdown and toe-off, and shank angular velocity at touchdown ( $p < 0.01$ ).

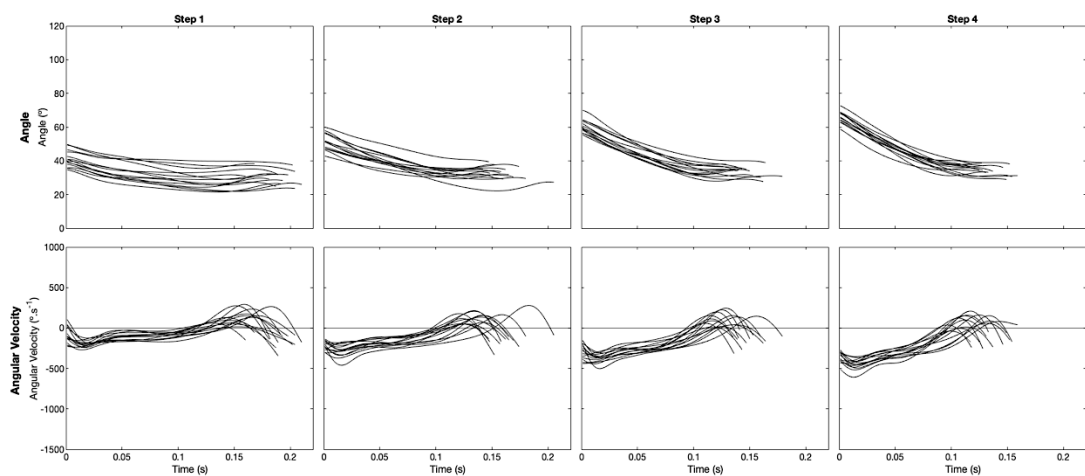


**Figure 4.6.** Segment angle-time and angular velocity-time history for the shank segment of the support leg during stance phase for steps one to four from each of the 14 sprinters.

**Table 4.8.** Shank angular kinematics from steps one to four (Mean  $\pm$  SD), with main effect of step number.

	Units	Step 1	Step 2	Step 3	Step 4	Main Effect (p)
<b>Shank</b>						
<u>Angle</u>						
Touchdown	(°)	41 $\pm$ 5	52 $\pm$ 5	61 $\pm$ 4	66 $\pm$ 4	<b>&lt; 0.01</b>
Toe-off	(°)	30 $\pm$ 4	33 $\pm$ 4	34 $\pm$ 3	35 $\pm$ 3	< 0.01
<u>Angular velocity</u>						
Touchdown	(°·s <sup>-1</sup> )	-87 $\pm$ 99	-216 $\pm$ 55	-284 $\pm$ 98	-355 $\pm$ 67	<b>&lt; 0.01</b>
Toe-off	(°·s <sup>-1</sup> )	-157 $\pm$ 77	-150 $\pm$ 72	-138 $\pm$ 87	-122 $\pm$ 105	0.50

Main effects highlighted in **bold** showed significant step-to-step differences across all steps through pairwise post-hoc comparisons ( $p < 0.05$ ).

While thigh angle decreased throughout the entire stance phase in most sprinters, thigh angle near toe-off began to increase for some sprinters for step one to three (Figure 4.7). However, this late-stance movement was less prominent with each step, with the thigh angle from only one sprinter beginning to increase near toe-off on step three, and none in step four (Figure 4.7). At touchdown, thigh orientation became more horizontal (i.e., anti-clockwise rotation of the proximal end) between steps one and two but remained relatively unchanged for steps two to four (Table 4.9), while its orientation at toe-off became progressively more horizontal (i.e., larger angle). Angular velocity of the thigh segment at both touchdown and toe-off progressively decreased (Table 4.9). Significant main effects of step number were observed in all of the thigh angular kinematics ( $p < 0.05$ ; Table 4.9).

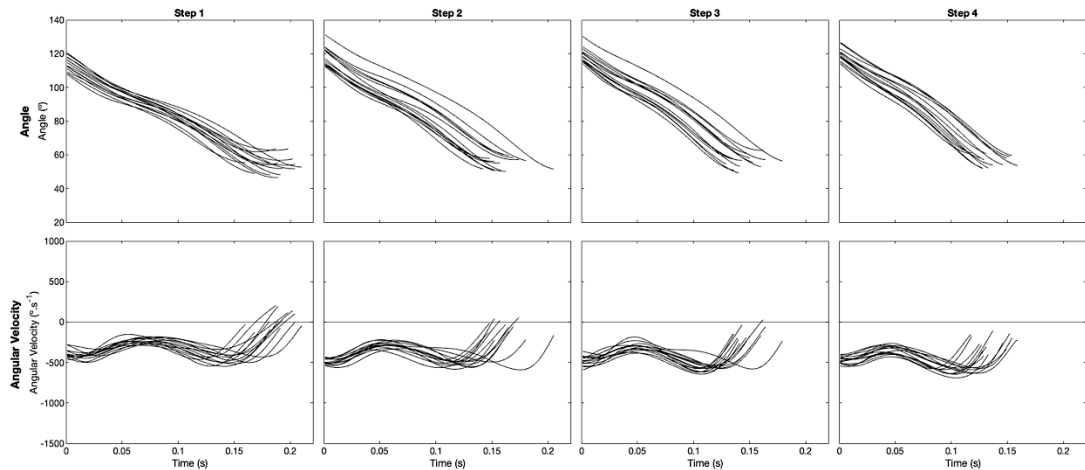


**Figure 4.7.** Segment angle-time and angular velocity-time history for the thigh segment of the support leg during stance phase for steps one to four from each of the 14 sprinters.

**Table 4.9.** Thigh angular kinematics from steps one to four (Mean  $\pm$  SD), with main effect of step number.

	Units	Step 1	Step 2	Step 3	Step 4	Main Effect (p)
<b>Thigh</b>						
<u>Angle</u>						
Touchdown	(°)	114 $\pm$ 4	119 $\pm$ 6	119 $\pm$ 4	119 $\pm$ 4	< 0.01
Toe-off	(°)	54 $\pm$ 5	55 $\pm$ 4	56 $\pm$ 4	57 $\pm$ 3	0.04
<u>Angular velocity</u>						
Touchdown	(°·s <sup>-1</sup> )	-391 $\pm$ 55	-492 $\pm$ 36	-476 $\pm$ 61	-467 $\pm$ 42	< 0.01
Toe-off	(°·s <sup>-1</sup> )	30 $\pm$ 104	-98 $\pm$ 107	-178 $\pm$ 110	-257 $\pm$ 97	<b>&lt; 0.01</b>

Main effects highlighted in **bold** showed significant step-to-step differences across all steps through pairwise post-hoc comparisons ( $p < 0.05$ ).

The trunk became progressively more vertical with each step at both touchdown and toe-off, and the angular velocity of the trunk at touchdown progressively increased over the four steps, while trunk angular velocity at toe-off fluctuated throughout the four steps (Table 4.10). Significant main effects were observed from steps one to four in all trunk kinematics ( $p < 0.01$ ), however there were no significant pairwise differences between adjacent steps.

**Table 4.10.** Trunk angular kinematics from steps one to four (Mean  $\pm$  SD), with main effect of step number.

	Units	Step 1	Step 2	Step 3	Step 4	Main Effect (p)
<b>Trunk</b>						
<u>Angle</u>						
Touchdown	(°)	29 $\pm$ 9	34 $\pm$ 8	36 $\pm$ 8	39 $\pm$ 8	< 0.01
Toe-off	(°)	40 $\pm$ 8	42 $\pm$ 9	45 $\pm$ 9	49 $\pm$ 8	< 0.01
<u>Angular velocity</u>						
Touchdown	(°·s <sup>-1</sup> )	-53 $\pm$ 60	-30 $\pm$ 46	-7 $\pm$ 62	36 $\pm$ 73	< 0.01
Toe-off	(°·s <sup>-1</sup> )	-20 $\pm$ 62	-70 $\pm$ 65	13 $\pm$ 53	-19 $\pm$ 71	< 0.01

### 4.3.3 Relationships between linear kinematics and RF

The relationship between  $RF_{MEAN}$  and mean normalised touchdown distance over the four steps was large and significant ( $r = 0.672$ ,  $p < 0.01$ ; Table 4.11). A very large, significant relationship was found between mean step frequency and  $RF_{MEAN}$  over the four steps ( $r = 0.715$ ,  $p < 0.01$ ). The relationship between  $RF_{MEAN}$  and all other linear kinematics ranged from trivial to moderate and were non-significant (Table 4.11).

**Table 4.11.** Mean ( $\pm$  SD) linear kinematics over four steps and correlation with  $RF_{MEAN}$ .

	Units	4 Step Mean	Correlation (r)
<b>Centre of Mass</b>			
Displacement at Touchdown <sup>^</sup>	(m)	-	-
Displacement at Toe-off <sup>^</sup>	(m)	-	-
Velocity at Touchdown	(m.s <sup>-1</sup> )	-	-
Velocity at Toe-off	(m.s <sup>-1</sup> )	-	-
Normalised Height at Touchdown		0.86 $\pm$ 0.03	0.000
Normalised Height at Toe-off		0.95 $\pm$ 0.04	-0.046
Normalised TDD <sup>‡</sup>		-0.03 $\pm$ 0.04	-0.672**
Normalised TOD <sup>‡</sup>		-0.89 $\pm$ 0.04	-0.428
<b>Spatiotemporal</b>			
Contact time	(s)	0.189 $\pm$ 0.014	-0.406
Flight time <sup>†</sup>	(s)	0.078 $\pm$ 0.017	-0.242
Normalised Step length <sup>§</sup>		1.44 $\pm$ 0.11	-0.296
Step frequency	(steps.s <sup>-1</sup> )	4.26 $\pm$ 0.29	0.715**
<b>Foot</b>			
Touchdown Velocity	(m.s <sup>-1</sup> )	0.32 $\pm$ 0.44	-0.398

<sup>^</sup>Relative to position at/time of movement onset. <sup>‡</sup>Touchdown distance. <sup>‡</sup>Toe-off distance. <sup>†</sup>Following contact phase. <sup>§</sup>Touchdown to next touchdown. \*\* Correlation is significant at the 0.01 level (2-tailed). Both displacement and velocity of the CM at touchdown and toe-off are expected to increase with each step and as such, these were not dependent variables and were included in the analysis.

### 4.3.4 Relationships between angular kinematics and RF

Relationships between the joint angular kinematics (four-step mean) and  $RF_{MEAN}$  are presented in Table 4.12. There was a very large significant relationship between mean ankle dorsiflexion range of motion and  $RF_{MEAN}$  ( $r = 0.735$ ,  $p < 0.01$ ). There were no other significant relationships between  $RF_{MEAN}$  and the other ankle joint angular kinematics (Table 4.12). There also were no significant relationships between the knee and hip angular kinematics and  $RF_{MEAN}$  (Table 4.12).

**Table 4.12.** Mean ( $\pm$  SD) joint angular kinematics over four steps and correlation with RF<sub>MEAN</sub>.

	Units	Mean	Correlation (r)
<b>Ankle</b>			
<u>Angle<sup>A</sup></u>			
Touchdown	(°)	102 $\pm$ 5	0.154
Dorsiflexion RoM	(°)	14 $\pm$ 3	0.728**
Peak dorsiflexion	(°)	88 $\pm$ 4	-0.258
Plantar flexion RoM	(°)	53 $\pm$ 3	0.110
Toe-off	(°)	140 $\pm$ 5	-0.141
<u>Angular velocity<sup>A</sup></u>			
Touchdown	(°·s <sup>-1</sup> )	-271 $\pm$ 66	-0.072
Peak Dorsiflexion	(°·s <sup>-1</sup> )	-457 $\pm$ 56	-0.449
Peak Plantar flexion	(°·s <sup>-1</sup> )	1147 $\pm$ 84	0.311
Toe-off	(°·s <sup>-1</sup> )	815 $\pm$ 118	-0.087
<b>Knee</b>			
<u>Angle</u>			
Touchdown	(°)	117 $\pm$ 5	-0.326
Early flexion RoM	(°)	0 $\pm$ 1	-0.292
Peak flexion	(°)	116 $\pm$ 5	-0.277
Extension RoM	(°)	41 $\pm$ 5	0.149
Peak extension	(°)	158 $\pm$ 5	-0.168
Late flexion RoM	(°)	0 $\pm$ 1	0.372
Toe-off	(°)	158 $\pm$ 5	-0.202
<u>Angular velocity</u>			
Touchdown	(°·s <sup>-1</sup> )	216 $\pm$ 70	-0.226
Peak Extension	(°·s <sup>-1</sup> )	636 $\pm$ 89	-0.167
Peak Flexion	(°·s <sup>-1</sup> )	-100 $\pm$ 83	-0.228
Toe-off	(°·s <sup>-1</sup> )	-27 $\pm$ 144	-0.413
<b>Hip</b>			
<u>Angle</u>			
Touchdown	(°)	114 $\pm$ 6	0.295
Extension RoM	(°)	59 $\pm$ 5	-0.234
Toe-off	(°)	173 $\pm$ 6	0.098
<u>Angular velocity</u>			
Touchdown	(°·s <sup>-1</sup> )	549 $\pm$ 37	0.201
Peak Extension	(°·s <sup>-1</sup> )	604 $\pm$ 32	-0.268
Toe-off	(°·s <sup>-1</sup> )	116 $\pm$ 88	0.036

<sup>A</sup>Negative values are representative of dorsiflexion, positive for plantar flexion.\*\* Correlation is significant at the 0.01 level (2-tailed). RoM = range of motion.

Very large, significant relationships were observed between both foot and shank angle at touchdown and RF<sub>MEAN</sub> ( $r = -0.724$ ,  $p < 0.01$  and  $r = -0.764$ ,  $p < 0.01$ , respectively; Table 4.13). As these relationships were negative, they relate to higher RF<sub>MEAN</sub> being associated with more forward-orientated foot and shank segments (more acute angle; see Figures 4.5 and 4.6).

**Table 4.13.** Mean ( $\pm$  SD) segment angular kinematics over four steps and correlation with  $RF_{MEAN}$ .

	Units	Mean	Correlation (r)
<b>Foot</b>			
<u>Angle</u>			
Touchdown	( $^{\circ}$ )	164 $\pm$ 5	-0.724**
Toe-off	( $^{\circ}$ )	105 $\pm$ 4	-0.334
<u>Angular velocity</u>			
Touchdown	( $^{\circ}.s^{-1}$ )	-25 $\pm$ 66	0.408
Toe-off	( $^{\circ}.s^{-1}$ )	-1310 $\pm$ 121	0.214
<b>Shank</b>			
<u>Angle</u>			
Touchdown	( $^{\circ}$ )	55 $\pm$ 3	-0.764**
Toe-off	( $^{\circ}$ )	33 $\pm$ 3	-0.235
<u>Angular velocity</u>			
Touchdown	( $^{\circ}.s^{-1}$ )	-235 $\pm$ 69	-0.309
Toe-off	( $^{\circ}.s^{-1}$ )	-142 $\pm$ 65	-0.511
<b>Thigh</b>			
<u>Angle</u>			
Touchdown	( $^{\circ}$ )	118 $\pm$ 3	-0.252
Toe-off	( $^{\circ}$ )	55 $\pm$ 4	0.076
<u>Angular velocity</u>			
Touchdown	( $^{\circ}.s^{-1}$ )	-456 $\pm$ 32	-0.174
Toe-off	( $^{\circ}.s^{-1}$ )	-126 $\pm$ 96	0.304
<b>Trunk</b>			
<u>Angle</u>			
Touchdown	( $^{\circ}$ )	34 $\pm$ 8	-0.151
Toe-off	( $^{\circ}$ )	44 $\pm$ 8	-0.180
<u>Angular velocity</u>			
Touchdown	( $^{\circ}.s^{-1}$ )	-14 $\pm$ 48	-0.272
Toe-off	( $^{\circ}.s^{-1}$ )	-24 $\pm$ 55	-0.223

\*\* Correlation is significant at the 0.01 level (2-tailed).

There were no strong or significant relationships found between  $RF_{MEAN}$  and the four-step average for the other foot angular kinematics and the thigh and trunk angle and angular velocity variables (Table 4.13).

#### 4.3.5 Relationships between kinematics favourable for RF and initial acceleration phase performance

Of the kinematic characteristics that were significantly related to  $RF_{MEAN}$ , only average normalised touchdown distance was also significantly related to NAHEP over the initial acceleration phase ( $r = 0.710$ ,  $p < 0.01$ ). Moderate, non-significant relationships with initial acceleration performance were found for each of the other measures related to  $RF_{MEAN}$ , all of which were in the same direction as the relationships between the respective variables and  $RF_{MEAN}$  (Table 4.14).

**Table 4.14.** Relationships between kinematic characteristics favourable for  $RF_{MEAN}$  and their relationship ( $r$ ) with initial acceleration phase performance (NAHEP).

Measure	Units	Correlation ( $r$ )
Normalised Touchdown Distance		-0.710**
Step Frequency	(steps.s <sup>-1</sup> )	0.434
Ankle Dorsiflexion RoM	(°)	0.458
Touchdown Foot Angle	(°)	-0.406
Touchdown Shank Angle	(°)	-0.330

\*\* Correlation is significant at the 0.01 level (2-tailed). RoM = range of motion.

Some of the kinematic variables measured were significantly related to NAHEP despite not being significantly related to  $RF_{MEAN}$ . The four-step average value for normalised toe-off distance was strongly and negatively related to NAHEP ( $r = -0.664$ ,  $p < 0.01$ ), a strong negative relationship was found with contact time ( $r = -0.738$ ,  $p < 0.01$ ), and hip angle at touchdown also was strongly and positively related to NAHEP ( $r = 0.536$ ,  $p < 0.05$ ).



## CHAPTER 5: DISCUSSION

### 5.1 Overview

This thesis aimed to investigate the relationships between kinematic characteristics and RF during the initial acceleration phase of sprinting. To achieve this, three research questions were systematically addressed. Firstly, through a preliminary investigation, research question one was addressed: “How strongly do RF-associated measures derived from the RF- $v_H$  profile, including the linearity of the fit, relate to initial acceleration phase performance?”. After identifying that linearity of the RF- $v_H$  profile was not related to initial acceleration performance (NAHEP) and that  $RF_{MEAN}$  was the only RF-associated measure strongly and significantly related to initial acceleration phase performance, the second research question was addressed to achieve the primary aim of this thesis: “What are the relationships between a sprinter’s kinematics and RF during the initial acceleration phase?”. Finally, after kinematic characteristics associated with  $RF_{MEAN}$  were identified, the relationships between such measures (i.e., kinematics significantly related to RF) and initial acceleration phase performance were investigated to assess the primary findings of this thesis in the context of acceleration performance and address the third research question; “How strongly do the kinematic characteristics, which are strongly related to RF, relate to initial acceleration phase performance?”.

This chapter will progress through each research question in turn, followed by discussion of the limitations and practical implications of this investigation, with lastly a conclusion which provides a summary of the key findings and implications of this thesis. As the second research question addressed the primary aim of this thesis, the findings associated with this question will be explored in greatest detail in this discussion. Therefore, there will be comparatively brief discussions around the first and third research questions, as they were a preliminary question to determine the RF-associated dependent variable to be used, and a supplementary question to assess the findings in the context of acceleration performance, respectively.

## **5.2 How strongly do RF-associated measures derived from the RF- $v_H$ profile, including the linearity of the fit, relate to initial acceleration phase performance?**

The first research question was addressed to evaluate a current gap in the sprint running literature with respect to the relationships between RF-associated measures derived from the RF- $v_H$  profile and performance during the initial acceleration phase. As outlined previously, existing research has highlighted the clear importance of RF and its associated measures (i.e.,  $RF_0$ ,  $D_{RF}$ ) for acceleration performance, even when performance is quantified using different measures (Morin et al, 2011; Rabita et al., 2015; Samozino et al., 2016; Bezodis et al., 2020). However, no previous research has investigated these RF measures during just the first four steps after block exit, which constitutes the initial acceleration phase. Bezodis et al. (2020) previously investigated ‘early acceleration’, which they defined as the block push followed by the first four steps on the track. Although it was not their primary focus, they created RF- $v_H$  profiles using data from the entire acceleration phase and observed that, for some sprinters, there were larger step-to-step variations in the RF- $v_H$  relationship during the first four steps, compared to the wider, whole acceleration profile (e.g., Figure 1.1). This observation raised a concern as to whether the step-to-step variation in RF is important to consider for acceleration performance, where sprinters who display a more or less linear decline in RF, with respect to  $v_H$ , may have more effective acceleration performance.

In the current study, there was a considerable amount of variation ( $R^2$  range over the group = 0.63 to 0.98) between sprinters in the linearity of the decline in RF with respect to  $v_H$  as they progressed through the four steps. However, when looking at the whole group, the semi partial correlation, which accounted for performance up to first contact, revealed only a small, negative relationship between the linearity of the RF- $v_H$  profiles and performance ( $r = -0.280$ ), suggesting that the linearity of the RF- $v_H$  profile is at best weakly related to initial acceleration phase performance. High acceleration performance can therefore be achieved regardless of step-to-step variation in RF as velocity increases during the initial acceleration phase. Thus, step-to-step variation in RF- $v_H$  observed over these four steps should not be a performance-related concern for practitioners and coaches.

There was a large, significant relationship between  $RF_{MEAN}$  and initial acceleration performance ( $r = 0.683$ ,  $p < 0.01$ ), which supports the findings of Bezodis et al. (2020) that high  $RF_{MEAN}$  is associated with acceleration performance. However, in contrast to the findings of Bezodis et al. (2020), the two RF-derived measures of technical performance,  $RF_0$  and  $D_{RF}$ , were not strongly related to performance in the current study ( $r = -0.090$  and  $r = 0.333$ , respectively); where Bezodis et al. (2020) found a strong, positive relationship between  $RF_0$  and performance during early acceleration (NAHEP) ( $r = 0.59$ ,  $p < 0.01$ ), and a negative, trivial relationship between  $D_{RF}$  and performance ( $r = -0.04$ ). Although the current study accounted for differences in block phase performance using a semi partial correlation, the inclusion of the block push data point on the RF- $v_H$  profile (as used by Bezodis et al. (2020) when they investigated early acceleration) appears to have an effect on the fit of the linear trendline, by increasing the gradient and the y-intercept of the trendline (Figure 5.1). As the  $D_{RF}$  and  $RF_0$  measures are extracted from the gradient and y-intercept of the RF- $v_H$  profile, respectively, the difference in shape between the ‘early acceleration’ and ‘initial acceleration’ phase leads to different outcomes with respect to these RF-derived measures. This effect was evident in the data obtained from the sprinters in the current study (Figure 5.1), where assessing ‘early acceleration’ similar to Bezodis et al. (2020) (i.e., including the block phase push-off), led to different values for  $D_{RF}$  and  $RF_0$  compared to assessing the initial acceleration phase as considered in the current study.

The current thesis directly investigated the aforementioned concern by Bezodis et al. (2020), about the step-to-step variation in RF during the first four steps on the track which constitute the initial acceleration phase. As such, the block phase was not of interest for the current research question, and therefore the block phase push-off data point was not included in the RF- $v_H$  profiles created. During the analysis to address the first research question, a semi-partial correlation accounting for block phase performance was used for two objectives; firstly, to obtain comparable results to the study by Bezodis et al. (2020) despite differing research aims, and secondly to account for differences in performance between sprinters leading into the initial acceleration phase. However, as considerably different relationships were observed between performance and the RF-derived measures of  $D_{RF}$  and  $RF_0$  in the current thesis and the study by Bezodis et al. (2020), future research analysing features of the RF- $v_H$  profile should therefore explicitly report the range of values

(i.e., inclusion of the block push and following number of steps) included in the profile used.

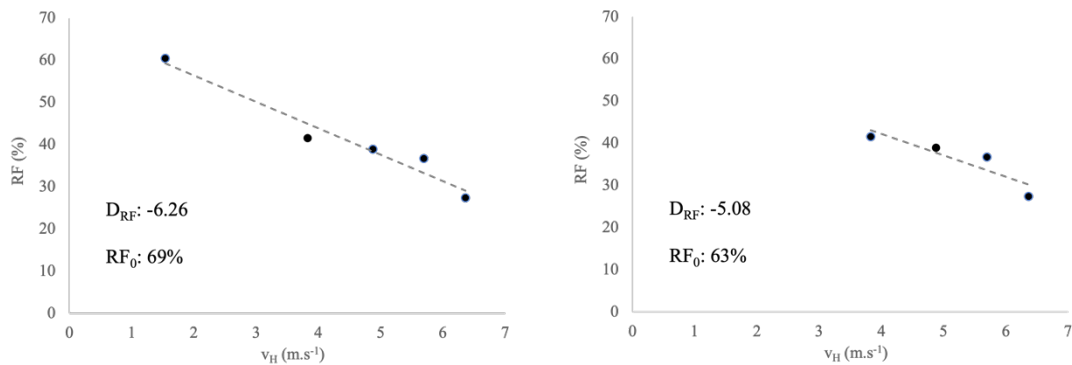


**Figure 5.1.** RF- $v_H$  profiles for one sprinter from the current thesis, created from left: ‘early acceleration’ (includes block exit; method used by Bezodis et al., 2020) and right: initial acceleration (excludes block exit; method used in this thesis) with linear trendlines fitted. Technical performance descriptors based on the slope ( $D_{RF}$ ) and y-intercept ( $RF_0$ ) of this trendline are stated in the bottom left of each plot.

In a number of previous studies, it has been demonstrated that, provided athletes are of a comparable performance level, the orientation of the force applied (i.e., RF) is more strongly related to acceleration performance than the resultant magnitude of the force applied (i.e.,  $F_R$ ) (Morin et al, 2011; Rabita et al., 2015; Samozino et al., 2016; Bezodis et al., 2020). The current thesis found a moderate correlation between  $F_R$  and NAHEP during the initial acceleration phase ( $r = 0.379$ ). As the relationship between RF and NAHEP during this phase was considerably stronger ( $r = 0.683$ ,  $p < 0.01$ ), this supports the aforementioned findings and extends their applicability to include assessment of performance during the initial acceleration phase in isolation. As the findings of this thesis suggest that  $RF_{MEAN}$  is the only significant predictor of performance among the GRF-derived and RF-associated measures of interest, research investigations of the initial acceleration phase need not be concerned by performance-related effects of any step-to-step variation in RF. As such, ‘technical performance’ during initial acceleration can be appropriately quantified using  $RF_{MEAN}$  over four steps. Therefore, for the purpose of subsequently addressing research question two, which addressed the primary aim of this thesis,  $RF_{MEAN}$  over four steps was used as the dependent variable of interest against which the average kinematic characteristics of the sprinter over the same four steps were correlated.

### **5.3 What are the relationships between a sprinter's kinematics and RF during the initial acceleration phase?**

The second research question was addressed by determining the whole body and stance leg kinematic features that were associated with achieving high  $RF_{MEAN}$  over the initial acceleration phase. This investigation revealed a number of kinematic characteristics at touchdown and during the stance phase that were strongly related to a high  $RF_{MEAN}$ . These findings suggested that lower limb kinematics around the stance foot, ankle, and shank at touchdown, and during early stance, were strongly associated with high 'technical performance' (i.e., high  $RF_{MEAN}$ ) during the initial acceleration phase. To elucidate the relationships between kinematic characteristics and a high  $RF_{MEAN}$ , the findings will be addressed firstly with respect to those present at touchdown, then during the stance phase, followed by the interactions between such kinematics at touchdown and during stance, and lastly spatiotemporal variables.

#### **5.3.1 Touchdown kinematics**

Significant negative relationships were found between angles of the foot and shank at touchdown and  $RF_{MEAN}$  ( $r = -0.724$  and  $r = -0.764$ , respectively;  $p < 0.01$ ). These negative relationships suggest that a more anterior orientation (i.e., more clockwise if viewed running left to right) of these lower limb segments, on average over the touchdown events of the four steps, were associated with achieving high RF.

Due to the conventions used in this thesis, a more anterior orientation of each of the respective segments is denoted by a smaller angle, hence, the orientation of these segments that were associated with RF were a more vertical foot and a more horizontal shank orientation in the sagittal plane at touchdown. As ankle angle at touchdown was not related to  $RF_{MEAN}$  ( $r = 0.154$ ), this suggests that sprinters who achieved higher RF did not typically have a more flexed or more extended ankle at touchdown. Therefore, these relationships suggest that more forward orientation of both the foot and shank segments at touchdown was more likely achieved primarily by a change in foot orientation, than by a change in shank orientation. This is likely the case because, on a mechanical basis, to achieve a more horizontal shank orientation without any change in foot orientation, the ankle joint must be dorsiflexed. However, if the foot orientation

becomes more vertical without any action at the ankle joint, the shank will inevitably become more horizontal (i.e., by anterior rotation). Therefore, as sprinters who achieved higher RF did not necessarily have a more flexed ankle, the segment orientations at touchdown that were associated with high RF were likely achieved by an active change in foot orientation (i.e., smaller angle), also leading to a consequent change in shank orientation at touchdown due to the lack of any change in ankle joint angles.

Touchdown distance, which is the difference in horizontal position between the whole-body CM and the toe of the stance leg at touchdown, was also significantly related to  $RF_{MEAN}$  over the initial acceleration phase. This relationship was strong and negative ( $r = -0.672$ ,  $p < 0.01$ ), suggesting that touching down with the base of support further behind the CM (i.e., a more negative touchdown distance) was associated with high RF. As touchdown distance progressively increased throughout the initial acceleration phase, the base of support shifted to be positioned in front of the whole-body CM by step four. This means that higher RF is not only associated with placing the base of support further behind the CM during the first steps (i.e., steps one and two), but also touching down with the foot less far ahead of the CM during later steps (steps three and four). Therefore, although it appears not possible to keep the stance foot behind the whole-body CM at touchdown throughout the initial acceleration phase, aiming to limit the increase in touchdown distance by keeping the stance foot as close to the whole-body CM as possible once touchdown distances become positive appears preferable.

As the whole-body CM position is a function of joint configurations and segment orientations of a linked system from the point of contact at the distal end (i.e., toe) to the vertex, a favourable touchdown distance could be the result of a range of different joint and segment kinematic characteristics. Although the motion of the CM is fixed during the flight phase prior to touchdown, a more negative (or less positive) touchdown distance could theoretically be created by a more forward leaning upper body or swing leg, or a more posteriorly extended stance leg, or a combination of both (Figure 5.2).

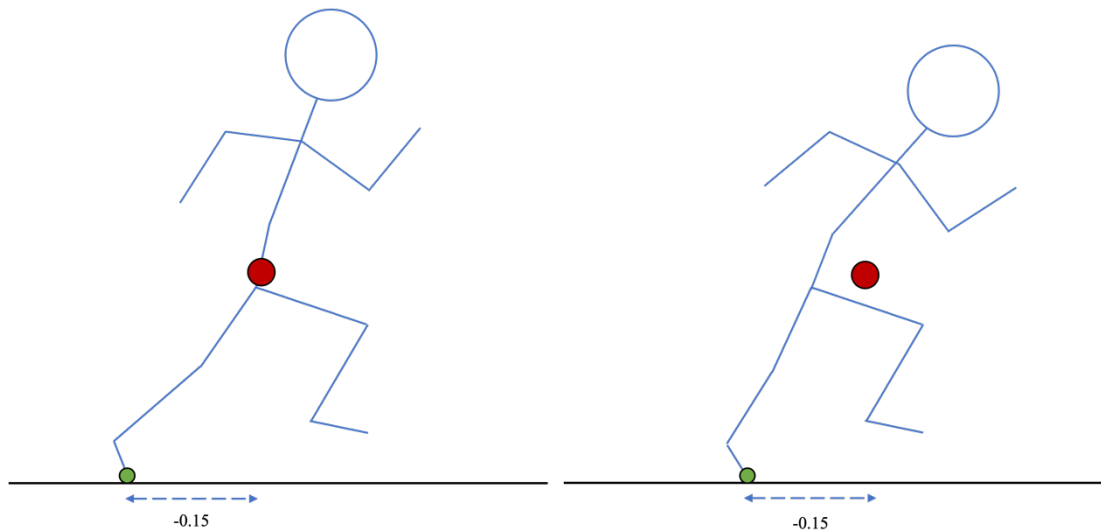


**Figure 5.2.** Representation of two examples of whole-body configurations with different angular kinematics to achieve the same touchdown distance. Left figure with a more posteriorly extended leg and more upright upper body, right figure with a more forward leaning upper body and less posteriorly extended leg. Red circle denotes the whole-body CM position, green circle denotes the base of support (toe marker), example normalised touchdown distance of -0.15 (arbitrary units).

To investigate the segment orientations associated with favourable touchdown distance, Pearson's correlations were conducted between normalised touchdown distance and each of the kinematics measured. These correlations revealed that the relationship between average trunk angle at touchdown and normalised touchdown distance was small and negative ( $r = -0.211$ ) (see appendix C). This suggests that athletes who achieved more favourable touchdown distance did not necessarily have either a smaller or larger trunk angle. Therefore, these relationships suggest that a more negative (or less positive) touchdown distance is related to a more posteriorly extended leg at touchdown (i.e., placing the base of support further behind the CM), as opposed to the upper body being more anteriorly orientated at touchdown.

Similar to its relationship with touchdown distance, the relationship between average trunk angle at touchdown over the four steps and  $RF_{MEAN}$  was also small and negative ( $r = -0.151$ ). This suggests that trunk angle was also unimportant in relation to producing high RF. It has been established that more forward orientations of the foot and shank at touchdown were associated with  $RF_{MEAN}$ . Therefore, it is more likely that the segment orientations of the stance leg facilitated negative touchdown distance and contributed to the production of high RF during the initial acceleration phase. The implications of such relationships between stance leg configuration, touchdown

distance, and RF, in conjunction with specific kinematics of interest during early stance (section 5.3.2), will be further discussed in section 5.3.3.

It is important to note that the current thesis focussed on kinematics of the stance leg and thus did not directly investigate characteristics related to the swing leg. The position of the swing leg during stance (i.e., more trailing or rotated through) could be a contributing factor for touchdown/toe-off distance, due to its effect on the whole-body CM position. Therefore, future research could also seek to investigate the kinematic characteristics of the swing leg in relation to RF during the initial acceleration phase to explore the effect that swing leg positions may have on creating favourable touchdown/toe-off distance.

### **5.3.2 Kinematics during stance**

Following touchdown, the ankle dorsiflexed for a short period during the early part of each stance phase (on average  $14 \pm 3^\circ$  of dorsiflexion). The average range of motion of this dorsiflexion at the ankle was very strongly and significantly related to  $RF_{MEAN}$  over four steps ( $r = 0.728$ ,  $p < 0.01$ ). As this relationship was positive, it means that larger dorsiflexion range of motion during early stance was associated with higher RF. At face value, this appears potentially surprising because coaching practice for sprinters often highlights the importance of a ‘stiff’ ankle for higher performance, and Nagahara and Zushi (2017) stressed the importance of ankle stiffness for improving sprinting performance, but the study by Nagahara and Zushi (2017) concerned the maximal velocity phase of sprinting. The finding of the current thesis suggests that, during the initial acceleration phase, allowing more dorsiflexion during early stance may be important for achieving high RF and is potentially more beneficial than a ‘stiffer’ ankle, for acceleration performance. Whilst Bezodis et al. (2017) found, during the step nearest 5 m, that sprinters who demonstrated higher RF had a greater amount of ankle dorsiflexion at touchdown, the current thesis extends this by identifying that the range of dorsiflexion motion following touchdown may also be important for RF. Although not statistically significant, the current thesis found that the peak velocity of ankle dorsiflexion was moderately related to  $RF_{MEAN}$  ( $r = -0.449$ ). This gives some indication that achieving greater dorsiflexion during early stance at a faster rate might be important for achieving high RF. However, as this finding was not



significant more research is needed to explore this potential factor and understand the potentially complex interactions surrounding the foot, ankle, and shank mechanics during the early stance phase. The findings with regard to dorsiflexion range of motion also warrant further investigation to explore the implications of active ankle stiffness or passive ankle flexibility for acceleration performance. For example, future research could compare the intention of having a more or less ‘stiff’ ankle by actively attempting to allow more and less dorsiflexion during sprint acceleration, or by applying additional external assistance to limit ankle dorsiflexion and understanding the performance implications of such limited motion during acceleration. Additionally, this could be explored through an observational and cross-sectional study to analyse if some sprinters passively possess more or less flexibility at the ankle which may impact their dorsiflexion range of motion during acceleration, with the effect of such characteristics on performance ultimately being considered. Additional participant information, such as the stiffness/sole properties of the shoes worn by each sprinter and their measured ankle flexibility, would have been useful for the discussion around such implications as presented above. However, the raw data used in this thesis were collected as part of an earlier project due to the restrictions imposed by the COVID-19 pandemic. To this end, such information was not available but would be useful to collect when conducting future research on sprint acceleration.

As discussed on a mechanical basis in relation to the changes in foot and shank orientation at touchdown, the early-stance dorsiflexion observed could be a function of a flattening of the foot (i.e., increase in foot segment angle), more anterior rotation of the shank (i.e., decrease in shank segment angle), or a combination of both. A qualitative assessment of the angle-time histories for the foot and shank segments (Figure 4.5 and Figure 4.6, respectively) suggest that, on average over the initial acceleration phase (particularly steps two to four), the shank angle decreases through approximately the same range and at a similar rate as the foot angle increases during early stance (i.e. shank and foot angles appear to display anti-phase coordination of near equal dominance, although more specific co-ordination analyses using vector coding would be required to quantify this in future studies). Therefore, on average over the initial acceleration phase, it appears that dorsiflexion at the ankle is typically a function of both the forward rotation of the shank and a flattening of the foot following touchdown. However, during step one, the relative contributions of the foot and shank

segments to early-stance dorsiflexion appear to be different from the following steps. Compared to steps two to four, foot angle during the first half of stance in step one remained relatively constant for most sprinters, and for those that flattened the foot, the angular velocity of the movement during early stance was less pronounced than in the following steps (Figure 4.5). Contrarily, the segment angular velocity-time history of the shank during early stance retained a relatively unchanged pattern across all steps in the majority of sprinters, despite the magnitude at touchdown typically decreasing progressively (Figure 4.6). The difference in angular velocity characteristics between the foot and shank suggests that, during the first step only, the early-stance dorsiflexion is likely caused by more anterior rotation of the shank than flattening of the foot. Donaldson et al. (2021) also found that coordination patterns between the foot and shank during step one were considerably different from each of the following steps during the initial acceleration phase. The findings of the current thesis determined that, for investigating relationships with RF, assessing kinematic characteristics on average over the initial acceleration phase was most appropriate. However, the aforementioned findings with respect to coordination of the foot and shank segments warrant further research to explore the potentially different relationships that may be present between kinematic characteristics and other performance measures (i.e., not associated with RF) during step one.

### **5.3.3 Kinematic interactions across stance**

The kinematic characteristics at touchdown and during stance which were found to be associated with achieving high  $RF_{MEAN}$  describe a postural position that includes anteriorly orientated lower limb segments at touchdown (more negative touchdown distance, smaller angles of the foot and shank). Followed by action of the ankle to facilitate anterior translation of the whole-body CM during early stance (greater ankle dorsiflexion range of motion), with possible implications for this ankle action to facilitate faster translation of the CM (peak dorsiflexion velocity). It has been clearly demonstrated in the sprint running literature that extension of the hip, knee, and ankle joints (in a proximal-to-distal sequence) occurs in each stance phase during the acceleration phase of maximal sprint efforts (Jacobs & van Ingen Schenau, 1992; Charalambous et al., 2012; Bezodis et al., 2014; Brazil et al., 2017; Bezodis et al.,

2019). The findings of this thesis may extend the understanding of an important interaction between the position of the whole-body CM at touchdown, anterior translation during early stance, and mid-to-late stance extension, when put into the context of the study by Jacobs and van Ingen Schenau (1992), which investigated patterns of intermuscular coordination during sprint acceleration. Their study described how the whole-body CM is translated and accelerated horizontally during stance by means of both rotation and extension of the stance leg around the base of support (Figure 2.9). Jacobs and van Ingen Schenau (1992) found that highly trained sprinters delayed the extension of their CM away from the base of support until the CM had been rotated further forwards, relative to the base of support (Figure 2.9). Although the measures of touchdown and toe-off distance were not reported by Jacobs and van Ingen Schenau (1992), their findings suggest that better performing sprinters adopted a whole-body orientation at toe-off that is similar to a more favourable (i.e., negative) toe-off distance. The findings of the current thesis suggest such a movement strategy is important for achieving high RF during the whole initial acceleration phase, where kinematic characteristics that position the whole-body CM further ahead of the base of support (i.e., contact foot) at touchdown and those that facilitate anterior translation during early stance before extension occurs, were strongly related to RF. The current findings also extend the findings by Jacobs and van Ingen Schenau (1992) to show that more favourable touchdown distance, facilitated by the repositioning of the stance leg more posteriorly during flight, may provide a benefit to both acceleration performance and RF capability. This is because adopting such a position at touchdown may reduce the requirement for the whole-body CM to rotate about the stance foot before leg extension can commence (i.e., the proximal to distal extension pattern described above can begin earlier because less rotation is required to get into favourable position). This links with theoretical findings by Bezodis et al. (2015), where sprinters' capability to produce high RF was found to increase with a more posteriorly positioned foot at touchdown. Bezodis et al. (2017) suggested that attempting to utilise both previously mentioned movement strategies (i.e., Jacobs & van Ingen Schenau (1992) and Bezodis et al. (2015)) by rotating the CM rapidly at touchdown (relative to the stance foot) with the stance foot further behind the CM, could exaggerate RF capability even further. This rapid rotation of the CM about the stance foot potentially links to the ankle dorsiflexion range of motion and peak dorsiflexion velocity findings from the current thesis. However, as previously

mentioned, the relationship between RF and peak dorsiflexion velocity was not significant, so further investigation is required to determine if this is the case.

#### **5.3.4 Spatiotemporal variables**

Average step frequency over four steps was very strongly related to  $RF_{MEAN}$  ( $r = 0.715$ ,  $p < 0.01$ ), while the relationship between average normalised step length and  $RF_{MEAN}$  was small and negative, but not significant ( $r = -0.296$ ). Previous studies have reported conflicting evidence on the relative importance of step length and step frequency for sprinting performance over a range of major sprint phases. However, it is important to consider the context of data collection and measures of sprint performance used by the different studies which likely explain the varied results reported. For example, Ito et al. (2006) found better sprinters had a larger step length between their first and second steps, when sprinters were classified using their 100 m personal best times. However, Nagahara et al. (2014a) found that the relative importance (i.e., for measured acceleration) of step length and step frequency changed depending on different sections of the sprint acceleration phase. Nagahara et al. (2014a) found that increasing step frequency was of most importance up to the third step but increasing step length was more important from the 5<sup>th</sup> to the 15<sup>th</sup> step. The results of the current thesis found that, for achieving high RF during the initial acceleration phase in isolation, higher step frequency is more strongly related to RF than higher step length.

The very strong relationship observed between step frequency and  $RF_{MEAN}$  may be indicative of a smaller vertical component of force being applied during each stance phase. As a large relative horizontal component ( $F_H$ ) of the resultant force vector ( $F_R$ ) is fundamentally required for achieving high RF, this is inherently accompanied by a relatively smaller vertical component of the vector. Nagahara et al. (2019b) found that step frequency increased in the initial two steps (through decreases in support time and flight time) when athletes were instructed to lean the body forward during acceleration. Nagahara et al. (2019b) suggested this change was caused by a notable decrease in vertical and braking impulse, without an increase in propulsive horizontal impulse. Therefore, a higher step frequency is possibly a function of the larger horizontal GRF component and smaller vertical component, and hence RF achieved, rather than being

a technical feature displayed by the sprinter that is associated with higher RF. However, due to the nature of the study design, the causality between interacting variables cannot be determined. As such, future investigation may be required if this interaction is to be investigated directly.

#### **5.4 How strongly do the kinematic characteristics, which are strongly related to RF, relate to initial acceleration phase performance?**

The third research question was addressed to ultimately determine if any of the RF-associated kinematic characteristics were related to performance, or to elucidate any potential conflicting findings between RF-associated kinematics and performance-associated kinematics. This investigation revealed that, among the RF-associated kinematics, only average normalised touchdown distance was also strongly and significantly related to performance over the initial acceleration phase ( $r = -0.710$ ,  $p < 0.01$ ). Each of the other kinematic characteristics of interest were moderately, but non-significantly, related to performance. However, each of the relationships observed with performance were in the same direction as those observed with  $RF_{MEAN}$ . Therefore, it can be concluded that, although they may not be directly beneficial to performance, the kinematic characteristics associated with high RF production, were not detrimental to initial acceleration phase performance.

Due to the exploratory nature of this thesis, the relationships between the dependent variables of interest (i.e., NAHEP,  $RF_{MEAN}$ , and normalised touchdown distance) and each of the measured kinematic and spatiotemporal variables were also analysed. A number of kinematic characteristics were strongly related to initial acceleration phase performance (NAHEP) but not strongly related to  $RF_{MEAN}$ . These were normalised toe-off distance, contact time, and touchdown hip angle ( $r = -0.664$ ,  $p < 0.01$ ;  $r = -0.738$ ,  $p < 0.01$ ;  $r = 0.536$ ,  $p < 0.05$ ; respectively; section 4.3.5). Contact time and touchdown hip angle were both also strongly related to normalised touchdown distance ( $r = 0.831$  and  $r = -0.746$ , respectively;  $p < 0.01$ ; appendix C). The strong relationship between NAHEP and a larger hip angle at touchdown again suggests that

greater performance may be achieved with the stance leg more posteriorly extended (i.e., due to a larger hip angle), relative to the upper body, which again suggests some interaction with the segment orientations comprising more favourable touchdown distance. The strong negative relationship between NAHEP and contact time, considering the strong positive relationship between normalised touchdown distance and contact time, may also suggest an important interaction between each of the aforementioned measures. If the contact foot is placed in a more anterior position compared to the CM at touchdown, there is theoretically more requirement for a long contact time to translate the whole-body CM into a more anterior position, relative to the foot (i.e., leaving foot in a posterior position), before extension occurs and toe-off is reached (i.e., resulting in a longer contact time). Therefore, where contact time is shorter, touchdown distance is less positive, and NAHEP is higher. This relationship also highlights an important consideration for the measured components comprising NAHEP and  $RF_{MEAN}$ , and the relationships between these measures and contact time. A mechanical link exists between NAHEP and  $RF_{MEAN}$ , as they both provide a quantity related to the propulsive impulse produced by the athlete. However, an important distinction between the two measures is the inclusion of the time component in NAHEP. Considering this distinction, it is to be expected that a stronger relationship was observed between contact time and NAHEP compared to  $RF_{MEAN}$ , as reduced contact time inherently increases NAHEP due to a smaller denominator in the calculation (i.e.,  $\Delta t$ ; equation 3.7).

The significant relationships found between NAHEP and normalised toe-off distance, contact time, and touchdown hip angle, reinforce the interaction between the lower limb segment configurations that comprise the favourable postural position for more negative touchdown distance and their association with initial acceleration phase performance. However, these relationships appear to contradict the traditional coaching paradigm of ‘front-side mechanics’ in sprint acceleration (Mann & Murphy, 2015). This coaching practice suggests that body segments that are positioned posteriorly to a theoretical straight line drawn through the upper body (i.e., trunk) are considered ‘back-side mechanics’, hence, those positioned anteriorly to such line are considered ‘front-side mechanics’. Mann and Murphy (2015) advocated that sprinters should be ‘front-side’ orientated from the very first step; stating that, for more than twenty years, coaches have attempted to optimise ‘front-side mechanics’ and minimise

‘back-side mechanics’ to increase acceleration performance. The findings of this thesis suggest that more negative touchdown and toe-off distance, hence maximising ‘back-side mechanics’, are strongly related to sprint acceleration performance. Haugen et al. (2017) also found that the relationship directions (i.e., with accelerated running performance) for most front- and back-side variables during accelerated running were opposite compared to how the theoretical concept has been described. Therefore, this thesis also provides some evidence to support the findings of Haugen et al. (2017), suggesting that optimising ‘back-side mechanics’ may be of more importance for sprint acceleration performance than ‘front-side mechanics’

As the majority of the RF-associated kinematics were not strongly related to performance, this suggests that each of the respective kinematic characteristics cannot solely be important for initial acceleration performance, rather that the interaction of a number of these kinematics may be required to achieve higher performance. From a series of stepwise multiple linear regressions (see appendix D) performed on pairs of kinematic characteristics strongly related to performance but not RF (i.e., normalised toe-off distance, contact time, and touchdown hip angle) and the kinematic characteristics strongly related to RF but not performance (i.e., step frequency, ankle dorsiflexion range of motion, touchdown foot angle, and touchdown shank angle), the only findings of statistical significance were the couples of ‘normalised toe-off distance; normalised touchdown distance’ and ‘normalised toe-off distance; ankle dorsiflexion range of motion’. These couples accounted for 66% and 60% of the variance (adjusted  $R^2$ ) in NAHEP, respectively, with relative importance (i.e.,  $\beta$ -coefficient) of -0.481;-0.549 and -0.666;0.461, respectively. Within these pairs, ‘normalised toe-off distance; ankle dorsiflexion range of motion’ provided the only notable insight. As ankle dorsiflexion range of motion combined with normalised toe-off distance to account for 60% of the variance in NAHEP, this suggests that higher performance can be achieved if sprinters dorsiflex more during early stance, but this further dorsiflexion must facilitate, or be accompanied by, more favourable toe-off distance (i.e., CM further ahead of the stance foot at toe-off). These multiple linear regressions to explore potential interactions between kinematic features were included as a supplementary approach to identify further ways to potentially investigate and understand the relationships between kinematic characteristics, RF, and initial acceleration phase performance in future research. Although outside of the scope of

the aim of the current thesis, future work could explore such methods with a larger sample size where more complex analyses using a regression-based approach with multiple variables are viable.

## **5.5 Limitations and considerations for future research**

The data presented in this thesis was collected from a cohort of fourteen trained male sprinters who completed maximal sprint efforts from a block start. This population was used so it was similar to that used in previous studies that have investigated acceleration performance from a block start (i.e., Bezodis et al. 2020). However, future research could potentially benefit from analysing the kinematic characteristics of interest presented in this thesis within other populations such as elite/world class sprinters or female sprinters to explore if athletes of a higher performance level or different sex exhibit the same or different kinematic characteristics to achieve high RF and performance during the initial acceleration phase. In extension to this, a larger sample size from any of the aforementioned populations would be of benefit to future investigations, allowing exploration of more complex regression analyses. As the data presented in this thesis was collected from a block start, the kinematic characteristics observed in the first steps on the track may be considerably different from those exhibited during a standing start. While athletes who practice other sports, where the ability to accelerate may be crucial for success, may be interested in the findings of this thesis, the practical implications of these findings may not be transferrable to other populations, compared to sprinters who typically start from a block start (Wild et al., 2018). This limitation may be particularly relevant for sprinters who participate in relay events and many team sports athletes. Therefore, future research could be conducted to investigate similar research questions in team sports athletes starting from a standing position should practitioners in these sports wish to understand the kinematic features associated with high RF producing abilities.

An additional methodological consideration is in respect to the modelling of the foot. In the current thesis, the foot segment was modelled as a rigid segment from the toe marker to the heel marker. However, as the foot is a deformable segment, where the interaction with the ground at each touchdown event may be affected by movement at the various joints within



the foot, greater consideration of the modelling of the foot may be warranted in future studies, particularly given the findings of the current thesis that the foot, ankle, and shank kinematics are associated with high RF. The current thesis used an end-to-end rigid segment definition for the foot to achieve a more global representation of the overall foot orientation without consideration for the within foot motion, whilst for calculating ankle angle an ankle joint centre-MTP joint centre segment definition was used to provide a closer representation of the true ankle kinematics. As the findings of the current thesis suggest that higher RF capability is more likely dictated by action around the ankle joint, through the interaction of the foot and shank, than more proximal segments, future research could consider adopting a more complex foot model including within-foot motion to extend the current understanding. However, if a multi-segment foot model is used, caution must be applied to the experimental protocol and marker model used to ensure that accurate multi-segment foot kinematics are obtained. As there is a possibility to introduce inaccuracies in data collected from a larger number of spike-mounted markers, recent studies have mounted markers on the foot by cutting holes in the running shoe to increase the accuracy of their findings (Trudeau et al., 2017). Therefore, it is advised that more detailed foot modelling in the context of sprinting should consider adopting such practices if such a detailed foot model is to be incorporated in future research in the current area of interest.

Due to the exploratory nature of this thesis, a large range of kinematic characteristics were measured and correlated with  $RF_{MEAN}$  to comprehensively determine the strength of the relationships between such measures and identify the most strongly related characteristics. However, undertaking a large number of statistical tests without applying a correction inherently increases the likelihood of a type I error (Field, 2017). A correction was not applied to the relationships comprising the primary findings of this thesis (i.e., relationships between kinematic characteristics and  $RF_{MEAN}$ ) because of the exploratory nature of this research and thus it was deemed that this was preferable above increasing the likelihood of a type II error. This has enabled the establishment of significant relationships that may exist between the measured variables which can then be used to inform future investigations with a smaller, more focused scope. Therefore, as a number of significant relationships were observed between kinematic characteristics, particularly those toward the distal end of the stance leg, and  $RF_{MEAN}$ , future research can focus on exploring these findings in more detail

without needing to consider some of the other variables considered in this thesis, and can thus utilise robust statistical analyses to more confidently determine the strength of the relationships observed as well as investigating potential explanations for them.

Lastly, as described in section 5.3.1, the current thesis focussed on kinematics of the stance leg and thus did not directly investigate characteristics related to the swing leg. However, future research could benefit from an investigation into the kinematic characteristics of the swing leg in relation to RF during the initial acceleration phase to explore the effect that swing leg positions may have on creating favourable touchdown/toe-off distance.

## **5.6 Practical implications**

The findings of the current thesis suggest that step-to-step variation in RF during the initial acceleration phase of sprinting is not related to performance, and that  $RF_{MEAN}$  is the only measure of ‘technical performance’ that is strongly related to performance during the initial acceleration phase. Therefore, sprinters and coaches should prioritise the production of a high RF over the whole initial acceleration phase above trying to ensure a consistent decline in RF as velocity increases. With respect to achieving this high  $RF_{MEAN}$ , and also for maximising acceleration performance, negative touchdown distance was the only measure to be strongly associated with both measures. As the trajectory of the CM is pre-determined during flight, sprinters who demonstrated this favourable whole-body position at touchdown likely achieved it by repositioning the stance leg during flight to touchdown with a more posteriorly extended leg. Therefore, the foot and shank segment angles were more forward at touchdown to position their contact foot further behind their CM (or less far in front as the initial acceleration phase progressed). Therefore, sprinters should attempt to reposition the stance leg to achieve this configuration during flight to maximise the difference in displacement between the whole-body CM and the contact foot at touchdown during each of the four steps that comprise the initial acceleration phase. Following touchdown, ankle dorsiflexion range of motion was very strongly related to  $RF_{MEAN}$ , suggesting that this forward rotation to potentially translate the CM more anteriorly during early stance is important

for achieving high RF. However, with regards to its importance for acceleration performance, this dorsiflexion during early-stance also potentially needs to lead to a more negative toe-off distance (i.e., the CM further ahead of the stance toe at toe-off). To maximise RF capability following touchdown during initial acceleration, sprinters and coaches should prioritise dorsiflexion at the ankle during early stance by attempting to actively dorsiflex above trying to maintain stiffness at the ankle, or by working to increase flexibility of the ankle to allow more passive dorsiflexion range of motion.

To allow the acute manipulation and long-term training of a sprinter's kinematics during the initial acceleration phase to mimic the favourable features highlighted in this thesis, coaches would need to design and implement drills during training. These drills should encourage the adoption of such movement strategies to enhance RF capability. Coaches may consider consulting strength and conditioning coaches or skill acquisition specialists to help to develop training programmes to achieve the technical or physical changes required so the athlete can adopt such favourable kinematic characteristics during sprint acceleration.

## **5.7 Thesis conclusion**

This thesis aimed to investigate the relationships between kinematic characteristics and RF during the initial acceleration phase of sprinting. A preliminary investigation into the relationships between RF-associated measures and initial acceleration performance was conducted to evaluate their relative importance as performance determinants and to assess the effect of step-to-step variation in RF on initial acceleration performance. The results revealed that  $RF_{MEAN}$  was the only significant predictor of performance (quantified by NAHEP), among the RF-associated measures of interest, and step-to-step variation in RF was not related to performance. As such, technical performance during initial acceleration can be appropriately quantified using mean RF over the four steps, and sprinters and coaches should prioritise the production of a high RF over the whole initial acceleration phase above trying to ensure a consistent decline in RF as velocity increases. To address the primary aim of this thesis, kinematic characteristics

averaged over four steps were then investigated in relation to  $RF_{MEAN}$ . At touchdown, a negative touchdown distance, where the stance foot was placed in a more posterior position relative to the CM, was found to be associated with a higher mean RF. The lower limb segment positions that likely comprised this negative touchdown distance, and were very strongly associated with high RF, were more a forward orientation of the foot and shank segments. Following touchdown, ankle dorsiflexion range of motion was very strongly related to  $RF_{MEAN}$ , suggesting that allowing more dorsiflexion during early stance through the initial acceleration phase is important for achieving high RF. On a higher level looking at spatiotemporal step characteristics, a very strong relationship was found between step frequency and  $RF_{MEAN}$ , which is likely a result of a lower proportion of the vertical component of the resultant force vector when high RF is achieved, leading to reduced contact and flight times. Although none of the kinematic characteristics associated with RF caused a detrimental effect to performance, only touchdown distance was strongly related to both RF and initial acceleration performance. Sprinters should attempt to maximise the difference in displacement between the whole-body CM and the contact foot at touchdown during each of the four steps comprising the initial acceleration phase. As the trajectory of the CM is pre-determined during flight, sprinters can achieve this through repositioning the stance leg during flight to touchdown with a posteriorly extended leg, where the foot and shank segments are orientated further forward. Following touchdown, sprinters and coaches should prioritise dorsiflexion at the ankle during early stance by attempting to actively dorsiflex above trying to maintain stiffness at the ankle, or by working to increase flexibility of the ankle to allow more passive dorsiflexion range of motion.

## REFERENCE LIST

- Ae, M., Tang, H. and Yokoi, T. (1992) 'Estimation of inertia properties of the body segments in Japanese athletes', *Biomechanisms*, 11, pp. 23–33. doi:10.3951/biomechanisms.11.23.
- Arsac, L.M. and Locatelli, E. (2002) 'Modeling the energetics of 100-m running by using speed curves of world champions', *Journal of Applied Physiology*, 92(5), pp. 1781–1788. doi:10.1152/jappphysiol.00754.2001.
- Batterham, A. and Hopkins, W. (2006) 'Making meaningful inferences about magnitudes', *International journal of sports physiology and performance*, 1, pp. 50–7. doi:10.1123/ijsp.1.1.50.
- Baumann, W. (1976) 'Kinematic and dynamic characteristics of the sprint start', *Biomechanics V-B*, pp. 194–199.
- Bayne, H. (2018) 'Force-velocity-power profiles of elite sprinters: inter-and intra-individual determinants of performance', *ISBS Proceedings Archive*, 36(1), Article. 245.
- Bayne, H., Donaldson, B. and Bezodis, N. (2020) 'Inter-limb coordination during sprint acceleration', *ISBS Proceedings Archive*, 38(1), p. 448.
- Bezodis, N.E., Colyer, S., Nagahara, R., Bayne, H., Bezodis, I.N., Morin, J.-B., Murata, M. and Samozino, P. (2020). 'Understanding ratio of forces during early acceleration: calculation considerations and implications for practice'. (Preprint) doi: 10.31236/osf.io/742nv.
- Bezodis, N.E., Colyer, S., Nagahara, R., Bayne, H., Bezodis, I.N., Morin, J.-B., Murata, M. and Samozino, P. (2021) 'Ratio of forces during sprint acceleration: A comparison of different calculation methods', *Journal of Biomechanics*, 127, p. 110685. doi:10.1016/j.jbiomech.2021.110685.
- Bezodis, N.E., North, J.S. and Razavet, J.L. (2017) 'Alterations to the orientation of the ground reaction force vector affect sprint acceleration performance in team sports athletes', *Journal of Sports Sciences*, 35(18), pp. 1817–1824. doi:10.1080/02640414.2016.1239024.
- Bezodis, N.E., Salo, A.I.T. and Trewartha, G. (2010) 'Choice of sprint start performance measure affects the performance-based ranking within a group of sprinters: which is the most appropriate measure?', *Sports Biomechanics*, 9(4), pp. 258–269. doi:10.1080/14763141.2010.538713.
- Bezodis, N.E., Salo, A.I.T. and Trewartha, G. (2014) 'Lower limb joint kinetics during the first stance phase in athletics sprinting: three elite athlete case studies', *Journal of Sports Sciences*, 32(8), pp. 738–746. doi:10.1080/02640414.2013.849000.

Bezodis, N.E., Salo, A.I.T. and Trewartha, G. (2015a) 'Relationships between lower-limb kinematics and block phase performance in a cross section of sprinters', *European Journal of Sport Science*, 15(2), pp. 118–124. doi:10.1080/17461391.2014.928915.

Bezodis, N.E., Trewartha, G. and Salo, A.I.T. (2015b) 'Understanding the effect of touchdown distance and ankle joint kinematics on sprint acceleration performance through computer simulation', *Sports Biomechanics*, 14(2), pp. 232–245. doi:10.1080/14763141.2015.1052748.

Bezodis, N.E., Willwacher, S. and Salo, A.I.T. (2019) 'The biomechanics of the track and field sprint start: A narrative review', *Sports Medicine*, 49(9), pp. 1345–1364. doi:10.1007/s40279-019-01138-1.

Brazil, A., Exell, T., Wilson, C., Willwacher, S., Bezodis, I.N. and Irwin, G. (2017) 'Lower limb joint kinetics in the starting blocks and first stance in athletic sprinting', *Journal of Sports Sciences*, 35(16), pp. 1629–1635. doi:10.1080/02640414.2016.1227465.

Charalambous, L., Irwin, G., Bezodis, I.N. and Kerwin, D. (2012) 'Lower limb joint kinetics and ankle joint stiffness in the sprint start push-off', *Journal of Sports Sciences*, 30(1), pp. 1–9. doi:10.1080/02640414.2011.616948.

Colyer, S.L., Graham-Smith, P. and Salo, A.I.T. (2019) 'Associations between ground reaction force waveforms and sprint start performance', *International Journal of Sports Science & Coaching*, 14(5), pp. 658–666. doi:10.1177/1747954119874887.

Colyer, S.L., Nagahara, R. and Salo, A.I.T. (2018) 'Kinetic demands of sprinting shift across the acceleration phase: Novel analysis of entire force waveforms', *Scandinavian Journal of Medicine & Science in Sports*, 28(7), pp. 1784–1792. doi:10.1111/sms.13093.

Crick, T. (2014) 'Event group endurance technical model: high speed and submaximal running - The Drive Phase' Available at: <https://www.ulearnathletics.com/> (Accessed: 5 January 2021).

Debaere, S., Delecluse, C., Aerenhouts, D., Hagman, F. and Jonkers, I. (2013) 'From block clearance to sprint running: Characteristics underlying an effective transition', *Journal of Sports Sciences*, 31(2), pp. 137–149. doi:10.1080/02640414.2012.722225.

Delecluse, C., Coppennolle, H.V., Willems, E., Leemputte, M.V., Diels, R. and Goris, M. (1995) 'Influence of high-resistance and high-velocity training on sprint performance', *Medicine & Science in Sports & Exercise*, 27(8), pp. 1203–1209.

di Prampero, P.E., Fusi, S., Sepulcri, L., Morin, J.B., Belli, A. and Antonutto, G. (2005) 'Sprint running: a new energetic approach', *The Journal of Experimental Biology*, 208(Pt 14), pp. 2809–2816. doi:10.1242/jeb.01700.

- Donaldson, B., Bayne, H. and Bezodis, N. (2020) ‘A comparison of trunk and shank angles between elite and sub-elite sprinters during sprint acceleration’, *ISBS Proceedings Archive*, 38(1), p. 744.
- Donaldson, B., Bayne, H. and Bezodis, N. (2021) ‘Step-to-step changes in foot-shank coordination during initial sprint acceleration’, *1st Conference of the South African Society of Biomechanics*.
- Dorel, S., Couturier, A., Lacour, J.-R., Vandewalle, H., Hautier, C. and Hug, F. (2010) ‘Force-velocity relationship in cycling revisited: benefit of two-dimensional pedal forces analysis’, *Medicine and Science in Sports and Exercise*, 42(6), pp. 1174–1183. doi:10.1249/MSS.0b013e3181c91f35.
- Dyson, G.H.G. (1973). *The mechanics of athletics*. 6th Edition. London: University of London Press.
- Field, A. (2017). *Discovering Statistics Using IBM SPSS Statistics*. 5<sup>th</sup> Edition. SAGE Publications Ltd.
- Golden, G., Pavol, M. and Hoffman, M. (2009) ‘Knee joint kinematics and kinetics during a lateral false-step maneuver’, *Journal of athletic training*, 44, pp. 503–10. doi: 10.4085/1062-6050-44.5.503.
- Hall, S.J. (2019) *Basic biomechanics*. 8<sup>th</sup> Edition. New York, NY : McGraw-Hill Education.
- Harland, M.J. and Steele, J.R. (1997) ‘Biomechanics of the sprint start’, *Sports Medicine*, 23(1), pp. 11–20. doi:10.2165/00007256-199723010-00002.
- Haugen, T., Danielsen, J., Alnes, L., McGhie, D., Sandbakk, O. and Ettema, G. (2017) ‘On the importance of “front-side mechanics” in athletics sprinting’, *International Journal of Sports Physiology and Performance*, 13. doi:10.1123/ijsp.2016-0812.
- Haugen, T., Del, F. and Seiler, S. (2019) ‘Sprint mechanical variables in elite athletes: Are force-velocity profiles sport specific or individual?’, *PLoS ONE*, 14. doi:10.1371/journal.pone.0215551.
- Hay, J. G. (1994) *The biomechanics of sports techniques*. 4th Edition. London: Prentice Hall International.
- Hof, A. (1996) ‘Scaling gait data to body size’, *Gait & Posture*, 4, pp. 222–223. doi:10.1016/0966-6362(95)01057-2.
- Hojka, V., Bacakova, R. and Kubovy, P. (2016) ‘Differences in kinematics of the support limb depends on specific movement tasks of take-off’, *Acta Gymnica*, 46(2), pp. 82–89. doi:10.5507/ag.2016.005.

- Hunter, J., Marshall, R. and McNair, P. (2004) 'Interaction of step length and step rate during sprint running', *Medicine & Science in Sports & Exercise*, 36(2), pp. 261–271. doi: 10.1249/01.MSS.0000113664.15777.53.
- Hunter, J.P., Marshall, R.N. and McNair, P. (2005) 'Relationships between ground reaction force impulse and kinematics of sprint-running acceleration', *Journal of Applied Biomechanics*, 21(1), pp. 31–43. doi:10.1123/jab.21.1.31.
- Ito, A., Ishikawa, M., Isolehto, J. and Komi, P. V. (2006) 'Changes in the step width, step length, and step frequency of the world's top sprinters during the 100 metres', *New Studies in Athletics*, 21, pp. 35–39.
- Jacobs, R. and van Ingen Schenau, G. J. (1992) 'Intermuscular coordination in a sprint push-off', *Journal of Biomechanics*, 25(9), pp. 953–965. doi: 10.1016/0021-9290(92)90031-u.
- Kawamori, N., Nosaka, K. and Newton, R.U. (2013) 'Relationships between ground reaction impulse and sprint acceleration performance in team sport athletes', *Journal of Strength and Conditioning Research*, 27(3), pp. 568–573. doi:10.1519/JSC.0b013e318257805a.
- Kugler, F. and Janshen, L. (2010) 'Body position determines propulsive forces in accelerated running', *Journal of biomechanics*, 43, pp. 343–8. doi: 10.1016/j.jbiomech.2009.07.041.
- Lockie, R.G., Murphy, A.J., Schultz, A.B., Jeffriess, M.D. and Callaghan, S.J. (2013) 'Influence of sprint acceleration stance kinetics on velocity and step kinematics in field sport athletes', *The Journal of Strength & Conditioning Research*, 27(9), pp. 2494–2503. doi:10.1519/JSC.0b013e31827f5103.
- Lockie, R.G., Murphy, A.J., Schultz, A.B., Knight, T.J. and de Jonge, X.A.K.J. (2012) 'The effects of different speed training protocols on sprint acceleration kinematics and muscle strength and power in field sport athletes', *Journal of Strength and Conditioning Research*, 26(6), pp. 1539–1550. doi:10.1519/JSC.0b013e318234e8a0.
- Mackala, K. (2007). Optimisation of performance through kinematic analysis of the different phases of the 100 metres. *New Studies in Athletics*, 22(2), pp. 7-16.
- Maćkała, K., Fostiak, M. and Kowalski, K. (2015) 'Selected determinants of acceleration in the 100m sprint', *Journal of Human Kinetics*, 45, pp. 135–148. doi:10.1515/hukin-2015-0014.
- Mann, R. and Murphy, A. (2015) *The Mechanics of Sprinting and Hurdling: 2015 Edition. CreateSpace Independent Publishing Platform.*
- Matsuo, A., Mizutani, M., Nagahara, R., Fukunaga, T. and Kanehisa, H. (2019) 'External mechanical work done during the acceleration stage of maximal sprint running and its association with running performance', *Journal of Experimental Biology*, 222(5). doi:10.1242/jeb.189258.



- Mero, A., Kuitunen, S., Harland, M., Kyröläinen, H. and Komi, P.V. (2006) 'Effects of muscle – tendon length on joint moment and power during sprint starts', *Journal of Sports Sciences*, 24(2), pp. 165–173. doi:10.1080/02640410500131753.
- Mero, A., Luhtanen, P. and Komi, P.V., (1983). 'A biomechanical study of the sprint start'. *Scandinavian Journal of Sports Science*, 5(1), pp.20-28.
- Moir, G., Sanders, R., Button, C. and Glaister, M. (2007) 'The effect of periodized resistance training on accelerative sprint performance', *Sports Biomechanics*, 6(3), pp. 285–300. doi:10.1080/14763140701489793.
- Morin, J.-B., Bourdin, M., Edouard, P., Peyrot, N., Samozino, P. and Lacour, J.-R. (2012) 'Mechanical determinants of 100-m sprint running performance', *European Journal of Applied Physiology*, 112(11), pp. 3921–3930. doi: 10.1007/s00421-012-2379-8.
- Morin, J.-B., Edouard, P. and Samozino, P. (2011) 'Technical ability of force application as a determinant factor of sprint performance', *Medicine and Science in Sports and Exercise*, 43(9), pp. 1680–1688. doi:10.1249/MSS.0b013e318216ea37.
- Morin, J.-B., Gimenez, P., Edouard, P., Arnal, P., Jimenez-Reyes, P., Samozino, P., Brughelli, M. and Mendiguchia, J. (2015) 'Sprint acceleration mechanics: the major role of hamstrings in horizontal force production', *Frontiers in Physiology*, 6. doi: 10.3389/fphys.2015.00404.
- Morin, J.-B., Samozino, P., Murata, M., Cross, M. R. and Nagahara, R. (2019) 'A simple method for computing sprint acceleration kinetics from running velocity data: Replication study with improved design', *Journal of Biomechanics*, 94, pp. 82–87. doi: 10.1016/j.jbiomech.2019.07.020.
- Murata, M., Takai, Y., Kanehisa, H., Fukunaga, T. and Nagahara, R. (2018) 'Spatiotemporal and kinetic determinants of sprint acceleration performance in soccer players', *Sports (Basel, Switzerland)*, 6(4). doi:10.3390/sports6040169.
- Nagahara, R. and Zushi, K. (2017) 'Development of maximal speed sprinting performance with changes in vertical, leg and joint stiffness', *The Journal of Sports Medicine and Physical Fitness*, 57(12), pp. 1572–1578. doi:10.23736/S0022-4707.16.06622-6.
- Nagahara, R., Amini, E., Marcon, K.C.C., Chen, P.-W., Chua, J., Eiberger, J., Futral, N.J.C., Lye, J., Pantovic, M.M., Starczewski, M., Sudsard, K., Sumartiningsih, S., Wang, C.-Y., William, T.B., Kasujja, T. and Gujar, T.A. (2019b) 'Influence of the intention to lean the body forward on kinematics and kinetics of sprinting for active adults', *Sports*, 7(6), p. 133. doi:10.3390/sports7060133.
- Nagahara, R., Kanehisa, H. and Fukunaga, T. (2020) 'Ground reaction force across the transition during sprint acceleration', *Scandinavian Journal of Medicine & Science in Sports*, 30(3), pp. 450–461. doi:10.1111/sms.13596.

- Nagahara, R., Kanehisa, H., Matsuo, A. and Fukunaga, T. (2019a) 'Are peak ground reaction forces related to better sprint acceleration performance?', *Sports Biomechanics*, pp. 1–10. doi: 10.1080/14763141.2018.1560494.
- Nagahara, R., Matsubayashi, T., Matsuo, A. and Zushi, K. (2014b) 'Kinematics of transition during human accelerated sprinting', *Biology Open*, 3(8), pp. 689–699. doi:10.1242/bio.20148284.
- Nagahara, R., Matsubayashi, T., Matsuo, A. and Zushi, K. (2017) 'Alteration of swing leg work and power during human accelerated Sprinting', *Biology Open*, 6, p. bio.024281. doi: 10.1242/bio.024281.
- Nagahara, R., Matsubayashi, T., Matsuo, A. and Zushi, K. (2018b) 'Kinematics of the thorax and pelvis during accelerated sprinting', *Journal of Sports Medicine and Physical Fitness*, 58(9), pp. 1253–1263. doi:10.23736/S0022-4707.17.07137-7.
- Nagahara, R., Mizutani, M., Matsuo, A., Kanehisa, H. and Fukunaga, T. (2018a) 'Association of sprint performance with ground reaction forces during acceleration and maximal speed phases in a single sprint', *Journal of Applied Biomechanics*, 34(2), pp. 104–110. doi: 10.1123/jab.2016-0356.
- Nagahara, R., Naito, H., Morin, J.-B. and Zushi, K. (2014a) 'Association of acceleration with spatiotemporal variables in maximal sprinting', *International Journal of Sports Medicine*, 35(9), pp. 755–761. doi: 10.1055/s-0033-1363252.
- Napier, C., Cochrane, C., Taunton, J. and Hunt, M. (2015) 'Gait modifications to change lower extremity gait biomechanics in runners: A systematic review', *British journal of sports medicine*, 49. doi:10.1136/bjsports-2014-094393.
- Newans, T., Bellinger, P., Dodd, K. and Minahan, C. (2019) 'Modelling the acceleration and deceleration profile of elite-level soccer players', *International Journal of Sports Medicine*, 40(5), pp. 331–335. doi: 10.1055/a-0853-7676.
- Otsuka, M., Shim, J.K., Kurihara, T., Yoshioka, S., Nokata, M. and Isaka, T. (2014) 'Effect of expertise on 3D force application during the starting block phase and subsequent steps in sprint running', *Journal of Applied Biomechanics*, 30(3), pp. 390–400. doi:10.1123/jab.2013-0017.
- Pavei, G., Zamparo, P., Fujii, N., Otsu, T., Numazu, N., Minetti, A. E. and Monte, A. (2019) 'Comprehensive mechanical power analysis in sprint running acceleration', *Scandinavian Journal of Medicine & Science in Sports*, 29(12), pp. 1892–1900. doi: <https://doi.org/10.1111/sms.13520>.
- Plamondon A. and Roy B. (1984) 'Kinematics and kinetics of sprint acceleration', *Canadian Journal of Applied Sport Sciences*, 9(1), pp. 42–52.
- Rabita, G., Dorel, S., Slawinski, J., Sàez-de-Villarreal, E., Couturier, A., Samozino, P. and Morin, J.-B. (2015) 'Sprint mechanics in world-class athletes: a new insight into the limits of human locomotion', *Scandinavian Journal of Medicine & Science in Sports*, 25(5), pp. 583–594. doi: 10.1111/sms.12389.

Robertson, D., Caldwell, G., Hamill, J., Kamen, G. and Whittlesey, S. (2013) *Research Methods in Biomechanics*. 2nd edition. Champaign, IL: Human Kinetics Publ.

Samozino, P. (2018) 'A simple method for measuring force, velocity and power capabilities and mechanical effectiveness during sprint running', in *Biomechanics of Training and Testing: Innovative Concepts and Simple Field Methods*, pp. 237–267. doi: 10.1007/978-3-319-05633-3\_11.

Samozino, P., Rabita, G., Dorel, S., Slawinski, J., Peyrot, N., Villarreal, E. S. de and Morin, J.-B. (2016) 'A simple method for measuring power, force, velocity properties, and mechanical effectiveness in sprint running', *Scandinavian Journal of Medicine & Science in Sports*, 26(6), pp. 648–658. doi: <https://doi.org/10.1111/sms.12490>.

Sandstrom R., (1983) 'Improvement of acceleration' in: 'Sprints and relays: contemporary theory, technique and training'. 52-55; 2nd edition. Los Altos (CA): TAFNEWS Press.

Schache, A.G., Lai, A.K.M., Brown, N.A.T., Crossley, K.M. and Pandy, M.G. (2019) 'Lower-limb joint mechanics during maximum acceleration sprinting', *Journal of Experimental Biology*, 222(22). doi:10.1242/jeb.209460.

Suzuki, Y., Ae, M., Takenaka, S. and Fujii, N. (2014) 'Comparison of support leg kinetics between side-step and cross-step cutting techniques', *Sports Biomechanics*, 13(2), pp. 144–153. doi: 10.1080/14763141.2014.910264.

Trudeau, M., Jewell, C., Rohr, E., Fischer, K., Willwacher, S., Brüggemann, G.-P. and Hamill, J. (2017) 'The calcaneus adducts more than the shoe's heel during running', *Footwear Science*, 9, pp. 1–7. doi: 10.1080/19424280.2017.1334712.

Van Caekenberghe, I., Segers, V., Aerts, P., Willems, P. and De Clercq, D. (2013) 'Joint kinematics and kinetics of overground accelerated running versus running on an accelerated treadmill', *Journal of the Royal Society Interface*, 10(84). doi:10.1098/rsif.2013.0222.

van Ingen Schenau, G.J., Jacobs, R. and de Koning, J.J. (1991) 'Can cycle power predict sprint running performance?', *European Journal of Applied Physiology and Occupational Physiology*, 63(3), pp. 255–260. doi:10.1007/BF00233857.

von Lieres und Wilkau, H., Irwin, G., Bezodis, N. E., Simpson, S. and Bezodis, I. N. (2018) 'Phase analysis in maximal sprinting: an investigation of step-to-step technical changes between the initial acceleration, transition and maximal velocity phases.' *SportRxiv*. doi: 10.31236/osf.io/bmhdg.

von Lieres und Wilkau, H., Irwin, G., Bezodis, N.E., Simpson, S. and Bezodis, I.N. (2017) 'Contributions to braking impulse during initial acceleration, transition and maximal velocity in sprinting', *ISBS Proceedings Archive*: 35(1), Article 261.

- Walker, J., Bissas, A., Paradisis, G.P., Hanley, B., Tucker, C.B., Jongerius, N., Thomas, A., von Lieres und Wilkau, H.C., Brazil, A., Wood, M.A., Merlino, S., Vazel, P.-J. and Bezodis, I.N. (2021) 'Kinematic factors associated with start performance in World-class male sprinters', *Journal of Biomechanics*, 124, p. 110554. doi:10.1016/j.jbiomech.2021.110554.
- Weyand, P.G., Sternlight, D.B., Bellizzi, M.J. and Wright, S. (2000) 'Faster top running speeds are achieved with greater ground forces not more rapid leg movements', *Journal of Applied Physiology*, 89(5), pp. 1991–1999. doi: 10.1152/jappl.2000.89.5.1991
- Wild, J. J., Bezodis, I. N., North, J. S. and Bezodis, N. E. (2018) 'Differences in step characteristics and linear kinematics between rugby players and sprinters during initial sprint acceleration', *European Journal of Sport Science*, 18(10), pp. 1327–1337. doi: 10.1080/17461391.2018.1490459.
- Willwacher, S., Herrmann, V., Heinrich, K., Funken, J., Strutzenberger, G., Goldmann, J.-P., Braunstein, B., Brazil, A., Irwin, G., Potthast, W. and Brüggemann, G.-P. (2016) 'Sprint start kinetics of amputee and non-amputee sprinters', *PloS One*, 11(11), p. e0166219. doi:10.1371/journal.pone.0166219.
- Winter, D. (2009) *Biomechanics and motor control of human movement*, 4th Edition. New Jersey: John Wiley & Sons. doi: 10.1002/9780470549148.ch5.
- Zameziati, K., Mornieux, G., Rouffet, D. and Belli, A. (2006) 'Relationship between the increase of effectiveness indexes and the increase of muscular efficiency with cycling power', *European Journal of Applied Physiology*, 96(3), pp. 274–281. doi:10.1007/s00421-005-0077-5.

## APPENDICES

### Appendix A: Residual analysis to select the cut-off frequency of the Butterworth low-pass filter used to smooth the kinematic data

The residual analysis was conducted, manually using chart and line tools in Excel, on the vertical and antero-posterior axes of four marker trajectories (toe, lateral ankle, lateral knee & hip markers) for three randomly chosen sprinters from the cohort following procedures by Winter (2009). The cut-off frequencies determined from the residual analysis for each axis for each marker were subsequently averaged across all markers for a participant and then averaged across all between participants to obtain an appropriate cut-off frequency for applying to the kinematic data (Table A1).

**Table (A1).** Cut-off frequencies for antero-posterior (A-P) and vertical (V) coordinate trajectories across toe, lateral ankle, lateral knee, and lateral hip markers on three participants, with determined cut-off frequency (Fc) for the kinematic data.

	Participant 1	Participant 5	Participant 10	
Toe A-P	13	13	13	
Toe V	15	14	13	
Lateral ankle A-P	12	15	12	
Lateral ankle V	14	18	14	
Lateral knee A-P	11	12	11	
Lateral knee V	14	17	13	
Lateral hip A-P	15	12	11	
Lateral hip V	14	16	16	
				<b>Fc</b>
Average	14	15	13	14

The residual analysis determined that the appropriate cut-off frequency for the Butterworth low-pass filter was 14 Hz, this frequency was used to apply the filter to all of the kinematic data presented in this thesis.

## Appendix B: Pairwise comparisons for significant effects between steps

For measures where a main effect of step number was identified, pairwise comparisons with Bonferroni adjustment were calculated to identify any pairwise significant effects between each of the four steps. For variables that did not show significant step-to-step differences across all steps, full details of these pairwise effects are presented below.

**Table (B1).** Significant step-to-step differences for measures where a significant main effect of step number over the four steps was identified.

Measure	Units	Step 1	Step 2	Step 3	Step 4
Average $F_R$ magnitude	(BW)	3 4	3 4	1 2	1 2
Peak $F_R$ magnitude	(BW)	4	3 4	2	1 2
Average $F_H$ component	(BW)	2 3 4	1 3 4	1 2	1 2
Peak propulsive $F_H$ component	(BW)	2 3 4	1 4	1	1 2
Peak braking $F_H$ component	(BW)	-	4	-	2
Average $F_V$ component	(BW)	3 4	3 4	1 2 4	1 2 3
Peak $F_V$ component	(BW)	3 4	3 4	1 2	1 2
AHEP	(W)	2 3 4	1	1	1
NAHEP		2 3 4	1	1	1
Normalised touchdown distance		2 3 4	1 3 4	1 2	1 2
Flight time	(s)	2 3 4	1 4	1	1 2
Step frequency	(steps.s <sup>-1</sup> )	3 4	4	1	1 2
Foot touchdown velocity	(m.s <sup>-1</sup> )	-	4	-	2
Ankle dorsiflexion RoM	(°)	3	4	1	2
Ankle plantar flexion RoM	(°)	4	4	4	1 2 3
Ankle angle at toe-off	(°)	4	-	-	1
Ankle angular velocity at touchdown	(°.s <sup>-1</sup> )	2 3 4	1 4	1	1 2
Ankle peak dorsiflexion velocity	(°.s <sup>-1</sup> )	2 3 4	1 4	1 4	1 2 3
Ankle angular velocity at toe-off	(°.s <sup>-1</sup> )	3 4	-	1	1
Knee early flexion RoM	(°)	-	-	-	-
Knee extension RoM	(°)	3 4	3 4	1 2 4	1 2 3
Knee late flexion RoM	(°)	-	-	-	-
Knee angular velocity at touchdown	(°.s <sup>-1</sup> )	3 4	4	1	1 2
Knee peak extension velocity	(°.s <sup>-1</sup> )	3 4	-	1	1
Knee peak flexion velocity	(°.s <sup>-1</sup> )	2	1	-	-
Knee angular velocity at toe-off	(°.s <sup>-1</sup> )	2 3 4	1 4	1	1 2
Hip angle at touchdown	(°)	3 4	-	1	1
Hip extension RoM	(°)	3	-	1	-
Hip angle at toe-off	(°)	4	4	4	1 2 3
Hip angular velocity at toe-off	(°.s <sup>-1</sup> )	3 4	4	1	1 2
Foot angle at touchdown	(°)	2 3 4	1 3 4	1 2	1 2
Foot angle at toe-off	(°)	3 4	4	1	1 2
Foot angular velocity at touchdown	(°.s <sup>-1</sup> )	3 4	3 4	1 2	1 2
Foot angular velocity at toe-off	(°.s <sup>-1</sup> )	3	-	1	-

Measure	Units	Step 1	Step 2	Step 3	Step 4
Shank angle at touchdown	(°)	2 3 4	1	1	1
Thigh angle at touchdown	(°)	3 4	-	1	1
Thigh angle at toe-off	(°)	-	4	-	2
Thigh angular velocity at touchdown	(°·s <sup>-1</sup> )	2 3 4	1	1	1
Trunk angle at touchdown	(°)	2 3 4	1 4	1	1 2
Trunk angle at toe-off	(°)	3 4	4	1	1 2
Trunk angular velocity at touchdown	(°·s <sup>-1</sup> )	3 4	4	1	1 2
Trunk angular velocity at toe-off	(°·s <sup>-1</sup> )	-	3 4	2	2

Numbers in each column represent steps where a significant step-to-step differences were observed ( $p < 0.05$ ) (e.g., for Average  $F_R$  magnitude on step 1, significant differences were observed with steps 3 and 4).

## Appendix C: Relationships between performance measures and all measured variables

**Table (C1).** Pearson's correlations for  $RF_{MEAN}$ , NAHEP, and normalised touchdown distance with kinematic and kinetic measures, including 95% confidence intervals.

Measure	Units		Correlation	Lower C.I.	Upper C.I.
Ankle dorsiflexion RoM	(°)	RFMEAN	0.728	0.321	0.908
		NAHEP	0.458	-0.096	0.795
		Normalised TDD	-0.683	-0.891	-0.238
Ankle plantar flexion RoM	(°)	RFMEAN	0.110	-0.447	0.605
		NAHEP	0.167	-0.399	0.641
		Normalised TDD	0.178	-0.389	0.648
CM displacement at touchdown	(m)	RFMEAN	-0.463	-0.798	0.090
		NAHEP	0.105	-0.450	0.602
		Normalised TDD	0.084	-0.467	0.589
Normalised CM height at touchdown	(m)	RFMEAN	0.000	-0.531	0.530
		NAHEP	0.147	-0.416	0.628
		Normalised TDD	-0.122	-0.613	0.437
CM velocity at touchdown	(m.s <sup>-1</sup> )	RFMEAN	-0.199	-0.660	0.371
		NAHEP	0.379	-0.190	0.757
		Normalised TDD	0.122	-0.437	0.613
Normalised toe-off distance		RFMEAN	0.428	-0.132	0.781
		NAHEP	0.664	0.206	0.883
		Normalised TDD	-0.334	-0.734	0.239
CM displacement at toe-off	(m)	RFMEAN	-0.507	-0.818	0.032
		NAHEP	-0.058	-0.571	0.487
		Normalised TDD	0.309	-0.265	0.721
Normalised CM height at toe-off	(m)	RFMEAN	-0.046	-0.563	0.497
		NAHEP	0.298	-0.276	0.716
		Normalised TDD	-0.272	-0.701	0.302
CM velocity at toe-off	(m.s <sup>-1</sup> )	RFMEAN	-0.151	-0.631	0.413
		NAHEP	0.339	-0.234	0.737
		Normalised TDD	0.120	-0.439	0.611
Contact time	(s)	RFMEAN	-0.406	-0.771	0.159
		NAHEP	-0.738	-0.912	-0.342
		Normalised TDD	0.831	0.537	0.945
$DRF$	(%·s/m)	RFMEAN	0.652	0.185	0.879
		NAHEP	0.333	-0.240	0.734
		Normalised TDD	-0.624	-0.868	-0.140
	(°)	RFMEAN	-0.724	-0.906	-0.313



Measure	Units		Correlation	Lower C.I.	Upper C.I.
Foot angle at touchdown		NAHEP	-0.406	-0.771	0.158
		Normalised TDD	0.597	0.097	0.856
Foot angle at toe-off	(°)	RFMEAN	-0.334	-0.734	0.239
		NAHEP	-0.333	-0.734	0.240
		Normalised TDD	0.038	-0.503	0.557
Foot angular velocity at touchdown	(°·s <sup>-1</sup> )	RFMEAN	0.408	-0.156	0.772
		NAHEP	-0.086	-0.589	0.466
		Normalised TDD	-0.223	-0.674	0.349
Foot angular velocity at toe-off	(°·s <sup>-1</sup> )	RFMEAN	0.214	-0.357	0.669
		NAHEP	0.176	-0.391	0.646
		Normalised TDD	-0.284	-0.708	0.291
Foot touchdown velocity	(m·s <sup>-1</sup> )	RFMEAN	-0.398	-0.767	0.168
		NAHEP	-0.430	-0.782	0.130
		Normalised TDD	0.616	0.127	0.864
Flight time	(s)	RFMEAN	-0.242	-0.685	0.331
		NAHEP	0.257	-0.317	0.693
		Normalised TDD	-0.297	-0.715	0.277
Hip angle at touchdown	(°)	RFMEAN	0.295	-0.280	0.714
		NAHEP	0.536	0.008	0.831
		Normalised TDD	-0.746	-0.915	-0.356
Hip angle at toe-off	(°)	RFMEAN	0.098	-0.456	0.598
		NAHEP	0.378	-0.191	0.757
		Normalised TDD	-0.261	-0.695	0.313
Hip angular velocity at touchdown	(°·s <sup>-1</sup> )	RFMEAN	0.201	-0.369	0.661
		NAHEP	-0.035	-0.555	0.505
		Normalised TDD	0.071	-0.478	0.58
Hip angular velocity at toe-off	(°·s <sup>-1</sup> )	RFMEAN	0.036	-0.504	0.556
		NAHEP	0.335	-0.237	0.735
		Normalised TDD	0.078	-0.472	0.584
Hip extension RoM	(°)	RFMEAN	-0.234	-0.680	0.339
		NAHEP	-0.213	-0.668	0.358
		Normalised TDD	0.580	0.071	0.849
Hip peak extension velocity	(°·s <sup>-1</sup> )	RFMEAN	-0.268	-0.699	0.306
		NAHEP	0.129	-0.431	0.617
		Normalised TDD	0.227	-0.345	0.676
Knee early flexion RoM	(°)	RFMEAN	-0.292	-0.712	0.283
		NAHEP	-0.012	-0.539	0.522
		Normalised TDD	0.463	-0.089	0.798
Knee late flexion RoM	(°)	RFMEAN	0.372	-0.198	0.754
		NAHEP	-0.273	-0.702	0.301

Measure	Units		Correlation	Lower C.I.	Upper C.I.
		Normalised TDD	0.035	-0.505	0.555
Knee angle at touchdown	(°)	RFMEAN	-0.326	-0.730	0.247
		NAHEP	0.044	-0.498	0.561
		Normalised TDD	-0.213	-0.668	0.358
Knee angle at toe-off	(°)	RFMEAN	-0.202	-0.662	0.368
		NAHEP	0.206	-0.364	0.664
		Normalised TDD	-0.051	-0.566	0.493
Knee angular velocity at touchdown	(°·s <sup>-1</sup> )	RFMEAN	-0.226	-0.676	0.346
		NAHEP	-0.269	-0.700	0.305
		Normalised TDD	0.058	-0.488	0.571
Knee angular velocity at toe-off	(°·s <sup>-1</sup> )	RFMEAN	-0.413	-0.774	0.151
		NAHEP	0.311	-0.263	0.722
		Normalised TDD	0.029	-0.510	0.551
Knee extension RoM	(°)	RFMEAN	0.149	-0.414	0.630
		NAHEP	0.136	-0.426	0.621
		Normalised TDD	0.156	-0.408	0.634
Knee peak flexion angle	(°)	RFMEAN	-0.277	-0.704	0.297
		NAHEP	0.044	-0.498	0.562
		Normalised TDD	-0.272	-0.701	0.303
Knee peak extension angle	(°)	RFMEAN	-0.168	-0.642	0.398
		NAHEP	0.184	-0.385	0.651
		Normalised TDD	-0.049	-0.565	0.494
Knee peak extension velocity	(°·s <sup>-1</sup> )	RFMEAN	-0.167	-0.641	0.399
		NAHEP	0.328	-0.245	0.731
		Normalised TDD	0.185	-0.383	0.652
Knee peak flexion velocity	(°·s <sup>-1</sup> )	RFMEAN	-0.228	-0.677	0.344
		NAHEP	0.394	-0.173	0.765
		Normalised TDD	-0.144	-0.626	0.419
Ankle peak plantar flexion velocity	(°·s <sup>-1</sup> )	RFMEAN	0.311	-0.263	0.722
		NAHEP	0.249	-0.324	0.689
		Normalised TDD	-0.164	-0.639	0.402
Average F <sub>H</sub> component	(BW)	RFMEAN	0.362	-0.209	0.749
		NAHEP	0.719	0.304	0.904
		Normalised TDD	-0.744	-0.914	-0.353
Average F <sub>R</sub> magnitude	(BW)	RFMEAN	-0.177	-0.647	0.391
		NAHEP	0.379	-0.189	0.757
		Normalised TDD	-0.415	-0.775	0.148
Average F <sub>V</sub> component	(BW)	RFMEAN	-0.200	-0.661	0.370
		NAHEP	0.347	-0.225	0.741
		Normalised TDD	-0.399	-0.767	0.167

Measure	Units		Correlation	Lower C.I.	Upper C.I.
Ankle peak dorsiflexion angle	(°)	RFMEAN	-0.258	-0.693	0.316
		NAHEP	0.129	-0.431	0.617
		Normalised TDD	-0.200	-0.661	0.369
Ankle peak dorsiflexion velocity	(°·s <sup>-1</sup> )	RFMEAN	-0.449	-0.791	0.107
		NAHEP	-0.520	-0.823	0.015
		Normalised TDD	0.743	0.35	0.913
Peak braking F <sub>H</sub> component	(BW)	RFMEAN	0.403	-0.162	0.769
		NAHEP	0.381	-0.187	0.758
		Normalised TDD	-0.558	-0.840	-0.039
Peak propulsive F <sub>H</sub> component	(BW)	RFMEAN	0.245	-0.329	0.686
		NAHEP	0.626	0.143	0.868
		Normalised TDD	-0.410	-0.773	0.154
Peak F <sub>R</sub> magnitude	(BW)	RFMEAN	-0.110	-0.605	0.447
		NAHEP	0.363	-0.207	0.749
		Normalised TDD	-0.407	-0.771	0.157
Peak F <sub>V</sub> component	(BW)	RFMEAN	-0.134	-0.620	0.427
		NAHEP	0.343	-0.230	0.739
		Normalised TDD	-0.411	-0.773	0.153
Linearity of the RF-v <sub>H</sub> fit (R <sup>2</sup> )		RFMEAN	-0.491	-0.810	0.054
		NAHEP	-0.280	-0.706	0.294
		Normalised TDD	0.136	-0.425	0.622
RF <sub>0</sub>	(%)	RFMEAN	-0.454	-0.794	0.100
		NAHEP	-0.090	-0.592	0.462
		Normalised TDD	0.493	-0.051	0.811
Shank angle at touchdown	(°)	RFMEAN	-0.764	-0.921	-0.392
		NAHEP	-0.330	-0.732	0.244
		Normalised TDD	0.364	-0.206	0.750
Shank angle at toe-off	(°)	RFMEAN	-0.235	-0.680	0.338
		NAHEP	-0.006	-0.535	0.527
		Normalised TDD	-0.187	-0.653	0.381
Shank angular velocity at touchdown	(°·s <sup>-1</sup> )	RFMEAN	-0.309	-0.721	0.265
		NAHEP	-0.443	-0.788	0.114
		Normalised TDD	0.272	-0.302	0.701
Shank angular velocity at toe-off	(°·s <sup>-1</sup> )	RFMEAN	-0.511	-0.820	0.026
		NAHEP	0.151	-0.412	0.631
		Normalised TDD	0.131	-0.430	0.619
Step frequency	(steps·s <sup>-1</sup> )	RFMEAN	0.715	0.297	0.903
		NAHEP	0.434	-0.126	0.784
		Normalised TDD	-0.466	-0.799	0.085
Normalised step length		RFMEAN	-0.296	-0.714	0.279

Measure	Units		Correlation	Lower C.I.	Upper C.I.
		NAHEP	0.412	-0.152	0.773
		Normalised TDD	-0.078	-0.584	0.472
Ankle angle at touchdown	(°)	RFMEAN	0.154	-0.410	0.633
		NAHEP	0.357	-0.214	0.746
		Normalised TDD	-0.540	-0.832	-0.013
Ankle angular velocity at touchdown	(°·s <sup>-1</sup> )	RFMEAN	-0.072	-0.580	0.477
		NAHEP	-0.072	-0.580	0.477
		Normalised TDD	0.197	-0.372	0.659
Thigh angle at touchdown	(°)	RFMEAN	-0.252	-0.690	0.322
		NAHEP	-0.392	-0.764	0.175
		Normalised TDD	0.677	0.229	0.889
Thigh angle at toe-off	(°)	RFMEAN	0.076	-0.473	0.583
		NAHEP	-0.311	-0.722	0.263
		Normalised TDD	-0.089	-0.592	0.463
Thigh angular velocity at touchdown	(°·s <sup>-1</sup> )	RFMEAN	-0.174	-0.645	0.393
		NAHEP	-0.392	-0.764	0.175
		Normalised TDD	0.526	-0.007	0.826
Thigh angular velocity at toe-off	(°·s <sup>-1</sup> )	RFMEAN	0.304	-0.270	0.719
		NAHEP	-0.374	-0.755	0.195
		Normalised TDD	0.046	-0.497	0.563
Ankle angle at toe-off	(°)	RFMEAN	-0.141	-0.625	0.421
		NAHEP	0.220	-0.352	0.672
		Normalised TDD	-0.047	-0.564	0.496
Ankle angular velocity at toe-off	(°·s <sup>-1</sup> )	RFMEAN	-0.087	-0.590	0.465
		NAHEP	0.126	-0.434	0.615
		Normalised TDD	0.092	-0.461	0.593
Trunk angle at touchdown	(°)	RFMEAN	-0.151	-0.631	0.413
		NAHEP	-0.134	-0.620	0.427
		Normalised TDD	0.211	-0.360	0.667
Trunk angle at toe-off	(°)	RFMEAN	-0.180	-0.649	0.388
		NAHEP	-0.057	-0.570	0.488
		Normalised TDD	0.090	-0.463	0.592
Trunk angular velocity at touchdown	(°·s <sup>-1</sup> )	RFMEAN	-0.272	-0.702	0.302
		NAHEP	0.027	-0.511	0.550
		Normalised TDD	-0.398	-0.767	0.168
Trunk angular velocity at toe-off	(°·s <sup>-1</sup> )	RFMEAN	-0.223	-0.674	0.348
		NAHEP	0.260	-0.314	0.694
		Normalised TDD	-0.159	-0.636	0.406

Normalised TDD = Normalised touchdown distance.

## Appendix D: Multiple linear regression results

Bivariate Pearson's correlations to address the primary aim of this thesis found some kinematic characteristics were strongly related to RF but not initial acceleration phase performance, and vice versa. This suggested that multivariate analyses may be required to thoroughly explore such relationships. Table D1 depicts a series of stepwise multiple linear regressions performed on variables strongly related to performance but not RF (normalised toe-off distance, contact time and touchdown hip angle), and those strongly related to RF but not performance (normalised touchdown distance, step frequency, ankle dorsiflexion range of motion, touchdown foot angle and touchdown shank angle) to assess their individual and combined share of the variance in initial acceleration phase performance (NAHEP).

**Table (D1).** Multiple linear regression between kinematic characteristics strongly related to performance but not RF and kinematic characteristics strongly related to RF but not performance to assess contribution to the variance in initial acceleration performance.

Measure		F	Adjusted R <sup>2</sup>	β-coefficient
NAHEP-related	RF-related			
Normalised Toe-off Distance	Normalised Touchdown Distance	13.4***	66%	-0.481* ; -0.549**
	Step Frequency	4.8*	37%	-0.587* ; 0.172
	Ankle Dorsiflexion RoM	10.4**	59%	-0.666** ; 0.461*
	Touchdown Foot Angle	8.1**	60%	-0.657** ; -0.394
	Touchdown Shank Angle	4.6*	36%	-0.622* ; -0.137
Contact time	Normalised Touchdown Distance	7.4**	50%	-0.481 ; -0.310
	Step Frequency	8.6**	54%	-0.672** ; 0.265
	Ankle Dorsiflexion RoM	6.7*	47%	-0.697* ; 0.077
	Touchdown Foot Angle	6.9*	56%	-0.689** ; -0.119
	Touchdown Shank Angle	10.0**	65%	-0.732** ; -0.315
Touchdown Hip Angle	Normalised Touchdown Distance	5.6*	50%	0.016 ; -0.698
	Step Frequency	5.4*	40%	0.555* ; 0.456
	Ankle Dorsiflexion RoM	3.0	23%	0.416 ; 0.277
	Touchdown Foot Angle	3.0	24%	0.457 ; -0.274
	Touchdown Shank Angle	3.3	26%	0.516 ; -0.294

β-coefficient pairs are presented as 'left ; right' referring to their corresponding measures in columns one and two. \* p < 0.05; \*\* p < 0.01; \*\*\* p < 0.001.